EFFECTS OF LONG-TERM EVOLUTION WAVEFORM ON SYNTHETIC APERTURE RADAR IMAGE QUALITY METRICS

THESIS

Blake M Colson, B.S.E.E., Captain, USAF

AFIT-ENG-MS-20-M-011

DEPARTMENT OF THE AIR FORCE
AIR UNIVERSITY

AIR FORCE INSTITUTE OF TECHNOLOGY

Wright-Patterson Air Force Base, Ohio

AFIT-ENG-MS-20-M-011

EFFECTS OF LONG-TERM EVOLUTION WAVEFORM ON SYNTHETIC APERTURE RADAR IMAGE QUALITY METRICS

THESIS

Presented to the Faculty

Department of Electrical and Computer Engineering

Graduate School of Engineering and Management

Air Force Institute of Technology

Air University

Air Education and Training Command

in Partial Fulfillment of the Requirements for the

Degree of Master of Science in Electrical Engineering

Blake M Colson, B.S.E.E., B.S.E.E.

Captain, USAF

March 2020

AFIT-ENG-MS-20-M-011

EFFECTS OF LONG-TERM EVOLUTION WAVEFORM ON SYNTHETIC APERTURE RADAR IMAGE QUALITY METRICS

THESIS

Blake M Colson, B.S.E.E., B.S.E.E.
Captain, USAF

Committee Membership:

Julie A Jackson, Ph.D
Chair

Richard K Martin,, Ph.D
Member

James R Lievsay,, Ph.D
Member

Abstract

As a greater demand by the private sector for bandwidth drives spectrum allocations away from defense, new methods for coexistence in the spectrum are being explored. One of the prominent areas in defense for this coexistence is passive radar. This mode of radar system allows for data collection by referencing signals already established in the environment of interest. Some of the most prolific signals currently available are those used for mobile communication networks. In particular, Long-Term Evolution (LTE) is a common waveform that could be leveraged for discrete collection of image intelligence. Seeking to build a base of knowledge, simulations of synthetic aperture radar (SAR) systems are carried out using the LTE framework. Variations in waveform content, structure, and signal components are established and used to generate point-spread function (PSF) responses characterizing the image domain impacts of given fluctuations. Overall, PSF responses for most variations are highly similar, incurring slight losses as pulses contain varied data types and slight gains when maximizing the amount of user data contained in pulses. Notable sidelobes in range profiles occur at predictable intervals and may be easily managed for adequately-sized scenes. Peak sidelobe ratio (PSLR) and integrated sidelobe ratio (ISLR) results show marginal improvement when pulses are varied over the aperture. Range and cross-range resolution, while remaining mostly unchanged throughout variations, are observed to be worse in simulation than is expected. The work presented here is meant to serve as a starting point of overall LTE characterization as a radar waveform and establish basic metrics of comparison for future efforts.

Table of Contents

Page

List of Figures

List of Tables

EFFECTS OF LONG-TERM EVOLUTION WAVEFORM ON SYNTHETIC APERTURE RADAR IMAGE QUALITY METRICS

I. Introduction

1.1 General Issue

As a greater demand by the private sector for bandwidth drives spectrum allocations away from defense, new methods for coexistence in the spectrum are being explored. One of the prominent areas in defense for this coexistence is passive radar. This mode of radar system allows for data collection by referencing signals already established in the environment of interest. Some of the most prolific signals currently available are those used for mobile communication networks.

Cell towers provide excellent opportunities for utilization as reference waveform generators without the need to transmit specific and powerful signals that create the possibility for system detection through signal monitoring and local interference. Presently, mobile telecommunications networks are implementing the most up-to-date versions of 3rd Generation Partnership Project's Long-Term Evolution (LTE) standard for mobile information transfer. Advancing the study of LTE use for synthetic aperture radar (SAR) systems could provide knowledge to the benefit of the warfighter, enabling discrete collection of image intelligence throughout the world while mitigating possibilities of local signal interference and alleviating pressure of government demand for increasingly populated spectrum.

1.2 Problem Statement

The use of LTE for radar applications is currently underrepresented in the field with much of the research being based around specific waveform structure [1, 2]. There is also potential for later versions of LTE to be more dynamic than is currently achievable. Overall effects of the use of LTE waveforms with parameter variation occurring at several levels of the structure should be evaluated with the intent to inform the mitigation of any undesirable effects introduced by either deterministic characteristics or variations in the waveform pulse-to-pulse.

1.3 Research Objectives

This research aims to establish baseline image-domain effects for several types of LTE variation in comparison with traditional radar methods. Further the performance of variations will be quantified using several image quality metrics to include range and cross-range resolutions, peak sidelobe ratio (PSLR), and integrated sidelobe ratio (ISLR). This work intends to establish a foothold in how LTE variation generally affects a point-spread function (PSF) to be further broken down and analyzed by future researchers.

1.4 Methodology

This research will utilize simulation with ideal assumptions to model a monostatic SAR system. A monostatic model is used in order to build a base of knowledge toward the eventual application of LTE to passive radar simulation and research. Basic variations of the LTE waveform will flow from utilizing a single section of the overall structure, for a given pulse length, to progression through the LTE structure pulse-to-pulse as new, random user data is generated. Following these variations, modifica-

tion of specific waveform parameters — to include bandwidth, user-data modulation scheme, cyclic prefix type, and number of control channels — will take place along with progression through the LTE structure and user-data generation.

1.5 Contributions

This research lays the groundwork for understanding impacts of LTE waveform variations in the image domain. Variations in waveform content and structure establish a base of comparison for modification of waveform parameters effecting bandwidth, user data modulation, number of control channels, and cyclic prefix (CP) length. The results of these simulations paint a picture of which waveform components most influence PSF outcomes and how. From this point, a greater depth of understanding may be built in order to optimize waveform selection and application to passive SAR.

1.6 Thesis Overview

In Chapter II, the SAR processing chain and PSF image quality metrics used throughout simulations are discussed. The radar information is followed by an overview of the LTE waveform structure, contents, and parameters of interest. Chapter III provides more information regarding LTE resource allocation across subcarriers and simulates three foundational waveform scenarios at four pulse-lengths corresponding to the major LTE time structures. Chapter IV builds upon the simulations accomplished in Chapter III by introducing variation to waveform bandwidth, user data modulation, control channel content, and CP length while progressing through LTE structure pulse to pulse. Finally, simulation results and key impacts are outlined in Chapter V, followed by recommendations for future efforts stemming from this work.

II. Background

2.1 Chapter Overview

This chapter equips the reader with background to synthetic aperture radar (SAR) imaging concepts, Long-Term Evolution (LTE) waveform structure, and image quality metrics. Enabling research is reviewed and assumptions for simulations are discussed in preparation for experimentation in following chapters.

2.2 Synthetic Aperture Radar

SAR systems, like traditional radar, propagate a waveform and process reflected energy to determine scatterer properties. For traditional radar systems, a single pulse is needed to determine target range and velocity using pulse return time and the Doppler shift, respectively. However, this method must be expanded upon for SAR systems. Because radar scenes typically include multiple scatterers, as shown in Figure 1, there is potential for those scatterers to be grouped in a single range contour despite being located at distinct positions in the scene. To alleviate scatterer range grouping, many pulses are propagated and processed over an aperture [3]. Being that an aperture is necessary to differentiate scatterers in range and cross-range, SAR is dependent upon receiver or target motion in spotlight and stripmap or inverse modes, respectively. The research laid out in this document utilizes spotlight-mode SAR in a monostatic configuration as depicted in Figure 2. The first step of processing scene information is matched filtering.

2.2.1 Matched Filter

Matched filtering is a primary method enabling radar receivers to generate useful scene information. While other methods of signal processing exist, such as the deramp

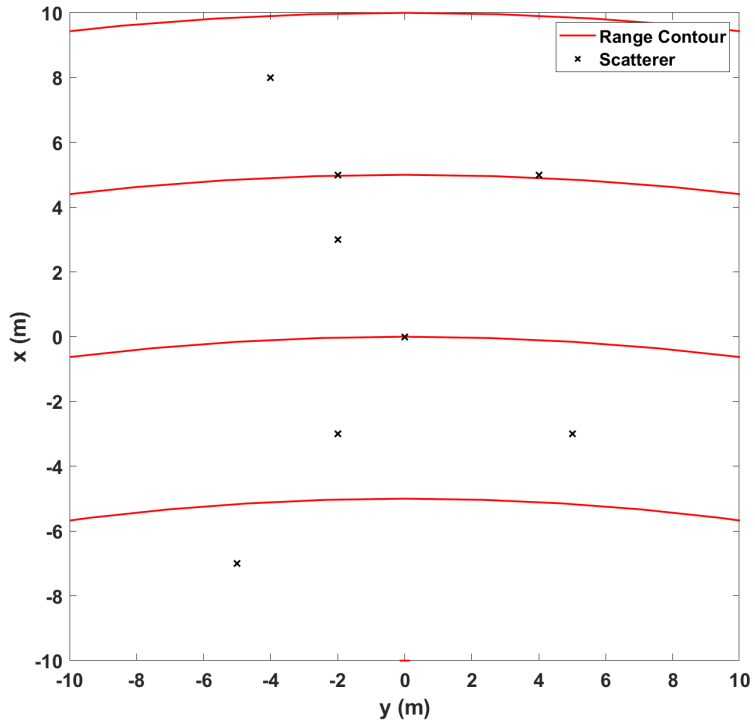

Figure 1: A typical SAR scene includes multiple scatterers that may lie between range contours and, thereby, lie within a single range cell despite being separated in cross-range.

algorithm, they are typically used for specialized waveforms and attempt to emulate the matched filter (MF) property of maximizing target return signal-to-noise ratio (SNR) in the presence of noise [3]. The discrete MF output with transmitted signal $s[n]$ takes the form

$$r_{mf}[n] = s[n] * s^*[-n], \tag{1}$$

where reference signal $s^*[-n]$ is the impulse response of the MF [4]. A MF output for an linear-frequency modulation (LFM) pulse is depicted in Figure 3.

In order to leverage the MF for radar applications, the scene effects $g[n]$ on $s[n]$ must be taken into account. The ideal discrete-time MF, given fast time[1] sample n

[1]For radar applications, fast time refers to the time a single pulse spends being transmitted and received, whereas slow time refers to the interval of time pulses are being transmitted and received

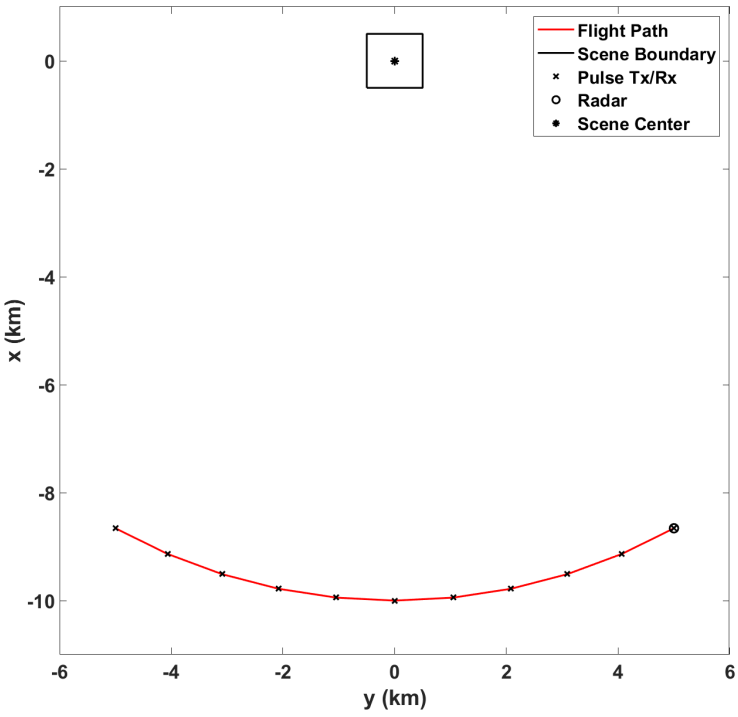

Figure 2: Spotlight mode SAR places scene center at a non-moving point for the duration of collection apertures. In this case, the aperture follows the flight path of an aircraft housing the radar and encompasses azimuth extent $\Delta\phi$ at constant grazing angle ψ and range from scene center R_0.

and collection azimuth ϕ, is described by

$$r[n, \phi] = s[n, \phi] * g[n, \phi] * s^*[-n, \phi], \tag{2}$$

where $s[n, \phi]$ is the transmitted signal, $g[n, \phi]$ is the scene reflectivity, and $s^*[-n, \phi]$ is the reference signal. The matched filter output $r[n, \phi]$, given effects of $g[n, \phi]$ on $s[n, \phi]$ is defined as a range profile.

over the entirety of an aperture.

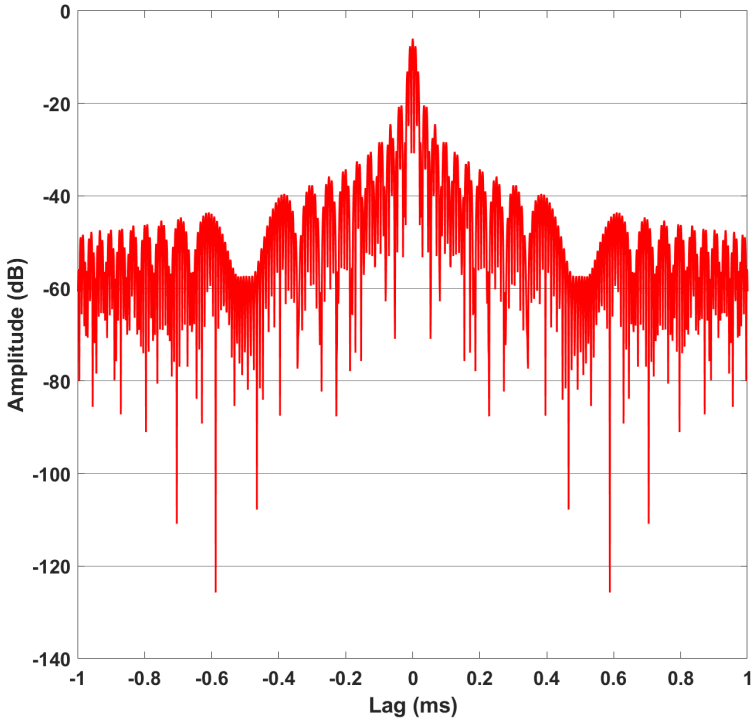

Figure 3: MF output for LFM waveform with 1 ms length.

2.2.2 Range Profiles

Range profiles are the point in the processing chain where target range information becomes prominent. By implementing Equation (2) for a single pulse, scatterers may be detected and displayed in a range profile as shown in Figure 4.

By using time-domain MF response peaks to determine round-trip pulse return time T_m from the m^{th} target, range R_m is quantified using

$$R_m = \frac{cT_m}{2}, \tag{3}$$

where c is the speed of light. Because SAR system standoff is often significantly greater than the scene extent, the range of targets may be redefined in terms of the

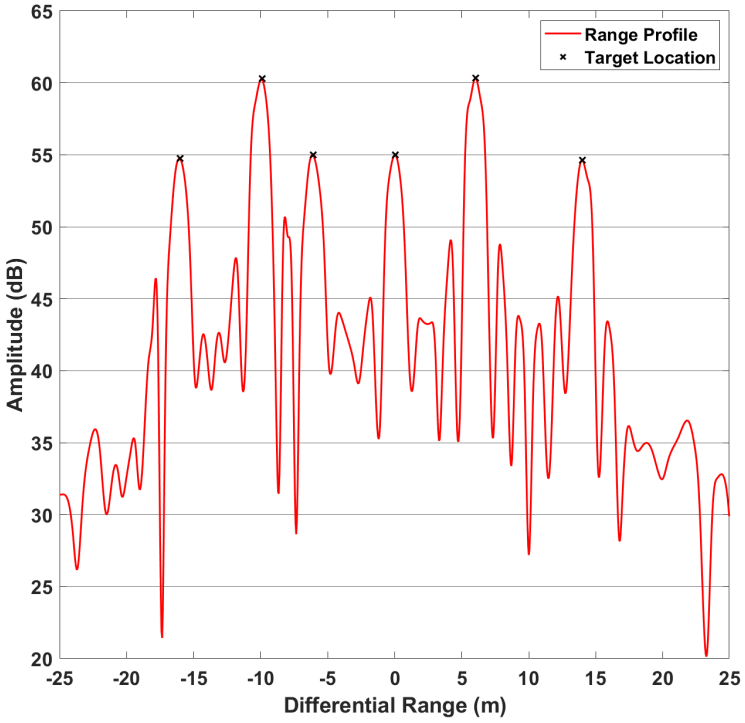

Figure 4: Range profile generated through use of the MF for a linear-frequency modulated pulse.

differential range

$$\Delta R_m = -2(x_m \cos\phi \cos\psi + y_m \sin\phi \cos\psi + z_m \sin\psi). \tag{4}$$

ΔR_m places scene center at zero range and evaluates the distance of the m^{th} target from scene center along the line of sight of the SAR system. It should be noted that Equation (4) is specific to the case of monostatic systems under a far-field assumption, as is simulated throughout this research. Additionally, as mentioned in the introduction to Section 2.2, scenes being observed by SAR systems often include targets grouped in a range contour but separated in cross-range. Scatterer grouping in cross-range with separation in range is also a possibility within a scene. To differentiate scatterers grouped in either of these two dimensions, multiple range profiles

are produced over the extent of the system aperture. With range profiles established and knowledge of convolution properties [5], the Fourier transform may be applied to Equation (2) yielding

$$R[f, \phi] = S[f, \phi]G[f, \phi]S^*[f, \phi]. \tag{5}$$

The relationship expressed by $R[f, \phi]$ represents the spectral response of the range profile and is known as phase history.

2.2.3 Phase History

Phase history is a representation of both scene reflectivity magnitude and phase across the extent of a collection aperture. The phase history of a simplified scene containing point scatterers may be represented as

$$G[f, \phi] = \sum_{m=1}^{M} A_m e^{j\theta_m[f,\phi]}, \tag{6}$$

where A_m is the spatial frequency magnitude and θ_m is phase for M scatterers given frequency f and collection azimuth ϕ. When a scene is further simplified to contain only a single point scatterer at scene center, Equation (6) may be reduced to

$$G[f, \phi] = A_0 e^{j\theta_0[f,\phi]}. \tag{7}$$

While Equation (6) and Equation (7) yield specifically scene response, Equation (5) is used to determine phase history accounting for transmit signal. When there is a single scatterer at scene center, no phase changes occur pulse to pulse resulting in a zero-response phase history. In the case of multiple scatterers throughout the scene, phase history may be depicted like that in Figure 5. In order to proceed to the image domain, the phase history is utilized by one of several imaging algorithms. The work presented here makes use of the back-projection algorithm (BPA).

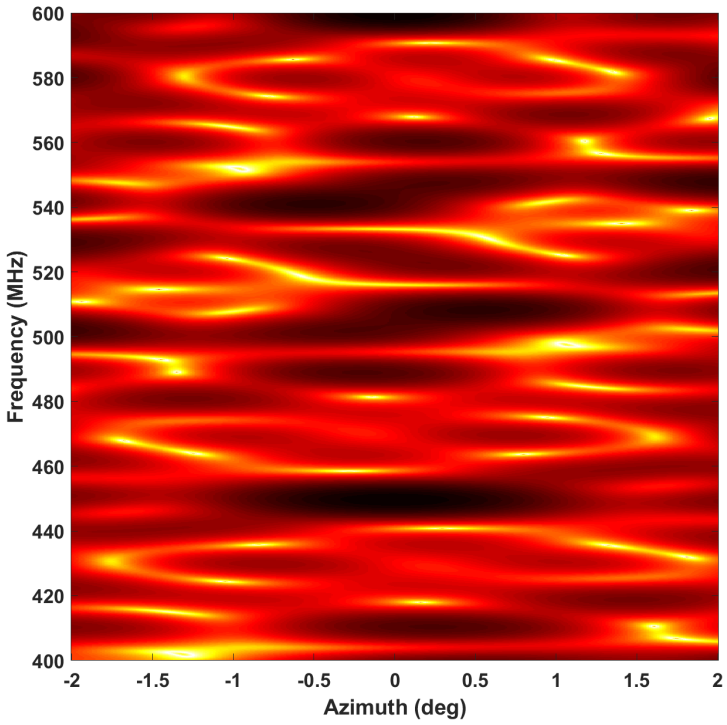

Figure 5: Phase history of scene depicted in Figure 1.

2.2.4 Back-Projection Algorithm

While several methods exist to convert radar data, whether range profile or phase history, the application of phase history in BPA is utilized throughout the course of this research. BPA is enabled by the inverse Radon transform, the primary function of which is to map phase history information to spatial domain range cells. This information mapping, in combination with its transformation to the spatial domain, result in an image depicting scene response to the transmitted waveform across the collection aperture. For more detailed information regarding this process, see [6].

2.2.5 Point-Spread Function

The point-spread function (PSF) is the image domain representation of reflectivity for a scene containing a single point scatterer located at scene center [7]. An example

PSF is shown in Figure 6. The PSF is used as a tool to observe the scatterer response to waveforms of interest. To that effect, the PSF is leveraged throughout this research to directly compare responses for several variations of the LTE waveform.

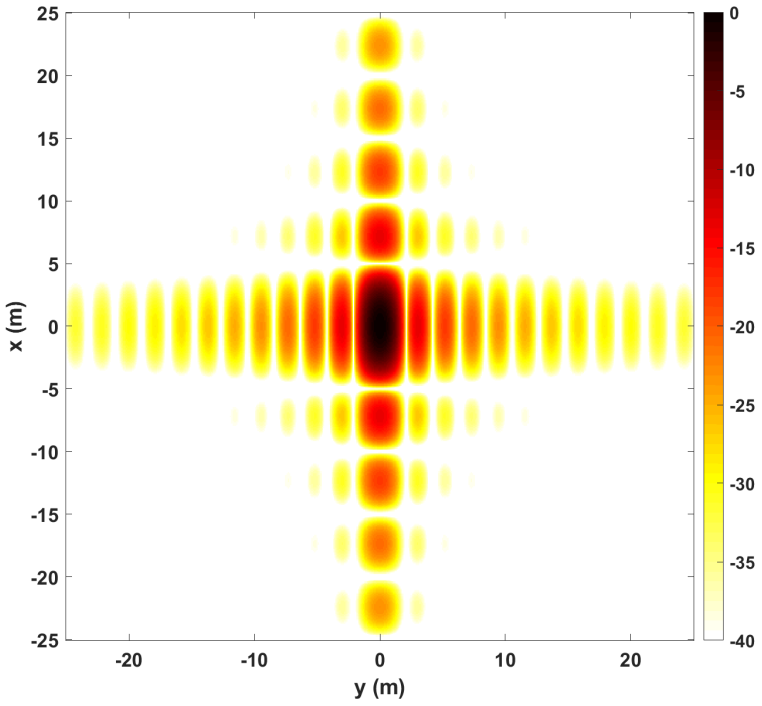

Figure 6: PSF using a LFM waveform.

2.3 Image Quality Metrics

Several metrics may be used in an attempt to determine quality of a PSF. The four metrics outlined below will serve as the basis for comparison between waveform variations and pulse-lengths throughout this research.

2.3.1 Range Resolution

Range resolution, defined as be the distance from scene center to the first PSF minimum in the range direction, is represented as

$$\delta R = \frac{c}{2B\cos\psi} \tag{8}$$

where B is the waveform bandwidth and ψ is the elevation angle of the system in radians, is a measure of how precisely the location of a target may be determined in the range direction [3]. As defined, the resolution of a target in the scene would be improved with increased bandwidth. Resolution in the range direction is a measure of the separation required between scatterers to detect them distinctly.

2.3.2 Cross-Range Resolution

Cross-range resolution shares a similar definition to range resolution, albeit in the direction normal to the range direction. Defined as the distance from scene center to the first PSF minimum in the cross-range direction, cross-range resolution is represented as

$$\delta R_{\otimes} = \frac{\lambda}{4sin(\frac{\Delta\phi}{2})cos(\psi)}, \tag{9}$$

cross-range resolution is dependent upon transmit wavelength λ, total aperture extent $\Delta\phi$ in radians, and elevation angle ψ in radians [8]. It should be noted that obtaining $\delta R_{\otimes}$ with this equation only holds under a small-angle assumption and begins to

break down for large apertures. Being that the waveforms used here are composed of several frequencies, the lowest transmit frequency is utilized for $\delta R_{\otimes}$ calculations. Using the lowest frequency results in a worst-case resolution to be considered for each case. In the same manner as δR, $\delta R_{\otimes}$ is indicative of the space required between scatterers to distinguish multiple targets in cross-range.

2.3.3 Peak Sidelobe Ratio

The peak sidelobe ratio (PSLR) of a MF response,

$$PSLR_{dB} = 10 \log_{10} \frac{|I_s|}{|I_m|}, \tag{10}$$

is the ratio of most prominent sidelobe's amplitude I_s to that of the mainlobe's amplitude I_m [9]. This metric is indicative of the degree to which the response of a scatterer may obscure that of another nearby target.

2.3.4 Integrated Sidelobe Ratio

The integrated sidelobe ratio (ISLR), defined as

$$ISLR_{dB} = 10 \log_{10} \frac{E_s}{E_m}, \tag{11}$$

is the ratio of sidelobe energy E_s to the -3 dB mainlobe energy E_m [9]. These energy levels are defined as

$$E_s = \sum_{n=k_{3dB}}^{L} |r[n, \phi]|^2 \tag{12}$$

and

$$E_m = \sum_{n=1}^{k_{3dB}} |r[n, \phi]|^2, \tag{13}$$

where $r[n, \phi]$ is the range profile response and k_{3dB} is the 3 dB cutoff index.

2.4 Long-Term Evolution Waveform

LTE is an international standard for wireless communication systems developed by European Telecommunications Standards Institute 3rd Generation partnership Project. The intention of LTE was to improve both capacity and speed of wireless networks. First proposed in 2004, LTE has become a primary means of wireless data transfer across mobile networks. This being the case, the LTE waveform presents an excellent opportunity for exploitation by passive radar systems. All technical information regarding LTE throughout this section is sourced from [10] with supporting information from [11].

2.4.1 Frame Structure

The highest level of physical LTE waveform structure is known as a frame. There are two varieties of LTE frame, type 1 and type 2. To separate uplink (UL) and downlink (DL) signals, type 1 and type 2 frames leverage frequency-division duplexing (FDD) and time-division duplexing (TDD), respectively. Similarly to [1], a type 1 frame format is used due to its characteristic separation of UL and DL in the frequency domain which allows the entire DL spectrum to be exploited for passive radar purposes. A frame represents 10 ms of signal across all utilized frequencies. The frame may be broken down into ten subframes of 1 ms duration. Subframes are further split into two slots that each contain either six or seven orthogonal frequency-division multiplexing (OFDM) symbols, dependent on the cyclic prefix (CP) length. A visualization of these structures is shown in Figure 7 and Figure 8. The most basic structure of the frame, however, is the resource block.

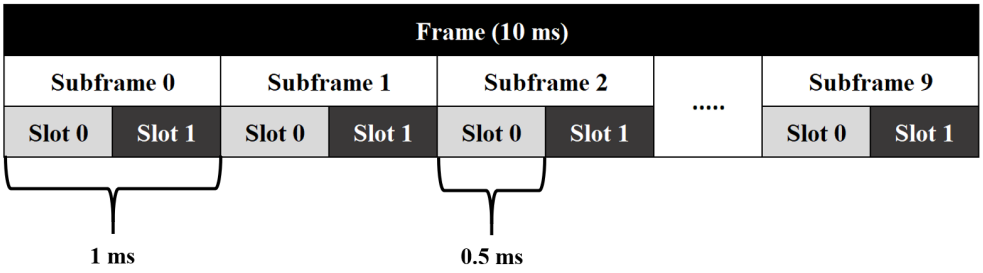

Figure 7: LTE type 1 frame structure [10].

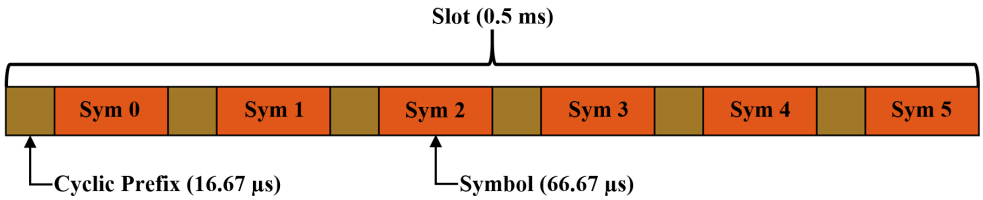

Figure 8: Slot structure for LTE waveform with extended CP length. When in the normal CP mode, the slot contains one additional symbol. While the usable symbol length for each mode is the same, the first symbol of the normal mode always has a slightly longer CP than the following six symbols to maintain LTE sample rate standards. Overall, the extended CP mode sees longer CP for each symbol over the normal mode [10].

2.4.2 Resource Block

A resource block (RB) represents one slot length in the time domain — either six or seven OFDM symbols — and 180 kHz of bandwidth made up of 12, 15 kHz wide subcarriers. Figure 9 depicts an example of the RB grid. A single RB is the minimum amount of waveform resources allocated to a user on an LTE network. However, no less than six and no more than 100 RBs, respectively equating to 72 and 1200 subcarriers, across the frequency domain may be transmitted by one carrier at any given time. These limits are established by the six LTE bandwidth modes expressed in Table 1. The effective bandwidth B_e of each mode is determined as

$$B_e = N_c B_c N_{RB}, \tag{14}$$

where N_c is 12 subcarriers per RB, B_c is 15 kHz, and N_{RB} is the number of RB for a given mode.

Each element in a RB is known as a resource element and contains a single modulated symbol representing all or part of the cell-specific reference signal (CSRS), primary synchronization signal (PSS), secondary synchronization signal (SSS), or one of several DL data channels[2].

[2]In the context of LTE communication, a channel is defined as data allocated to a specific purpose across the spectrum of the overall signal and not to a physical signal.

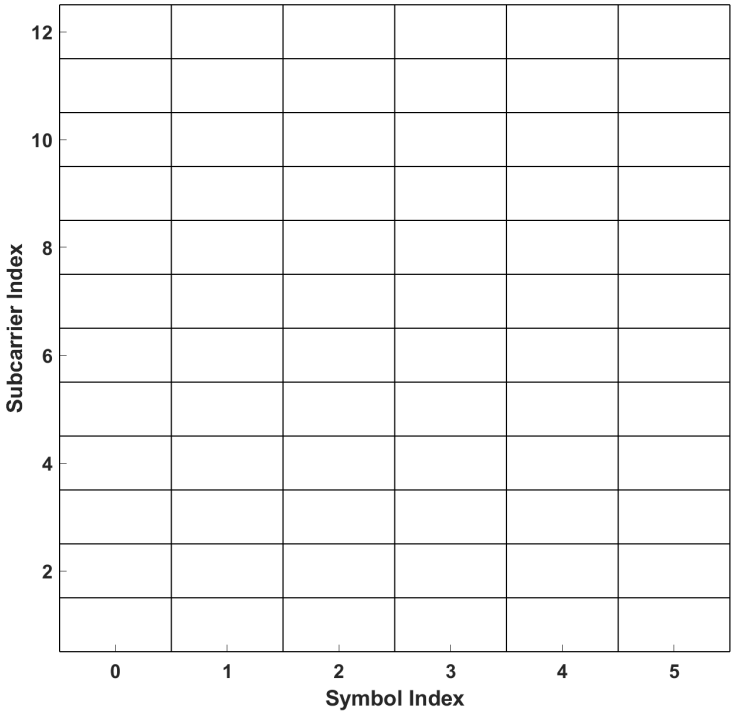

Figure 9: An empty resource block grid containing six OFDM symbols across 12 subcarriers. In this configuration, each RB contains 72 resource elements. When using a normal CP with seven symbols per slot, the RB contains 84 resource elements.

Table 1: LTE bandwidth modes and associated effective bandwidth, RB, and subcarrier allocations for each.

B (MHz)	B_e (MHz)	N_{RB}	N_f
1.4	1.08	6	72
3	2.7	15	180
5	4.5	25	300
10	9	50	600
15	13.5	75	900
20	18	100	1200

2.4.3 Downlink Contents

The LTE DL contains several types of signals that each relay specific information to be used for communication between the cell and user equipment. The DL reference signal is known as the CSRS. The CSRS is leveraged by user equipment to determine cell transmission power and perform channel estimation. The resource elements that the reference is mapped to are dependent upon the physical cell identity. For a given cell identity, these reference elements appear at the same location in each slot making the CSRS a mostly constant aspect of the LTE waveform when applied to spotlight-mode SAR.

The DL also contains the PSS and SSS used to synchronize frames at user equipment. These two signals are also used to determine physical cell identity of the transmitter. The PSS is comprised of a 62 Zadoff Chu Sequence and is mapped to 72 active subcarriers—centered on DC—in slot 0 and slot 10. The SSS is comprised of a 62 scrambling sequence and is mapped to 72 active subcarriers—similarly centered on DC—in slot 0 and slot 10. The SSS in slot 0 is different than that in slot 10 and different equations are used to generate symbols for oddly versus evenly indexed resource elements.

Several DL channels are present throughout an LTE frame and data from more than one of these channels may be transmitted during one OFDM symbol, depen-

dent upon the current slot and symbol indices. Each channel carries process-specific information used for communication between the cell and user equipment. The DL channels include physical broadcasting channel (PBCH), physical control format indicator channel (PCFICH), physical downlink control channel (PDCCH), physical hybrid ARQ indicator CH (PHICH), and physical downlink shared channel (PDSCH)[3].

PBCH contains the master information block. This channel utilizes quadrature phase-shift keying (QPSK) modulation and is mapped to six RB, regardless of cell bandwidth, centered around the DC subcarrier in subframe 0 of each frame. Mapping of PBCH to resource elements occurs such that PCFICH, PHICH, and reference signals are not overwritten.

PDSCH is dedicated to carrying user data modulated using QPSK, 16-quadrature amplitude modulation (16QAM), or 64-quadrature amplitude modulation (64QAM). Modulated data is allocated to resource elements not already being filled by other DL channels. The PDSCH makes up the vast majority of LTE DL information and is what would be best leveraged in a passive SAR system. While it is a very real possibility for other data channels to have some amount of repetition frame-to-frame, user data is most likely to be pseudo-random in each OFDM symbol. The fact that user data dominates each LTE frame, combined with the random nature of its generation, may be leveraged in radar applications to assume a new and unique waveform pulse-to-pulse. This method of application is similar to noise radar with differences being notable in that LTE DL power levels may be comparably greater than noise radar applications due to the working nature of communications waveforms and the desire for signal to cover significant distances. The nature of the randomness of PDSCH information and, thereby, the randomness of LTE itself lies in the necessity to cater the data to varied individual users.

[3]Throughout this work, PDSCH and waveform user data are synonymous

2.4.4 Time-Varying Parameters

Many aspects of the LTE waveform vary with time frame-by-frame. Of primary interest to this research are the signal bandwidth, user-data modulation scheme, cyclic prefix length, and control format indicator (CFI). These parameters may vary dynamically to best serve the users within a given cell or meet the needs of a network provider.

Varying the bandwidth of an LTE signal is dependent on provider allocations and network signal conditions. Being that bandwidth is allocated to providers, it is atypical that the bandwidth for a given cell would vary much if at all. At most, the bandwidth may vary frame-to-frame. Practically, however, any variation in bandwidth would necessitate the use of multiple frames before a change takes place, ensuring delivery of current user-data and synchronization information. Based on Equation (8), variations in bandwidth pulse-to-pulse are expected to affect δR of radar returns, the resulting resolution being most negatively affected by the smallest bandwidth observed.

Similarly to bandwidth, varying user-data modulation scheme is dependent upon network signal conditions. Specifically the user equipment (UE) SNR at the cell affects which scheme is utilized. For degraded SNR, a lower throughput modulation may be preferred. Should improvements in SNR occur, the modulation may be shifted to schemes with greater bit rates. For LTE, user-data modulation types are limited to QPSK, 16QAM, and 64QAM.

The CP for each OFDM symbol is made up a section of the end of the given symbol appended to the beginning of that symbol and it varies dependent on multipath effects and inter-symbol interference (ISI), favoring a normal CP when conditions permit. A normal CP allows for seven OFDM symbols to be allocated to each slot in the LTE frame. The first of these seven symbols contains a longer CP than the following six,

which have uniformly sized CP. An extended CP allocates only six OFDM symbols to each slot in the LTE frame, all having uniform CP lengths. Regardless of CP type, slot-length remains constant at 0.5 ms. The ramifications of the CP on radar, especially for symbol-length pulses, include the introduction of characteristic sidelobes resulting from the correlation of CP and corresponding section of the OFDM symbol when matched filtering.

The CFI varies dependent on several conditions to include bandwidth and code rate throughput. The CFI takes on a value of 1, 2, or 3 to indicate the number of OFDM symbols being utilized by the PDCCH at the beginning of each subframe. The codewords associated with each of the CFI options is shown in Table 2. These codewords may be beneficial for radar applications being that they occupy, dependent upon cell identity, specific frequencies in the first OFDM symbol of each subframe and are entirely deterministic.

Table 2: CFI value and bit patterns representing them.

CFI	Codeword $< b_0, b_1, \ldots, b_{31} >$
1	<0,1,1,0,1,1,0,1,1,0,1,1,0,1,1,0,1,1,0,1,1,0,1,1,0,1,1,0,1,1,0,1>
2	<1,0,1,1,0,1,1,0,1,1,0,1,1,0,1,1,0,1,1,0,1,1,0,1,1,0,1,1,0,1,1,0>
3	<1,1,0,1,1,0,1,1,0,1,1,0,1,1,0,1,1,0,1,1,0,1,1,0,1,1,0,1,1,0,1,1>

2.5 Relevant Research

The research provided in this thesis attempts to broaden the view of works such as [1, 2]. In [1], Evers and Jackson emphasize the LTE CSRS in an analysis of its ambiguity function. The work presented here differs from [1] in that variations of waveform content, structure, and parameters are applied to determine image domain impacts. Further, simulations in this work preserve all data inherent to LTE in order to arrive at general conclusions regarding the root cause of imaging domain effects.

Taylor, in [2], aims at characterizing LTE effects on space-time adaptive processing for passive bistatic radar ground moving target indication (GMTI). In many ways, [2] is the GMTI flavor of the work presented here being that modulation scheme and bandwidth variations are examined. However, [2] does not consider pulse-lengths longer than one symbol.

In addition to the works of Evers, Jackon, and Taylor, significant portions of this research utilized [7, 9] for radar fundamentals and [10] for LTE information.

2.6 Assumptions

Several assumptions are made regarding the experimental setup to represent a SAR system. An aperture of 1 degree is established with pulses being transmitted and received every $\delta\phi$ of 0.01 degrees under a move-stop-move assumption. That is to say that at each system azimuth location, a pulse is transmitted, received, and processed before moving to the next azimuth location in the aperture. A constant elevation angle of 30 degrees using far-field assumptions applied to imaging algorithms. The system is monostatic in nature allowing for the ideal matched filtering of the transmitted waveform with the scene response as described in Equation (2). Cell identity is assumed to remain unchanged pulse-to-pulse in accordance with the use of a single cell as a reference in the real world. Though it was discussed in Section 2.4 that

variations in parameters of interest typically occur on a multi-frame basis, variation of the parameters will occur pulse-to-pulse to observe effects of a more dynamic waveform. Further assumptions are made dependent upon variations being observed and will be discussed in the relevant sections of Chapter III and Chapter IV. It should be noted that all pulse-lengths presented in this work produce range profiles extending no less than about 50 km. While much shorter pulse lengths are typical of radar systems, the intention of this research is to establish basic effects of LTE as a radar waveform with the potential to enable selection of desirable attributes of the signal for shorter pulse duration in practical systems. The scene size for the PSF generated in each case explored here is significantly smaller than even the shortest range profile. With this in mind, expected sidelobes due to CP matching are expected to be well outside the scenes presented here but should be considered if using a live waveform.

III. Basic LTE Variation Effects

3.1 Chapter Overview

This section outlines the overarching methodology for Long-Term Evolution (LTE) waveform generation and steps through basic variation schemes to establish imaging effects rooted in fundamental waveform channel and structure diversity. A point-spread function (PSF) and range profile ensemble for each variation type are generated and analyzed using the image quality metrics outlined in Chapter II.

3.2 Waveform Generation

As discussed in Section 2.4, the LTE waveform is the result of several parameters. Similarly to [2], generating a LTE signal is made easier through the use of the MATLAB™ LTE Toolbox. The toolbox generates LTE signals subframe by subframe. An Evolved Node B (eNB) structure is defined to establish waveform parameters and passed to a downlink (DL) creation tool, along with a defined data stream, to produce the LTE waveform, resource grid, and secondary structure containing additional waveform information. The eNB parameters may be adjusted manually or a preset structure, selected from Table 3, may be employed.

This research explores the synthetic aperture radar (SAR) imaging effects created by variation in the LTE reference waveform over time. These parameter changes may be simulated to randomly vary or remain constant throughout an aperture. Variation of signal parameters occurs pulse to pulse for frame-, subframe-, slot-, and symbol-length pulses. For frame- and subframe-length pulses, variations are introduced directly through the main eNB structure passed to the LTE toolbox. In order to apply variations to slot- and symbol-length pulses, multiple instances of the current subframe are generated and the applicable slot or symbol extracted.

Table 3: All preset options offered by the MATLAB™ LTE toolbox along with their key parameters.

Preset Option	Key Parameters
R.0	(Port0, 1 RB, 16QAM, CellRefP=1, R=1/2)
R.1	(Port0, 1 RB, 16QAM, CellRefP=1, R=1/2)
R.2	(Port0, 50 RB, QPSK, CellRefP=1, R=1/3)
R.3	(Port0, 50 RB, 16QAM, CellRefP=1, R=1/2)
R.4	(Port0, 6 RB, QPSK, CellRefP=1, R=1/3)
R.5	(Port0, 15 RB, 64QAM, CellRefP=1, R=3/4)
R.6	(Port0, 25 RB, 64QAM, CellRefP=1, R=3/4)
R.7	(Port0, 50 RB, 64QAM, CellRefP=1, R=3/4)
R.8	(Port0, 75 RB, 64QAM, CellRefP=1, R=3/4)
R.9	(Port0, 100 RB, 64QAM, CellRefP=1, R=3/4)
R.10	(TxDiversity—SpatialMux, 50 RB, QPSK, CellRefP=2, R=1/3)
R.11	(TxDiversity—SpatialMux—CDD, 50 RB, 16QAM, CellRefP=2, R=1/2)
R.12	(TxDiversity, 6 RB, QPSK, CellRefP=4, R=1/3)
R.13	(SpatialMux, 50 RB, QPSK, CellRefP=4, R=1/3)
R.14	(SpatialMux—CDD, 50 RB, 16QAM, CellRefP=4, R=1/2)
R.25	(Port5, 50 RB, QPSK, CellRefP=1, R=1/3)
R.26	(Port5, 50 RB, 16QAM, CellRefP=1, R=1/2)
R.27	(Port5, 50 RB, 64QAM, CellRefP=1, R=3/4)
R.28	(Port5, 1 RB, 16QAM, CellRefP=1, R=1/2)
R.31-3A FDD	(CDD, 50 RB, 64QAM, CellRefP=2, R=0.85-0.90)
R.31-3A TDD	(CDD, 68 RB, 64QAM, CellRefP=2, R=0.87-0.90)
R.31-4	(CDD, 100 RB, 64QAM, CellRefP=2, R=0.87-0.90)
R.43 FDD	(Port7-14, 50 RB, QPSK, CellRefP=2, R=1/3)
R.43 TDD	(SpatialMux, 100 RB, 16QAM, CellRefP=4, R=1/2)
R.44 FDD	(Port7-14, 50 RB, QPSK, CellRefP=2, R=1/3)
R.44 TDD	(Port7-14, 50 RB, 64QAM, CellRefP=2, R=1/2)
R.45	(Port7-14, 50 RB, 16QAM, CellRefP=2, R=1/2)
R.45-1	(Port7-14, 39 RB, 16QAM, CellRefP=2, R=1/2)
R.48	(Port7-14, 50 RB, QPSK, CellRefP=2, R=1/2)
R.50 FDD	(Port7-14, 50 RB, 64QAM, CellRefP=2, R=1/2)
R.50 TDD	(Port7-14, 50 RB, QPSK, CellRefP=2, R=1/3)
R.51	(Port7-14, 50 RB, 16QAM, CellRefP=2, R=1/2)
R.6-27RB	(Port0, 27 RB, 64QAM, CellRefP=1, R=3/4)
R.12-9RB	(TxDiversity, 9 RB, QPSK, CellRefP=4, R=1/3)
R.11-45RB	(CDD, 45 RB, 16QAM, CellRefP=2, R=1/2)

Throughout the basic variations explored here, an aperture of 1 degree is utilized with pulses being transmitted and received every $\delta\phi$ of 0.01 degrees. Platform range from scene center is assumed to be 10,000 m while elevation angle is maintained at 30 degrees above the horizon. The test environment is depicted in Figure 2. For each pulse-length, waveform eNB parameters of interest are set as outlined in Table 4. It

should be noted that while the bandwidth mode is set to be 20 MHz, the effective bandwidth is 18 MHz due to guard bands on either end of the waveform spectrum. Given these fixed parameters, Equations (8) and (9) are utilized to determine an expected δR of 9.6 meters and $\delta R_{\otimes}$ between 13.1 and 13.4 meters for all pulse-lengths.

An example resource grid is shown in Figure 10. When using wider bandwidths, more resource block (RB) are allocated to the grid in accordance with Table 1 and as shown in Figure 11. In both Figures 10 and 11 there is a distinct inactive zone in subframe 5 (zero-base indexed). Within this subframe, the primary synchronization signal (PSS), secondary synchronization signal (SSS), and cell-specific reference signal (CSRS) are evident centered around the carrier frequency. While not obvious in these examples, the PSS and SSS are also contained in Subframe 0 while the CSRS populates specific elements throughout the entire resource grid. These signals are repeated in the same locations frame to frame regardless of signal bandwidth, cyclic prefix (CP), modulation type, or number of control symbols.

Table 4: Parameters established to key eNB variables for basic waveform variations.

Bandwidth Mode (MHz)	20
Center Frequency (MHz)	750
PDSCH Modulation	QPSK
CP Length	Extended
Control Channels	1

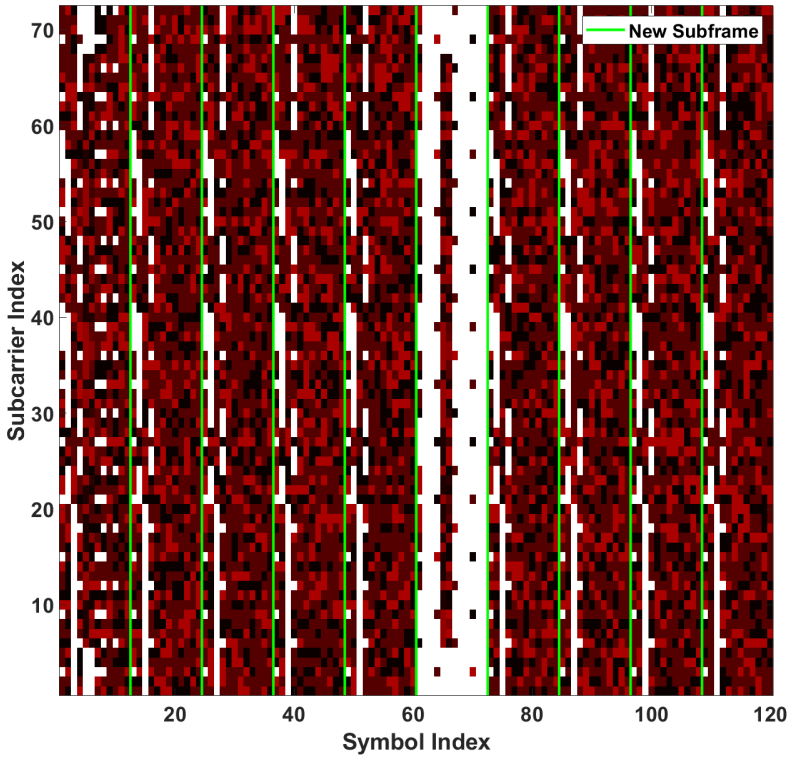

Figure 10: The resource grid for a 1.4 MHz bandwidth-mode LTE waveform with extended CP. Areas in white represent inactive resource elements while all other colors are indicative of complex values assigned to that resource element. Green lines extending across all subcarriers indicate the start of a new subframe.

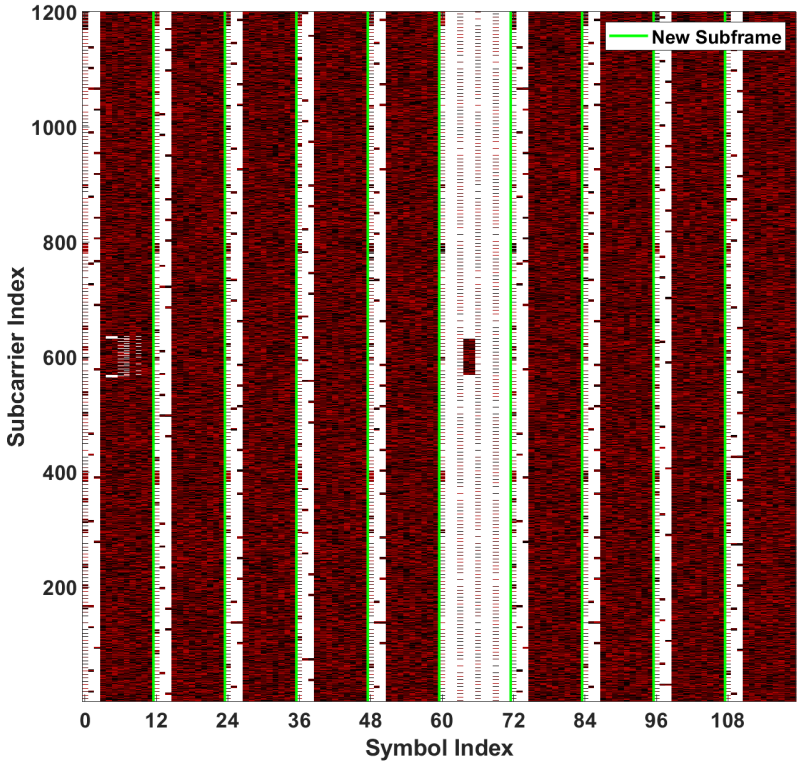

Figure 11: The resource grid for a 20 MHz bandwidth-mode LTE waveform with extended CP. Areas in white represent inactive resource elements while all other colors are indicative of complex values assigned to that resource element. Green lines extending across all subcarriers indicate the start of a new subframe.

3.3 Fixed User Data Effects

To start exploration into LTE effects, a pre-determined and unchanging segment of the framework is chosen and used for each pulse in the aperture.

3.3.1 Methodology and Assumptions

As much as possible, the section of waveform used for each pulse-length contains user data. For a frame-length pulse, the entire framework is utilized. For subframe-, slot-, and symbol-length pulses, Table 5 outlines the framework segments utilized. Example resource grids and time-domain waveforms for these segments are shown in Figures 12 and 13, respectively. It is expected that maximizing physical downlink shared channel (PDSCH) user data in the reference waveform should result in a PSF with lower sidelobe levels due to the random nature of the PDSCH signal. Frame- and subframe-length pulses contain a greater degree of LTE cell and synchronization information. Though the duration of frame- and subframe-length pulses is expected to reduce variation in the PSF by way of being mostly PDSCH user data, the cell and synchronization information contained in the waveform could result in the appearance of significant sidelobes.

In this section, every pulse in the aperture at each pulse-length is identical and unchanging. For shorter pulse-lengths, no progression through the LTE framework occurs. The purpose of this simulation is to establish a baseline for performance utilizing a known, repeating waveform. The PSF of each pulse-length is normalized to its own maximum.

Table 5: Subframe, slot, and symbol indices for each pulse length used. All indices are zero-based. Frame-wide symbol indexing enumerates symbols in the frame from 0 through 119 for extended CP. The frame-wide indexing may be used to locate associated pulse length segments in graphical depictions like that in Figure 12.

Pulse Length	$k_{Subframe}$	k_{Slot}	k_{Symbol}	Frame-Wide Symbol Index
Frame	N/a	N/a	N/a	0 - 119
Subframe	1	N/a	N/a	12 - 23
Slot	1	1	N/a	18 - 23
Symbol	1	1	1	19

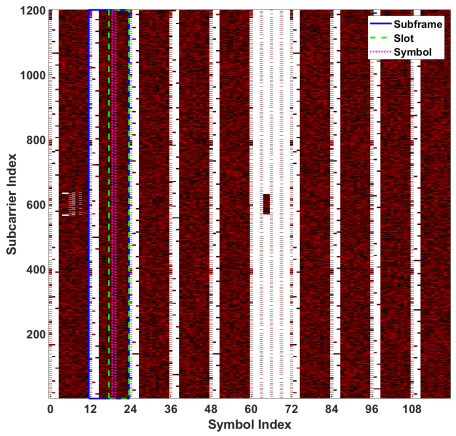

(a) Frame-length pulse

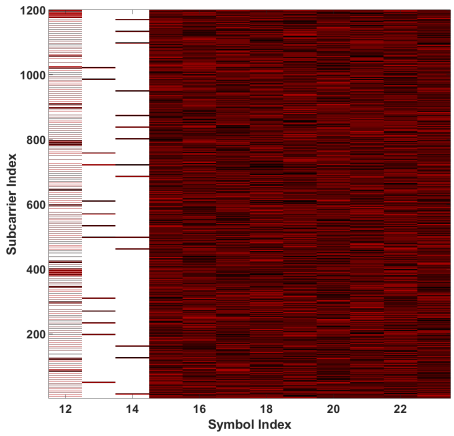

(b) Subframe-length pulse

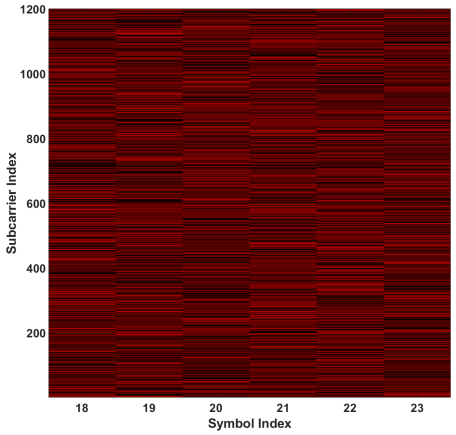

(c) Slot-length pulse

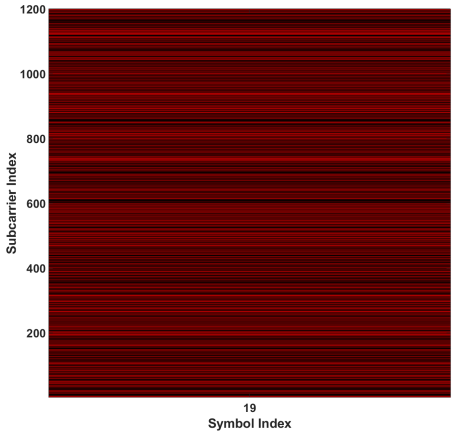

(d) Symbol-length pulse

Figure 12: Example resource grids for each pulse length. The resources allocated to a frame-length pulse are shown in (a) along with the location of other, shorter pulse-length resources within the frame. (b), (c), and (d) enlarge the corresponding areas of the overall framework and depict examples of resources allocated for the given pulse length.

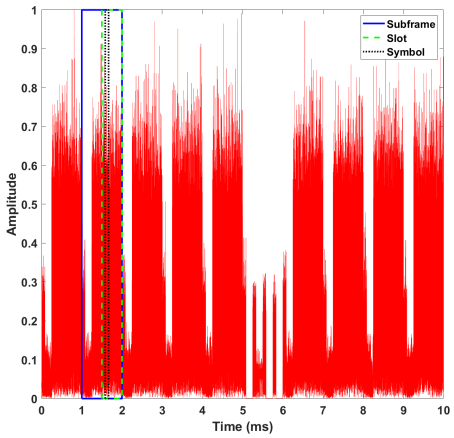

(a) Frame-length pulse

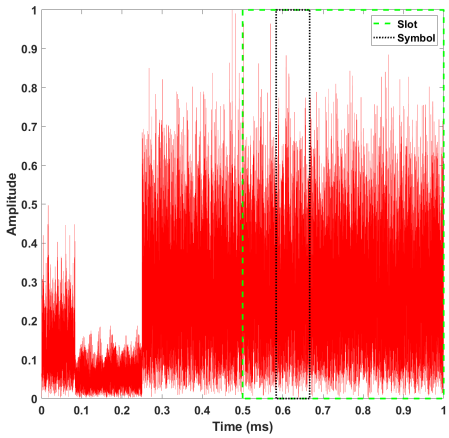

(b) Subframe-length pulse

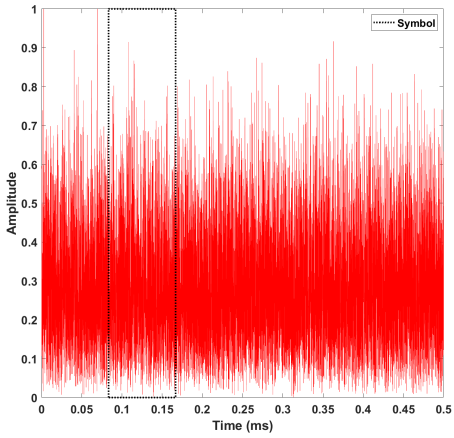

(c) Slot-length pulse

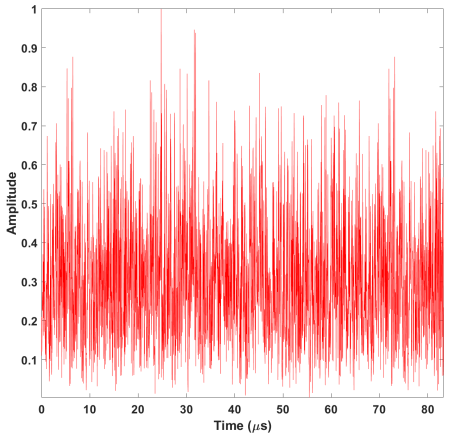

(d) Symbol-length pulse

Figure 13: Example waveforms for each pulse length derived from Figure 12. A frame-length pulse is shown in (a) along with the location of other, shorter pulse-lengths within the frame. (b), (c), and (d) enlarge the corresponding areas of the frame-length pulse.

3.3.2 Results

3.3.2.1 Frame

In this section, each pulse consists of one LTE frame, see Figures 12a and 13a, which is 10 ms in length. Because the pulse is a full LTE frame, all cell and user data channels, see Section 2.4.3, are contained in every pulse. Referencing Figure 14a, the PSF yields δR of 9.6 meters and $\delta R_{\otimes}$ of 13.2 meters. The peak sidelobe ratio (PSLR) and integrated sidelobe ratio (ISLR) resulting from Figure 14b are -6.68 dB and 9.27 dB, respectively.

It is evident that prominent sidelobes exists near the range profile mainlobe. The most prominent sidelobes, as expected, are due to the aligning of orthogonal frequency-division multiplexing (OFDM) symbol[1] CP with the associated piece of symbol. These two sidelobes occur about 20 km — the range-duration of one OFDM symbol not including CP length — away from the peak of the mainlobe. Overall, these sidelobes contribute negligibly to the PSF due to their distance from scene center. Looking at the range profile more closely to the mainlobe in Figure 14c, smaller sidelobes are evident. These smaller sidelobes indicate potential structural content matching between the CP and other sections of the corresponding OFDM symbols in the waveform. These distinct supplementary sidelobes occur at 3.3, 6.6, and 9.9 km. Due to the various resources allocated to a frame-length pulse, it is difficult to determine what may cause sidelobes closer to the mainlobe than those caused by CP matching.

[1]The CP-generated sidelobes occur at a distance of one OFDM symbol without its associated CP. This results in a sidelobe distance of about 20 km rather than the nearly 25 km range implied by the length of a symbol when including its CP

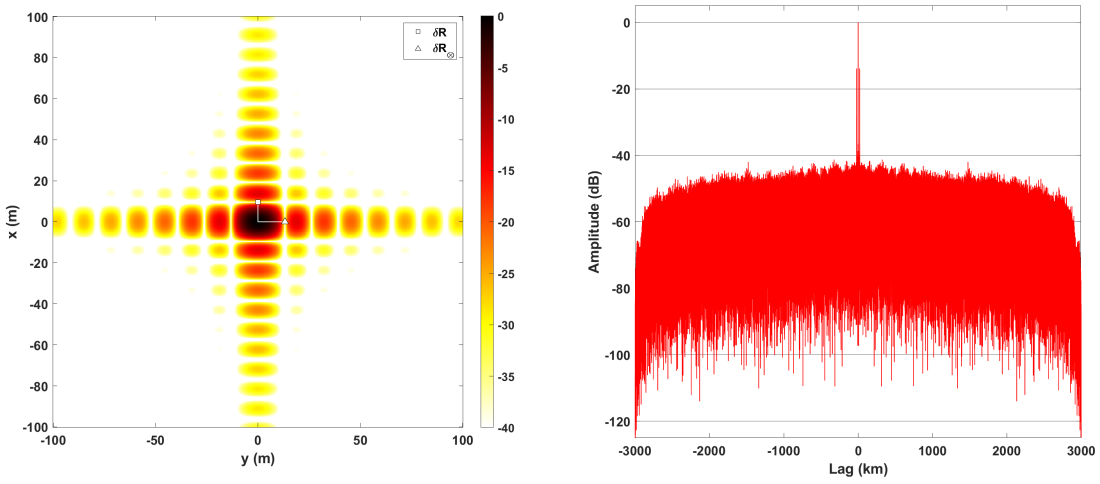

(a) PSF

(b) Range Profile

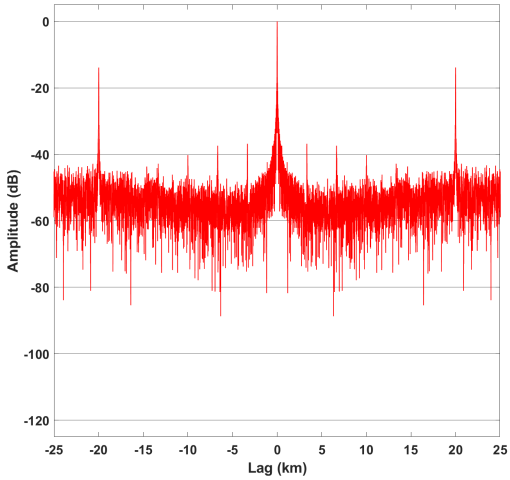

(c) Magnified Range Profile

Figure 14: Resulting PSF and range profile utilizing identical, repeating, frame-length pulses. Range profile yields a PSLR of -6.68 dB and a ISLR of 9.27 dB.

3.3.2.2 Subframe

In this section, each pulse consists of one LTE subframe, see Figures 12b and 13b, which is 1 ms in length. Subframe 1 is selected for this simulation. This subframe is selected to eliminate effects of PSS, SSS, and physical broadcasting channel (PBCH) data and maximize user data in the waveform. Data contained in the waveform includes CSRS, physical control format indicator channel (PCFICH), physical downlink control channel (PDCCH), physical hybrid ARQ indicator CH (PHICH), and PDSCH. The PCFICH, PDCCH, and PHICH are contained in the first three OFDM symbols of the subframe. The remaining nine symbols are made up primarily of PDSCH user data. CSRS elements are spaced across the bandwidth in four of the 12 OFDM symbols contained in the subframe. Referencing Figure 15a, the PSF yields δR of 9.6 meters and $\delta R_{\otimes}$ of 13.2 meters. The PSLR and ISLR resulting from Figure 15b are -6.63 dB and 13.65 dB, respectively.

The PSF using identical, subframe-length pulses over the aperture is virtually indistinguishable from that of identical, frame-length pulses. Much like the frame-length pulse, the most prominent sidelobes in the range profile are a result of CP matching and are inconsequential to the PSF. Looking within the range of the CP sidelobes, there is a supplementary sidelobe evident at 3.3 km. Also like the frame-length pulse case, determining the root cause of these subordinate sidelobes is troublesome due to the number of resources allocated to a subframe.

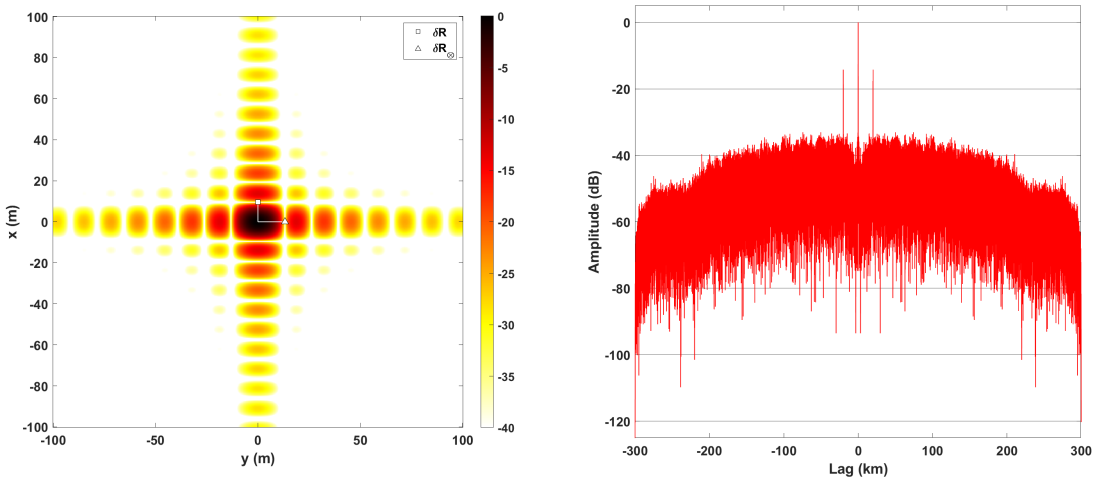

(a) PSF

(b) Range Profile

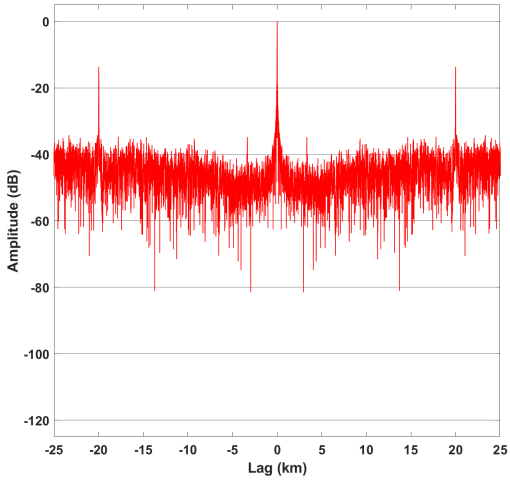

(c) Magnified Range Profile

Figure 15: Resulting PSF and range profile utilizing identical, repeating, subframe-length pulses. Range profile yields a PSLR of -6.63 dB and a ISLR of 13.65 dB.

3.3.2.3 Slot

In this section, each pulse consists of one LTE slot, see Figures 12c and 13c, which is 0.5 ms in length. Slot 1 of subframe 1 is selected for this simulation. Use of this specific slot further reduces the number of channels within the time-domain waveform, eliminating effects of PCFICH, PDCCH, and PHICH. The slot is made up primarily of PDSCH user data with CSRS elements spaced across the bandwidth in the first and fifth symbols. Referencing Figure 16a, the PSF yields δR of 9.6 meters and $\delta R_{\otimes}$ of 13.2 meters. The PSLR and ISLR resulting from Figure 16b are -6.53 dB and 13.97 dB, respectively.

Again, the resulting PSF is identical to that produced using frame-length pulses. The lack of alteration to the PSF is due to the bandwidth and aperture characteristics of the pulses. Because the pulses from case to case only differ in their length and data content, the overarching effects of bandwidth and aperture sampling dominate in the PSF outcomes. There are no notable sidelobes other than those resulting from CP matching. Lack of sidelobes closer to the mainlobe is an indication that subsidiary sidelobes using longer pulse-lengths are likely an effect of PCFICH, PDCCH, and/or PHICH data.

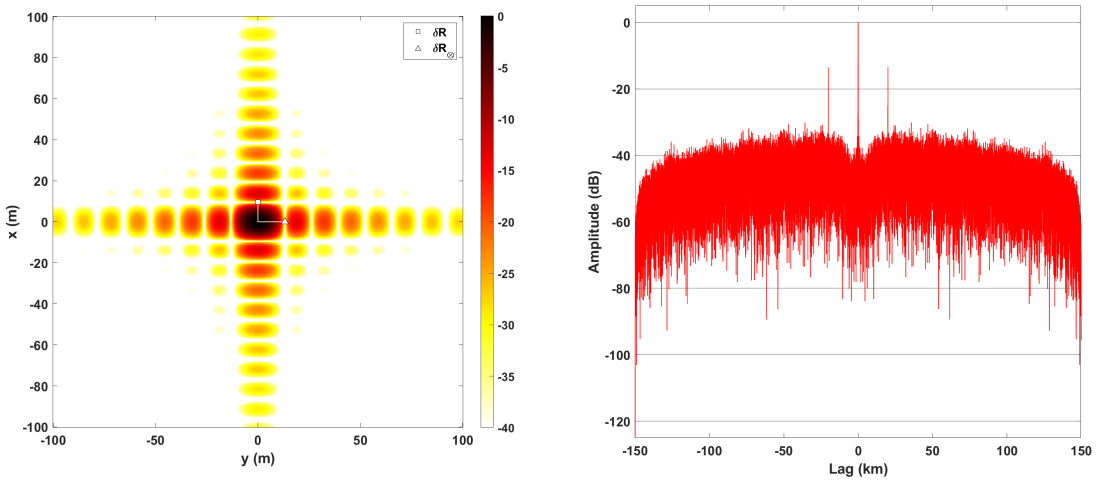

(a) PSF

(b) Range Profile

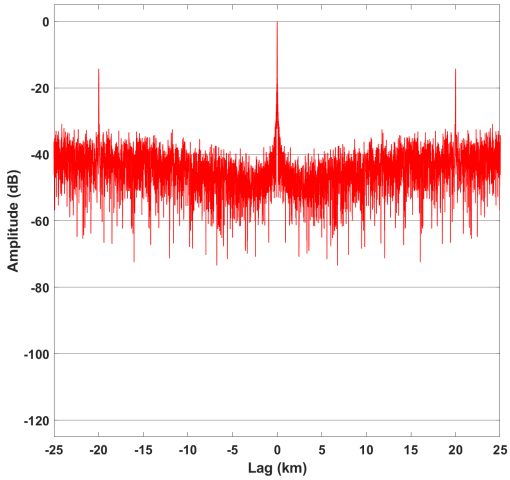

(c) Magnified Range Profile

Figure 16: Resulting PSF and range profile utilizing identical, repeating, slot-length pulses. Range profile yields a PSLR of -6.53 dB and a ISLR of 13.97 dB.

3.3.2.4 Symbol

In this section, a 83.3 μs-length pulse consisting of one OFDM symbol, see Figures 12d and 13d, including the CP is used. Symbol 1 of slot 1, subframe 1 is selected for this simulation. This particular symbol contains only PDSCH user data. Referencing Figure 17a, the PSF yields δR of 9.6 meters and $\delta R_{\otimes}$ of 13.2 meters. The PSLR and ISLR resulting from Figure 17b are -6.53 dB and 15.33 dB, respectively.

As discussed regarding slot-length pulses, the PSF for identical, symbol-length pulses is essentially unchanged due to bandwidth and aperture sampling effects. The only notable sidelobes in the symbol-length range profile are those created by CP matching, indicating that PDSCH sidelobe effects are negligible.

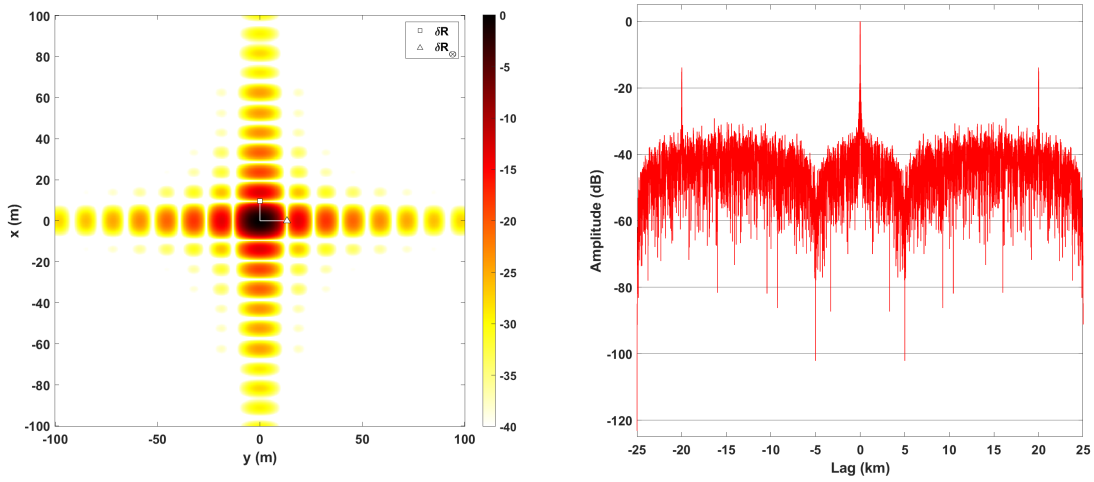

(a) PSF (b) Range Profile

Figure 17: Resulting PSF and range profile utilizing identical, repeating, symbol-length pulses. Range profile yields a PSLR of -6.53 dB and a ISLR of 15.33 dB.

3.4 Variable User Data Effects

Next, the PDSCH user data is varied while maintaining the use of specific locations in the LTE framework every pulse. Varying user data while maintaining a fixed location in the LTE framework provides information on whether PDSCH content affects the intra-symbol sidelobes[2] observed in Section 3.3.

3.4.1 Methodology and Assumptions

Similarly to the methodology for Section 3.3, the simulated waveforms contain as much user data as possible for the given pulse-length. These framework locations are identical to those in Section 3.3 for each pulse-length. The distinction here is that new, randomly generated PDSCH data is applied to the framework pulse to pulse. The PSF of each pulse-length is normalized to the maximum of the corresponding fixed-data pulse-length PSF from Section 3.3. It is expected that variation of PDSCH

[2]Intra-symbol sidelobes are those notable sidelobes observed in proximity to the mainlobe that are not beyond the primary sidelobes created by CP matching when filtering the return signal.

data will slightly reduce PSF while maintaining the overall response observed up to this point. Range profiles are expected to be much the same as they were for identical pulses with the caveat that some user data may result in better quality metrics than others.

3.4.2 Results

3.4.2.1 Frame

In this section, each pulse consists of one LTE frame, see Figures 12a and 13a, which is 10 ms in length. Because the pulse is a full LTE frame, all cell and user data channels, see Section 2.4.3, are contained in every pulse. The PDSCH resources are randomly generated for each new pulse. Referencing Figure 18a, the PSF yields δR of 9.6 meters and $\delta R_{\otimes}$ of 13.2 meters. The best-case PSLR and ISLR resulting from Figure 19 are -6.71 dB and 9.21 dB, respectively.

As expected, PSF response when varying PDSCH pulse to pulse is reduced slightly. In the case of frame-length pulses, the loss is 0.01 dB. Due to the effect of bandwidth and aperture sampling on the PSF, δR and $\delta R_{\otimes}$ are unchanged from Section 3.3.2.1. Looking more closely at one realization of the range profiles in Figure 18b, intra-symbol sidelobes are evident occurring every 3.3 km until the CP sidelobe occurs at about 20 km from scene center. The interval of 3.3 km corresponds to 1/6 the length of one symbol when excluding the CP length.

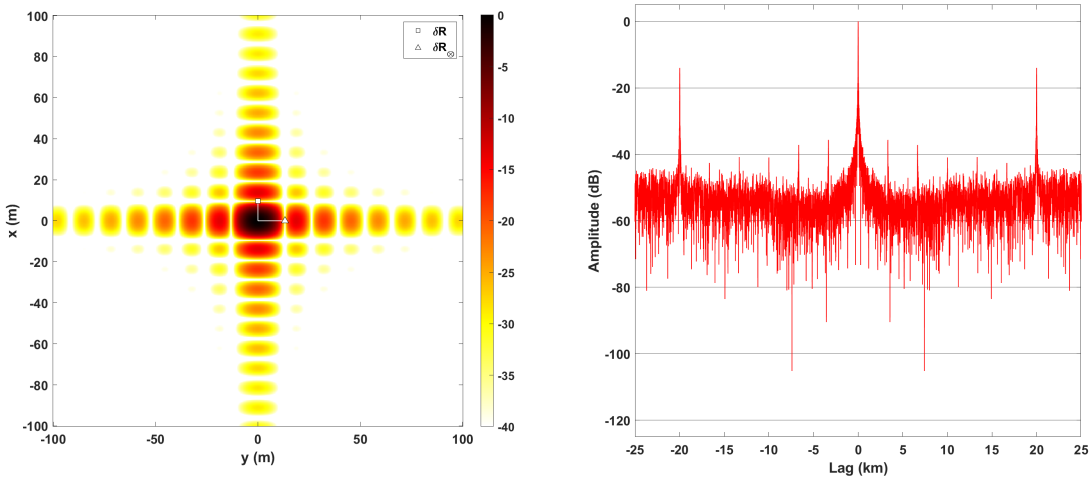

(a) PSF

(b) Magnified Range Profile

Figure 18: Resulting PSF and single range profile realization utilizing variable-data, frame-length pulses.

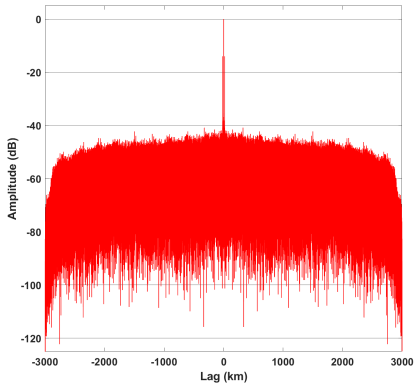

(a) Best Case, PSLR = -6.71 dB

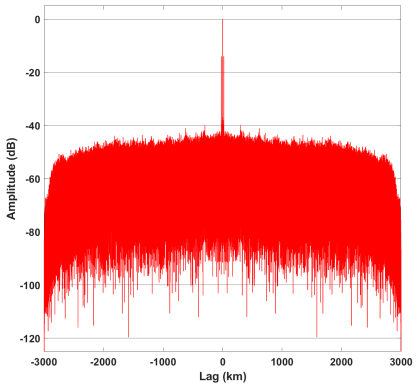

(b) Best Case, ISLR = 9.21 dB

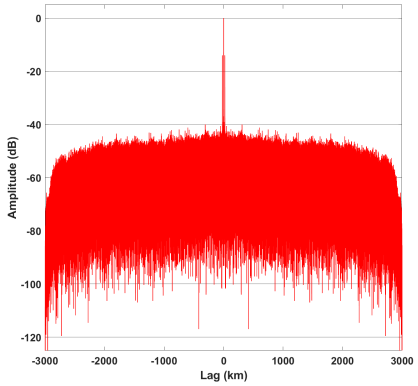

(c) Median Case, PSLR = -6.67 dB

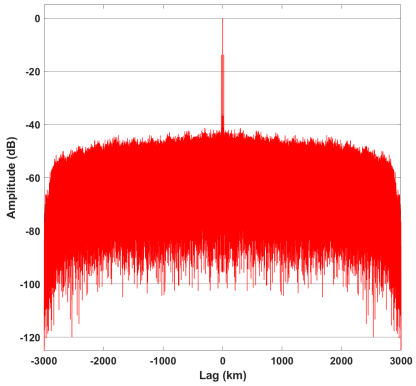

(d) Median Case, ISLR = 9.26 dB

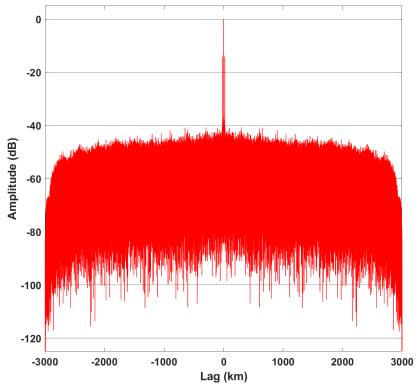

(e) Worst Case, PSLR = -6.64 dB

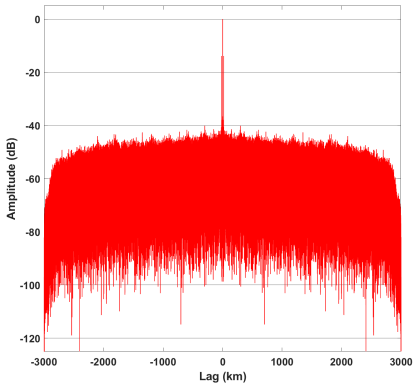

(f) Worst Case, ISLR = 9.29 dB

Figure 19: Range profiles for given cases of PSLR and ISLR utilizing variable-data, frame-length pulses over the aperture.

3.4.2.2 Subframe

In this section, each pulse consists of one LTE subframe, see Figures 12b and 13b, which is 1 ms in length. Subframe 1 is selected for this simulation in order to eliminate effects of PSS, SSS, and PBCH and maximize user data in the waveform. Data contained in the waveform includes CSRS, PCFICH, PDCCH, PHICH, and PDSCH. The PCFICH, PDCCH, and PHICH are contained in the first three OFDM symbols of the subframe. The remaining nine symbols are made up primarily of PDSCH user data. CSRS elements are spaced across the bandwidth in four of the 12 OFDM symbols contained in the subframe. Referencing Figure 20a, the PSF yields δR of 9.6 meters and $\delta R_{\otimes}$ of 13.2 meters. The best-case PSLR and ISLR resulting from Figure 21 are -6.78 dB and 13.58 dB, respectively.

PSF response is observed to incur a minor loss of 0.01 dB, but is otherwise unaffected by varying PDSCH. δR and $\delta R_{\otimes}$ remain consistent due to the unchanging structure of each pulse. Considering Figure 20b, notable intra-symbol sidelobe are evident at 3.3 km.

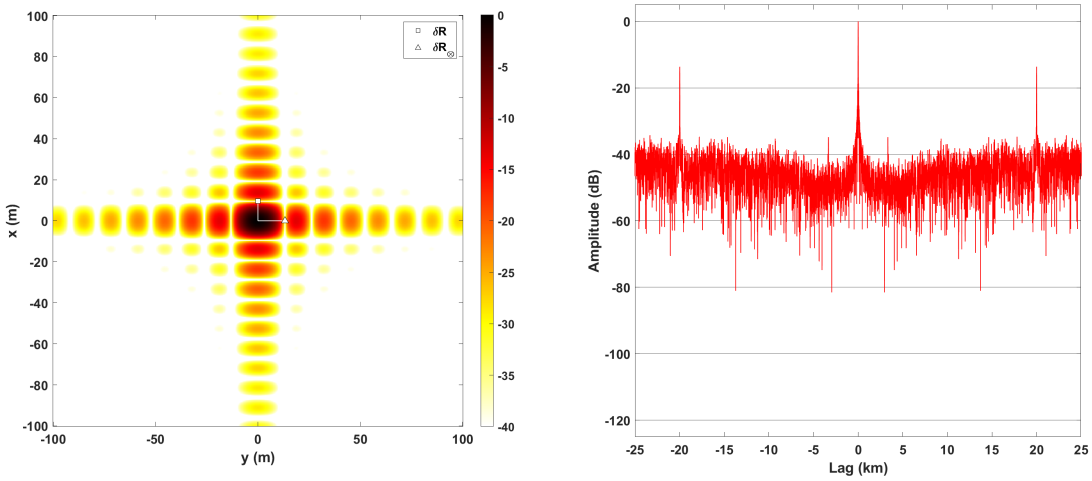

(a) PSF

(b) Magnified Range Profile

Figure 20: Resulting PSF and single range profile realization utilizing variable-data, subframe-length pulses.

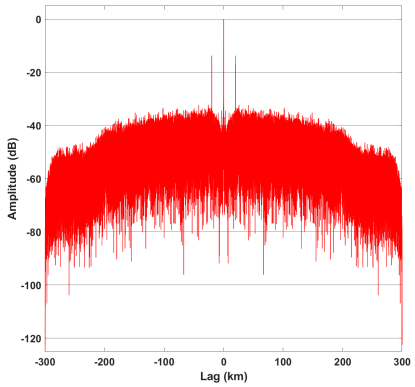

(a) Best Case, PSLR = -6.78 dB

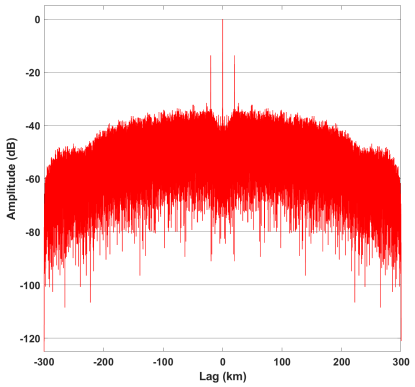

(b) Best Case, ISLR = 13.58 dB

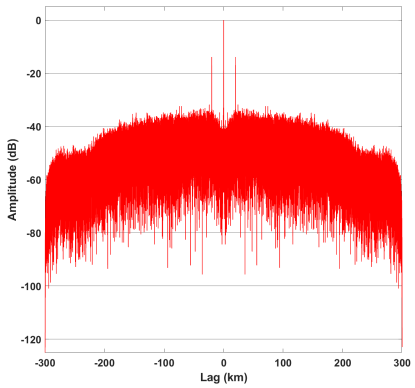

(c) Median Case, PSLR = -6.65 dB

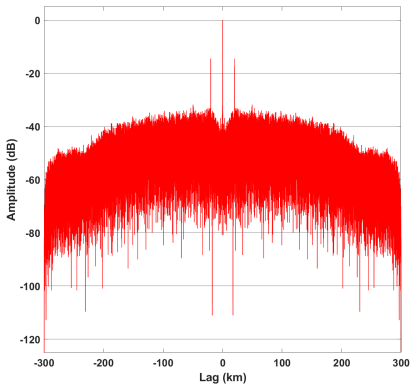

(d) Median Case, ISLR = 13.68 dB

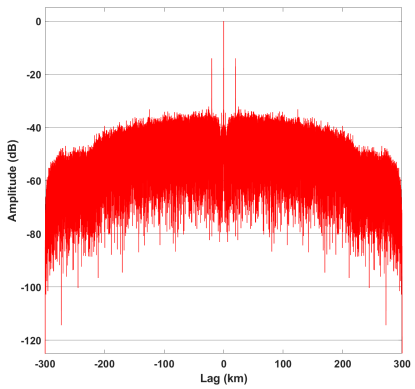

(e) Worst Case, PSLR = -6.54 dB

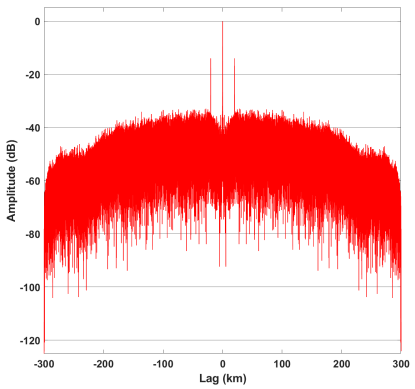

(f) Worst Case, ISLR = 13.78 dB

Figure 21: Range profiles for given cases of PSLR and ISLR utilizing variable-data, subframe-length pulses over the aperture.

3.4.2.3 Slot

In this section, each pulse consists of one LTE slot, see Figures 12c and 13c, which is 0.5 ms in length. Slot 1 of subframe 1 is selected for this simulation. Use of this specific slot further reduces the number of channels within the time-domain waveform, eliminating effects of PCFICH, PDCCH, and PHICH. The slot is made up primarily of PDSCH user data with CSRS elements spaced across the bandwidth in the first and fifth symbols. Referencing Figure 22a, the PSF yields δR of 9.6 meters and $\delta R_{\otimes}$ of 13.2 meters. The best-case PSLR and ISLR resulting from Figure 23 are -6.80 dB and 13.85 dB, respectively.

In the case of slot-length pulses, the PSF loss is slightly more at 0.02 dB. Ambiguities in range and cross-range are likewise virtually the same as for previous simulations. CP-generated sidelobes are the only noteworthy ambiguities in Figure 22b. The lack of intra-symbol sidelobes when varying user data further supports the notion that the channels contained within slot 1, subframe 1 inconsequentially affect the PSF.

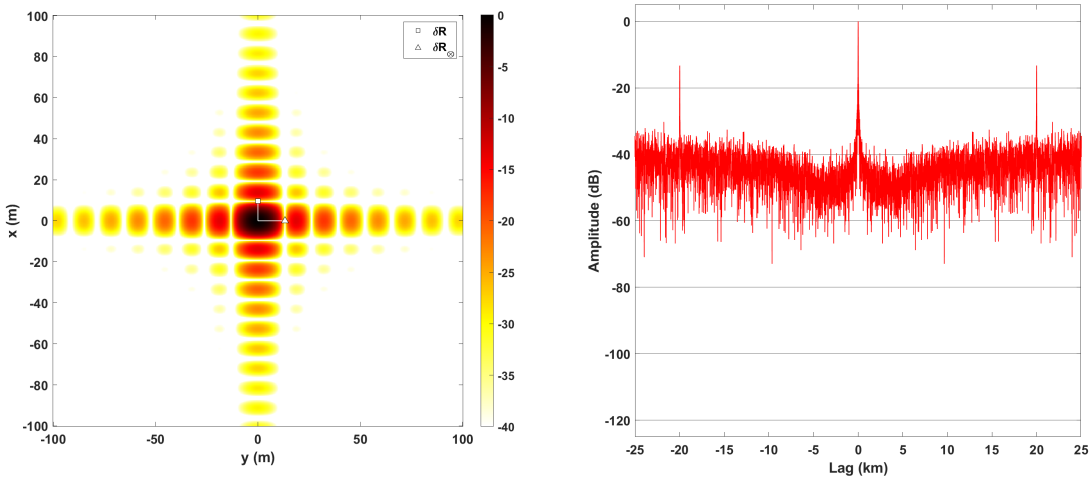

(a) PSF

(b) Magnified Range Profile

Figure 22: Resulting PSF and single range profile realization utilizing a variable-data, slot-length pulses.

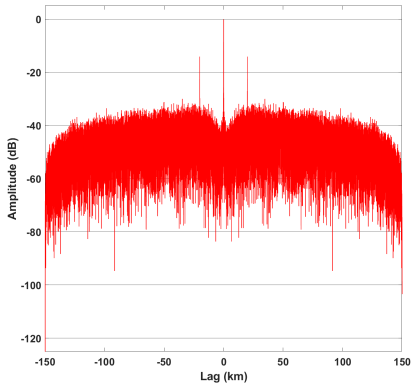

(a) Best Case, PSLR = -6.80 dB

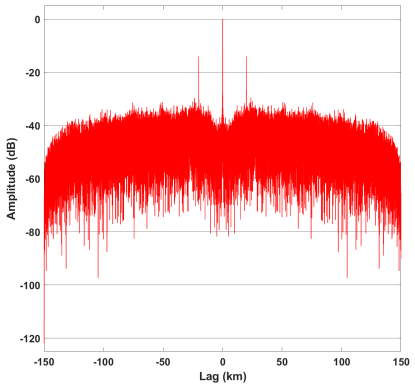

(b) Best Case, ISLR = 13.85 dB

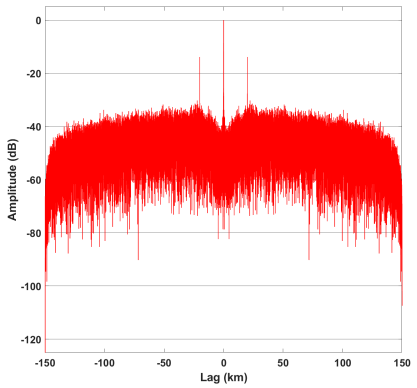

(c) Median Case, PSLR = -6.63 dB

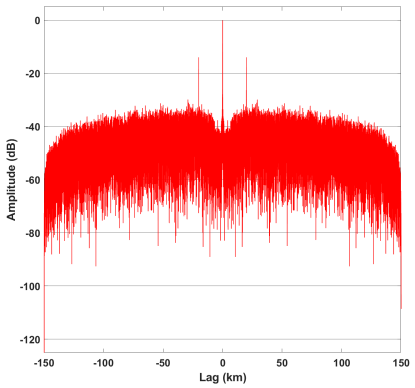

(d) Median Case, ISLR = 13.97 dB

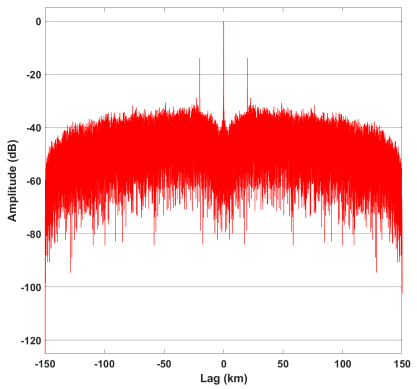

(e) Worst Case, PSLR = -6.49 dB

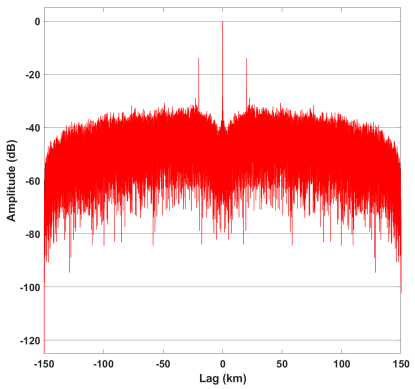

(f) Worst Case, ISLR = 14.41 dB

Figure 23: Range profiles for given cases of PSLR and ISLR utilizing variable-data, slot-length pulses over the aperture.

3.4.2.4 Symbol

In this section, each pulse consists of one OFDM symbol, see Figures 12d and 13d, which is 83.3 μs in length. Note that the symbol includes a CP. Symbol 1 of slot 1, subframe 1 is selected because it contains only user data. Referencing Figure 24, the PSF yields δR of 9.6 meters and $\delta R_{\otimes}$ of 13.2 meters. The best-case PSLR and ISLR resulting from Figure 25 are -7.00 dB and 15.21 dB, respectively.

Here a slightly more significant PSF loss is observed at 0.04 dB. Range profiles are markedly similar to those for fixed-data simulations, containing major sidelobes only where CP matching occurs at about 20 km.

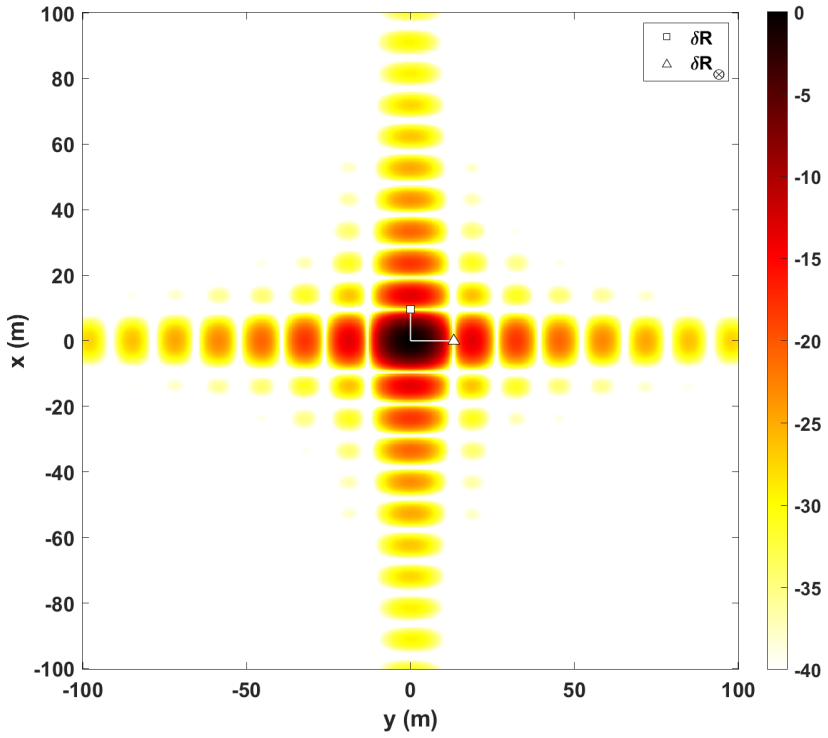

Figure 24: Resulting PSF utilizing a variable-data, symbol-length pulses.

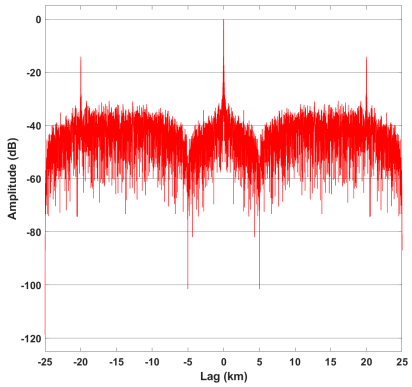

(a) Best Case, PSLR = -7.00 dB

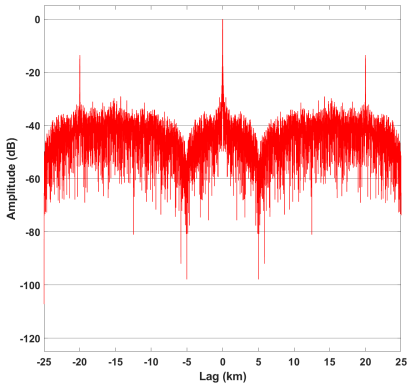

(b) Best Case, ISLR = 15.21 dB

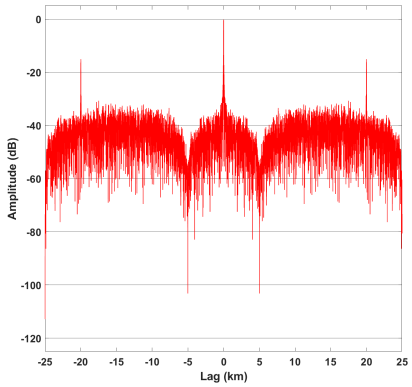

(c) Median Case, PSLR = -6.64 dB

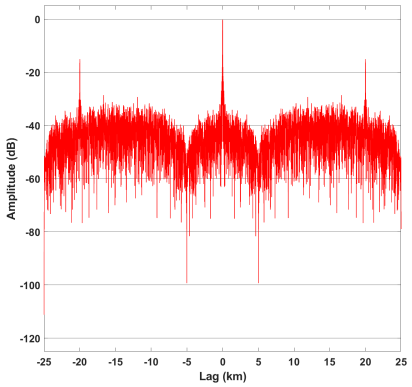

(d) Median Case, ISLR = 15.37 dB

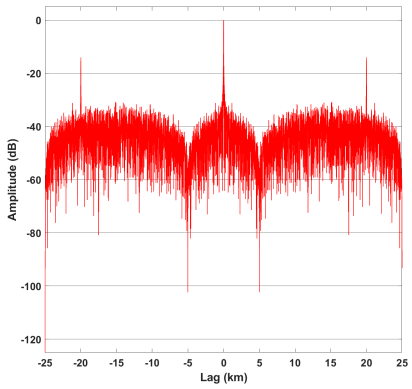

(e) Worst Case, PSLR = -6.33 dB

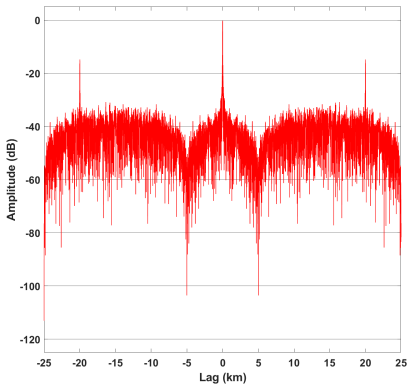

(f) Worst Case, ISLR = 16.05 dB

Figure 25: Range profiles for given cases of PSLR and ISLR utilizing variable-data, symbol-length pulses over the aperture.

3.5 Framework Progression Effects

A final basic variation considered here is the transition of pulses through the LTE framework while also generating new PDSCH user data pulse to pulse.

3.5.1 Methodology and Assumptions

Every frame-length waveform emitted is indexed and has the potential to contain new data on one or more non-PDSCH channels. As each new frame is indexed, so too are the subframes, slots, and symbols. Throughout this section, each new pulse will be generated from the next pulse-length structure in the LTE framework. User data is newly generated for every pulse as well. Novel image effects are expected, especially for shorter-duration pulses, due to potential for portions of the framework containing varying ratios of PDSCH data.

3.5.2 Results

3.5.2.1 Frame

In this section, each pulse consists of one LTE frame, see Figures 12a and 13a, which is 10 ms in length. Because the pulse is a full LTE frame, all cell and user data channels, see Section 2.4.3, are contained in every pulse. New PDSCH data is generated and the frame index iterated for each subsequent pulse. Iterative frame indexing introduces potential variation to CSRS, PDCCH, and PHICH channels as reference and control information change to meet network needs. Referencing Figure 26a, the PSF yields δR of 9.6 meters and $\delta R_{\otimes}$ of 13.2 meters. The best-case PSLR and ISLR resulting from Figure 27 are -6.71 dB and 9.23 dB, respectively.

While expected that the PSF would experience some loss, the PSF for progressive, frame-length pulses virtually matches that for fixed-data simulations. Likewise, range profiles are fairly consistent, resulting in tight image metrics, as seen in Figure 27.

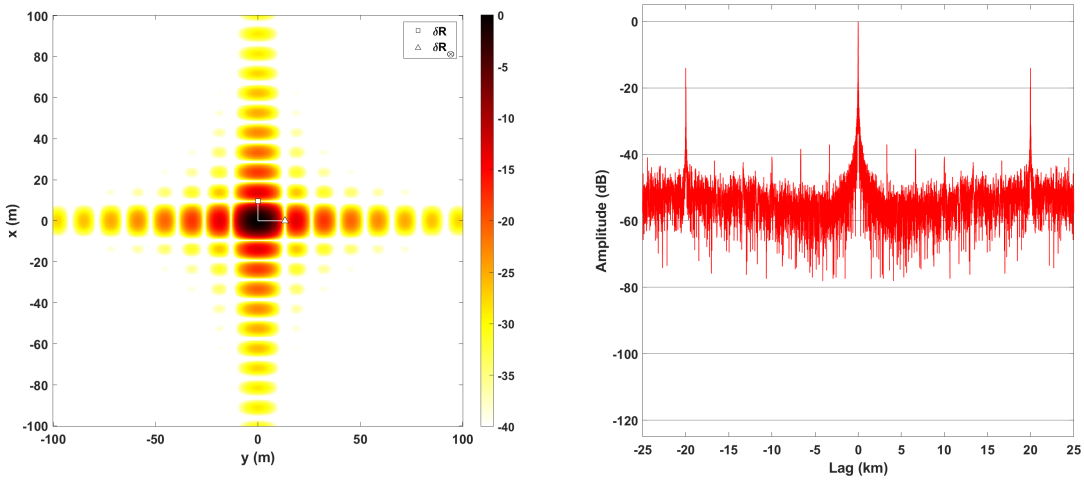

(a) PSF

(b) Magnified Range Profile

Figure 26: Resulting PSF and single range profile realization utilizing a progressive, variable-data, frame-length pulses.

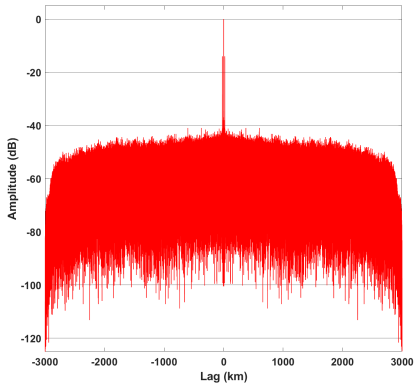

(a) Best Case, PSLR = -6.71 dB

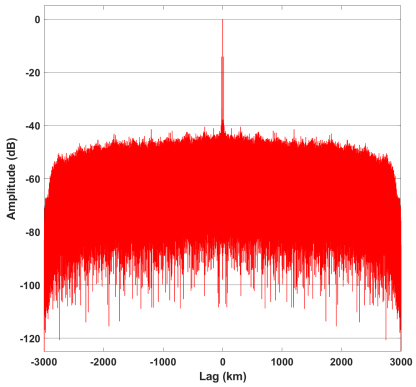

(b) Best Case, ISLR = 9.23 dB

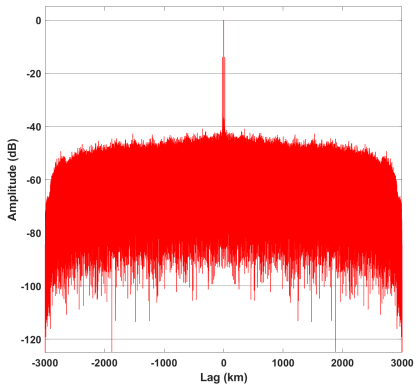

(c) Median Case, PSLR = -6.67 dB

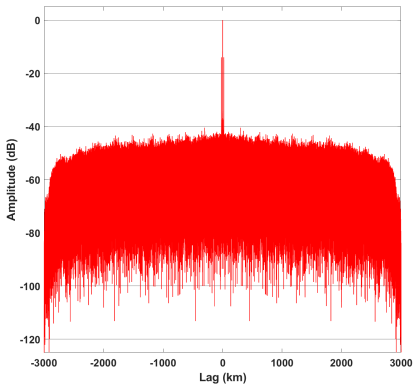

(d) Median Case, ISLR = 9.26 dB

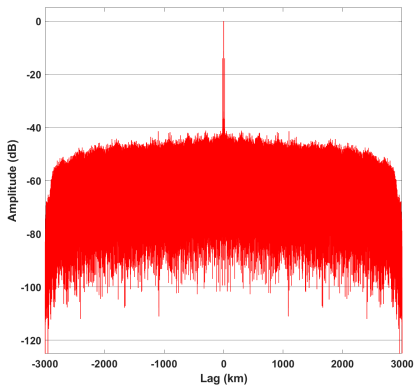

(e) Worst Case, PSLR = -6.64 dB

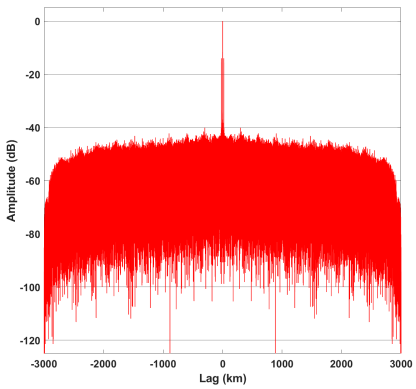

(f) Worst Case, ISLR = 9.29 dB

Figure 27: Range profiles for given cases of PSLR and ISLR utilizing LTE structure progressing, variable-data, frame-length pulses over the aperture.

3.5.2.2 Subframe

In this section, each pulse consists of one LTE subframe, see Figures 12b and 13b, which is 1 ms in length. New PDSCH data is generated and the subframe index iterated for each subsequent pulse. The frame index is likewise iterated when necessary to maintain proper framework progression of the waveform across the aperture. At minimum, any given pulse contains CSRS, PCFICH, PDCCH, PHICH, and PDSCH information. As the subframe index is iterated, some pulses will contain all cell and user data channels. Referencing Figure 28a, the PSF yields δR of 9.6 meters and $\delta R_{\otimes}$ of 13.2 meters. The best-case PSLR and ISLR resulting from Figure 29 are -6.77 dB and 13.60 dB, respectively.

PSF response is observed to incur a loss of 0.86 dB, but otherwise maintains a response shape consistent with previous configurations at the subframe level. While δR is unchanged, $\delta R_{\otimes}$ does worsen slightly. remain consistent due to the unchanging structure of each pulse. Considering Figure 28b, which depicts a range-magnified view of Figure 29e, two major intra-symbol sidelobes are evident at 6.6 km and 13.2 km. This particular range profile occurs on pulse 96 of 101, which corresponds to frame 9, subframe 5. Looking back to Figure 11, the subframe that generates this notable range profile does not contain any user data.

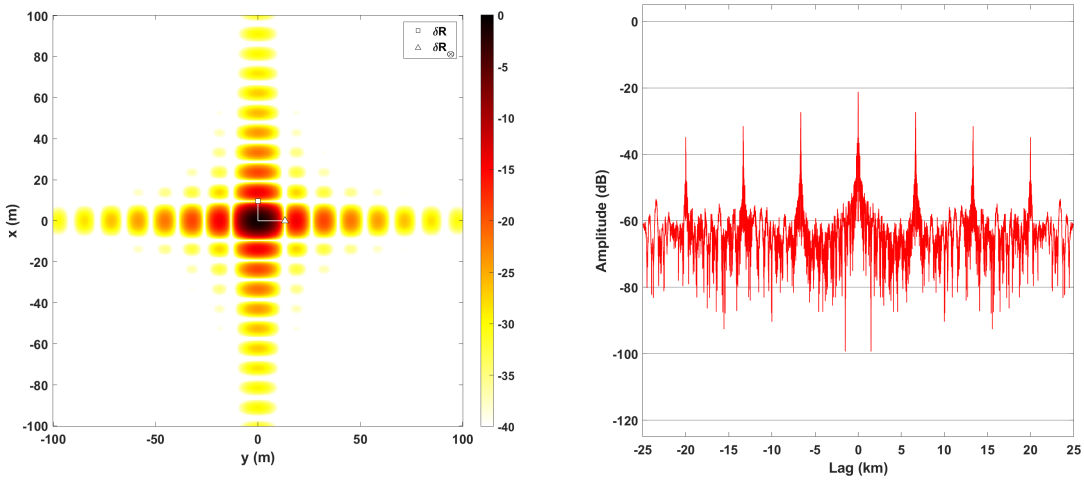

(a) PSF

(b) Magnified Range Profile

Figure 28: Resulting PSF and single range profile realization utilizing a progressive, variable-data, subframe-length pulses.

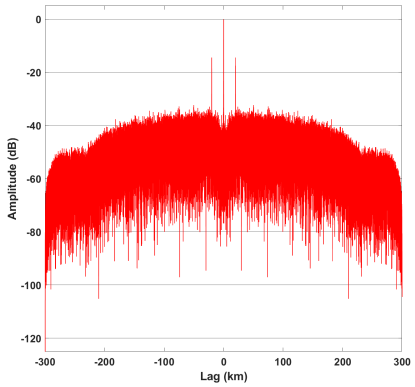

(a) Best Case, PSLR = -6.77 dB

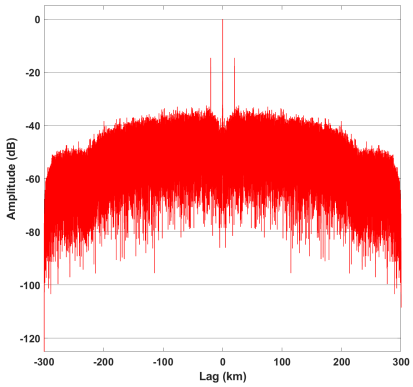

(b) Best Case, ISLR = 13.60 dB

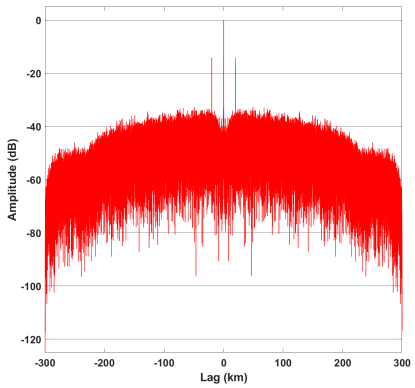

(c) Median Case, PSLR = -6.63 dB

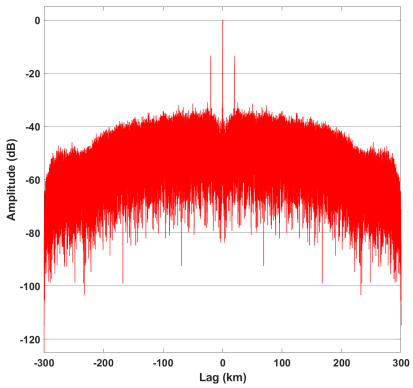

(d) Median Case, ISLR = 13.69 dB

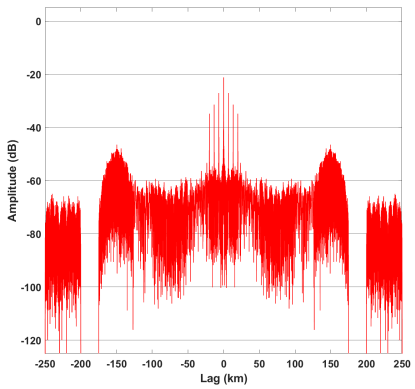

(e) Worst Case, PSLR = -2.93 dB

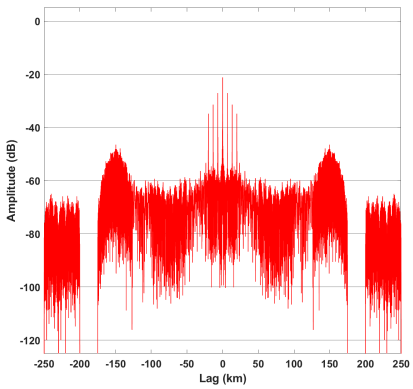

(f) Worst Case, ISLR = 24.44 dB

Figure 29: Range profiles for given cases of PSLR and ISLR utilizing LTE structure progressing, variable-data, subframe-length pulses over the aperture.

3.5.2.3 Slot

In this section, each pulse consists of one LTE slot, see Figures 12c and 13c, which is 0.5 ms in length. New PDSCH data is generated and the slot index iterated for each subsequent pulse. The frame and subframe indices are likewise iterated when necessary to maintain proper framework progression of the waveform across the aperture. At minimum, any give pulse contains CSRS information. As the slot index is iterated, pulses will contain several combinations of cell and/or user data channels. Referencing Figure 30a, the PSF yields δR of 9.6 meters and $\delta R_{\otimes}$ of 13.2 meters. The best-case PSLR and ISLR resulting from Figure 31 are -6.84 dB and 13.86 dB, respectively.

A loss of 3.09 dB is observed in the PSF when normalized against the PSF generated in Section 3.3.2.3. Cross-range ambiguities are also evident in Figure 30a at about 70 meters from scene center. These cross-range sidelobes are an effect of aperture pulse density. The inclusion of sparse-signal pulses that result in range profiles like those displayed in Figures 31e and 31f, effectively decrease the aperture's pulse density. Increasing the number of pulses in the aperture lessens the impact of sparse-signal pulses, thereby diminishing cross-range effects observed here. The range profiles referenced are generated from subframe 5 in each frame. The sparse nature of this specific subframe results in the near-null response observed in Figure 31e. It should be noted that these areas are not completely null and have a value approaching $-\infty$. The extremely low response is due to matching of the pulse in such a way that sections with no signal align to sections containing signal.

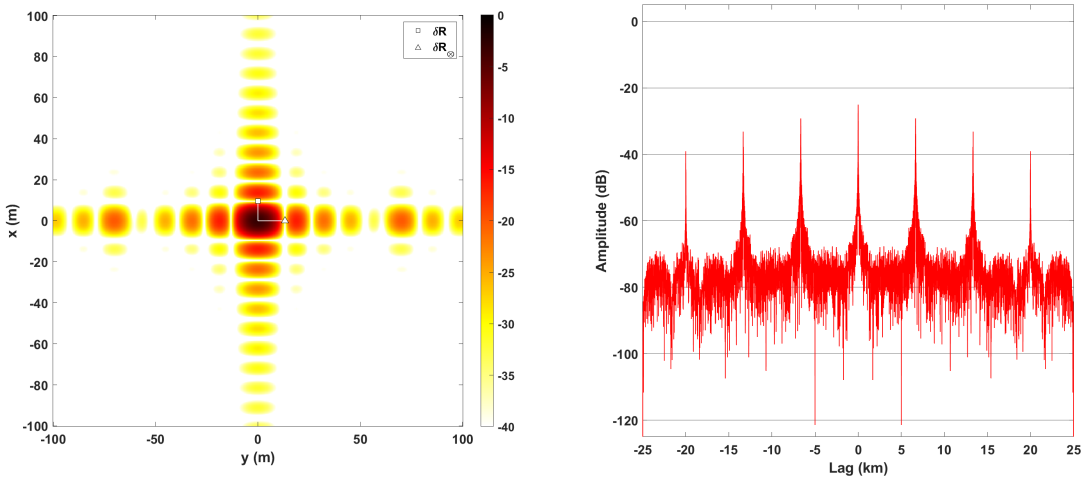

(a) PSF

(b) Magnified Range Profile

Figure 30: Resulting PSF and single range profile realization utilizing a progressive, variable-data, slot-length pulses.

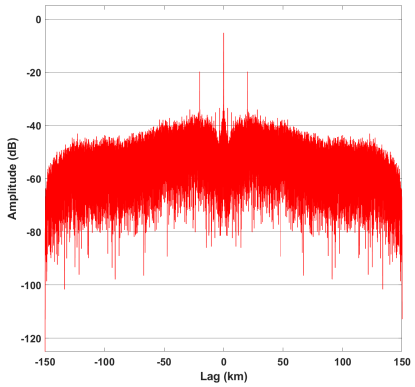

(a) Best Case, PSLR = -6.84 dB

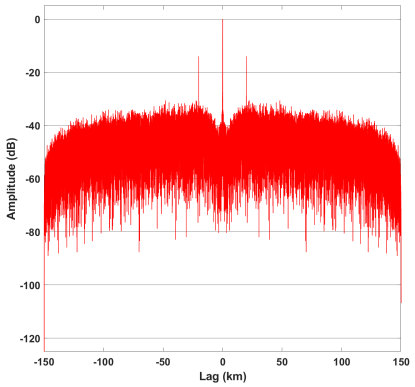

(b) Best Case, ISLR = 13.86 dB

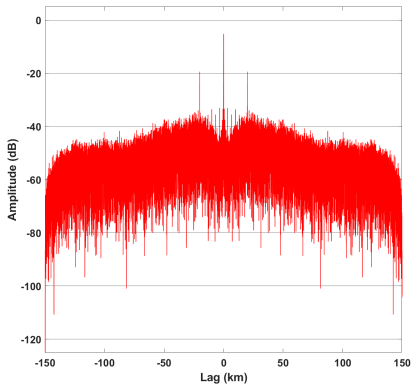

(c) Median Case, PSLR = -6.63 dB

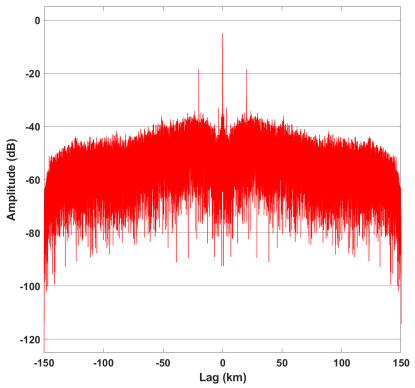

(d) Median Case, ISLR = 16.29 dB

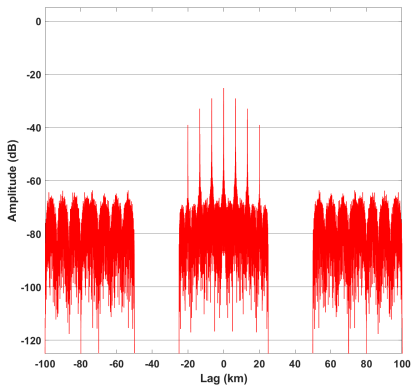

(e) Worst Case, PSLR = -1.96 dB

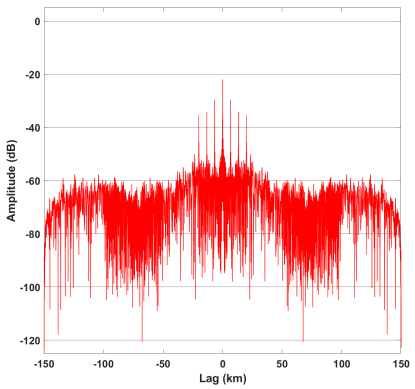

(f) Worst Case, ISLR = 25.53 dB

Figure 31: Range profiles for given cases of PSLR and ISLR utilizing LTE structure progressing, variable-data, slot-length pulses over the aperture.

3.5.2.4 Symbol

In this section, each pulse consists of one OFDM symbol, see Figures 12d and 13d, which is 83.3 μs in length. Note that the symbol includes a CP. New PDSCH data is generated and the symbol index iterated for each subsequent pulse. Frame, subframe, and slot indices are likewise iterated when necessary to maintain proper framework progression of the waveform across the aperture. At minimum, it is possible that a pulse will contain no signal whatsoever. This possibility only occurs at specific symbols within subframe 5 of each new frame. Otherwise, pulses may contain information from no less than one cell or user data channel. Referencing Figure 32, the PSF yields δR of 9.6 meters and $\delta R_{\otimes}$ of 12.4 meters. The best-case PSLR and ISLR resulting from Figure 33 are -6.90 dB and 15.18 dB, respectively.

Here a more significant PSF loss is observed at 3.42 dB. Range profiles are markedly similar to those for fixed- and varied-data simulations, containing major sidelobes only where CP matching occurs. For this particular method of waveform variation, the worst-case metric range profiles are completely flat as the corresponding pulses contain no signal. Notable cross-range effects are observed in the PSF resulting from the aperture pulse density, much like when using slot-length pulses. While $\delta R_{\otimes}$ appears to improve over expectations, the inconsistent sidelobes resulting from empty and sparse-signal pulses causes cross-range smearing and move the first cross-range minimum toward scene center. As more pulses are included in the aperture extent, $\delta R_{\otimes}$ degrades to expected bounds.. Significantly reduced response displayed in Figure 33a is an effect of empty symbol matching in slot 1, subframe 5.

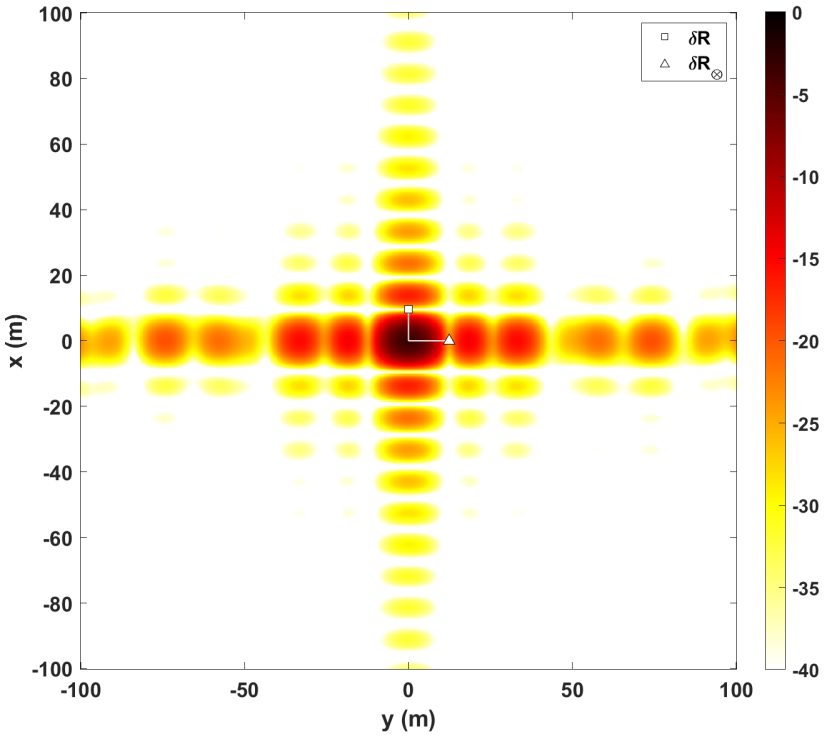

Figure 32: Resulting PSF utilizing a progressive, variable-data, symbol-length pulse.

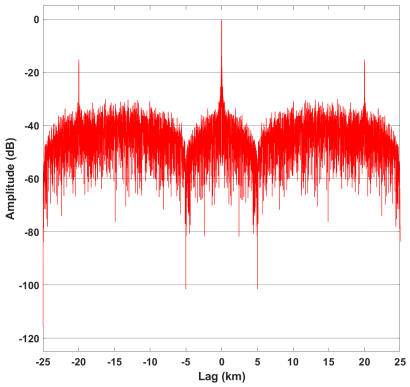

(a) Best Case, PSLR = -6.90 dB

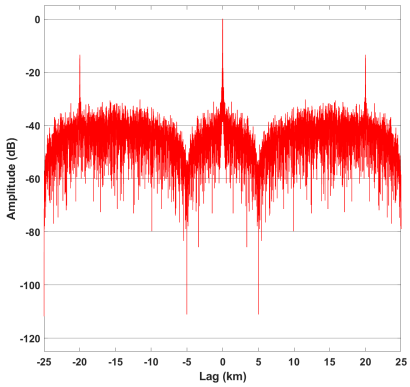

(b) Best Case, ISLR = 15.18 dB

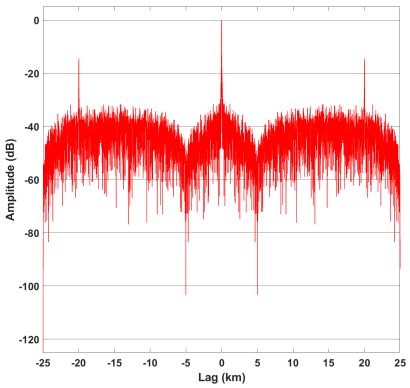

(c) Median Case, PSLR = -6.47 dB

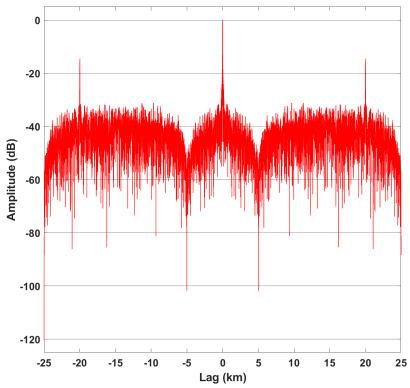

(d) Median Case, ISLR = 15.54 dB

Figure 33: Range profiles for given cases of PSLR and ISLR utilizing LTE structure progressing, variable-data, symbol-length pulses over the aperture. Worst-case results in a range profile of all zeros due to lack of any transmitted data in the symbol of interest.

3.6 Chapter Review

This chapter discussed basic variations of the LTE waveform and demonstrated image domain and range profile effects of those variations. PSF for all combinations of data variation and pulse-lengths are nearly indistinguishable with the exception of those in Sections 3.5.2.3 and 3.5.2.4. These two variable configurations resulted in increases to cross-range sidelobes that tie back to the impact of zero-valued range profiles on the aperture's pulse density.

As waveform bandwidth and aperture extent dominate δR and $\delta R_{\otimes}$, these metrics are within expected bounds across variations and pulse-lengths with the exception of symbol-length pulses progressing through the framework. The apparent improvement of $\delta R_{\otimes}$ for this case is due to non-uniform pulse repetition frequency rooted in changing frequency support pulse to pulse. Increasing the number of symbol-length pulses used across the aperture extent sees $\delta R_{\otimes}$ return to expected bounds. Range profiles across the board do not contain significant sidelobes within 3 km, lending support to the potential effectiveness of LTE as a useful waveform for considerably-sized SAR scenes. Range effects, across pulse-widths, within the 20 km range of the CP sidelobe are due in large part to PCFICH, PHICH, and CSRS information contained in the first symbol of each subframe. It is, however, difficult to discern which of these channels contributes most significantly to intra-symbol sidelobes in the range profiles. These notable sidelobes are not observed in the PSF due to their significant range from scene center and the conservative size of the scene.

Overall, PSLR improves with shorter pulse-lengths while ISLR is affected in the opposite manner, degrading with shorter pulse-lengths. Further, in the best-cases for each pulse length, both PSLR and ISLR improve marginally as more variation is introduced to the waveform. The primary trade off of additional variation is lower peak PSF, due mostly to lack of signal in all or sections of pulses. All PSLR and

ISLR measures presented in the figures throughout this section are located in Table 6 for easy referencing.

The information gathered throughout this chapter provides a standard from which to work as more variations are applied to the waveform in Chapter IV to characterize the influences of a pulse-diverse LTE signal.

Table 6: PSLR and ISLR results from all cases of basic variations in decibels.

	Fixed Data		Variable Data		Progressive Data		
	PSLR	ISLR	Data	ISLR	PSLR	ISLR	
Frame	-6.68	9.27	-6.71	9.21	-6.71	9.23	Best
			-6.67	9.26	-6.67	9.26	Median
			-6.64	9.29	-6.64	9.29	Worst
Subframe	-6.63	13.65	-6.78	13.58	-6.77	13.6	Best
			-6.65	13.68	-6.63	13.69	Median
			-6.54	13.78	-2.93	24.44	Worst
Slot	-6.53	13.97	-6.8	13.85	-6.84	13.86	Best
			-6.63	13.97	-6.63	16.29	Median
			-6.49	14.41	-1.96	25.53	Worst
Symbol	-6.53	15.33	-7	15.21	-6.9	15.18	Best
			-6.64	15.37	-6.47	15.54	Median
			-6.33	16.05	NaN	NaN	Worst

IV. Advanced LTE Variation Effects

4.1 Chapter Overview

This chapter builds upon the concepts explored in Chapter III by varying specific waveform parameters in addition to generation of physical downlink shared channel (PDSCH) user data and Long-Term Evolution (LTE) framework progression pulse-to-pulse. The parameters of interest include waveform bandwidth, PDSCH modulation scheme, control format indicator (CFI) and number of control channels, and cyclic prefix (CP) length. A point-spread function (PSF) and range profile ensemble for each variation type are generated and analyzed using the image quality metrics outlined in Chapter II. The PSF of each pulse-length is normalized to the maximum of the Section 3.3 fixed-data configuration corresponding to given pulse-length.

4.2 Bandwidth Effects

The first parameter variation explored is bandwidth. As discussed in Chapter II, bandwidth allocated for a specific cell is dependent upon the carrier utilizing that particular cell. There is also potential for the bandwidth to change dependent upon user traffic. This section examines image effects introduced by varying waveform bandwidth pulse to pulse.

4.2.1 Methodology and Assumptions

While LTE broadcasts are unlikely to alter bandwidth on less than a multi-frame basis, this research explores more agile variations such that bandwidth varies pulse to pulse for each pulse-length. Because the impacts of bandwidth availability on radar are generally well known [9], the bandwidth of the waveform used varies randomly and with uniform distribution between 15 and 20 MHz. These two bandwidth modes

have effective bandwidths of 13.5 MHz and 18 MHz, respectively. Not only does this method of variation reduce expected range-spreading effects, interpolation of lower-bandwidth waveforms to match sample density of greater bandwidth waveforms using the MATLAB™ LTE Toolbox need not be considered. Evolved Node B (eNB) settings for PDSCH modulation, CP length, and CFI are constant and designated to be quadrature phase-shift keying (QPSK), extended, and three control symbols, respectively. PDSCH user data is generated and the frame index iterated for each subsequent pulse. The PSF for each pulse-length is normalized to the corresponding pulse-length maximum PSF from Section 3.3. Given fixed aperture parameters and using possible effective simulation bandwidths of 18 and 13.5 MHz centered at 750 MHz, Equations (8) and (9) are utilized to determine an expected δR between 9.6 and 12.8 meters and $\delta R_{\otimes}$ between 13.1 and 13.4 meters for all pulse-lengths.

4.2.2 Results

4.2.2.1 Frame

In this section, each pulse consists of one LTE frame, see Figures 12a and 13a, which is 10 ms in length. Because the pulse is a full LTE frame, all cell and user data channels, see Section 2.4.3, are contained in every pulse. New PDSCH data is generated, bandwidth selected, and the frame index iterated for each subsequent pulse. Referencing Figure 34a, the PSF yields δR of 10.8 meters and $\delta R_{\otimes}$ of 13.2 meters. The peak sidelobe ratio (PSLR) and integrated sidelobe ratio (ISLR) resulting from Figure 35 are -6.70 dB and 9.21 dB, respectively.

The PSF contains significant range spreading effects due to the varying nature of waveform bandwidth pulse to pulse over the aperture. Lower bandwidth pulses contribute to degraded resolution that is clearly evident not only in range, but cross-range as well. As a consequence, δR is greatly impacted producing a mainlobe response

nearly twice the expected resolution. In comparison to corresponding fixed-data PSF, bandwidth variation introduces a loss of 1.07 dB. Beneath the range spreading, the PSF patterns observed throughout Chapter III are clearly evident with range profiles also maintaining previously observed compositions of evenly-spaced intra-symbol sidelobes.

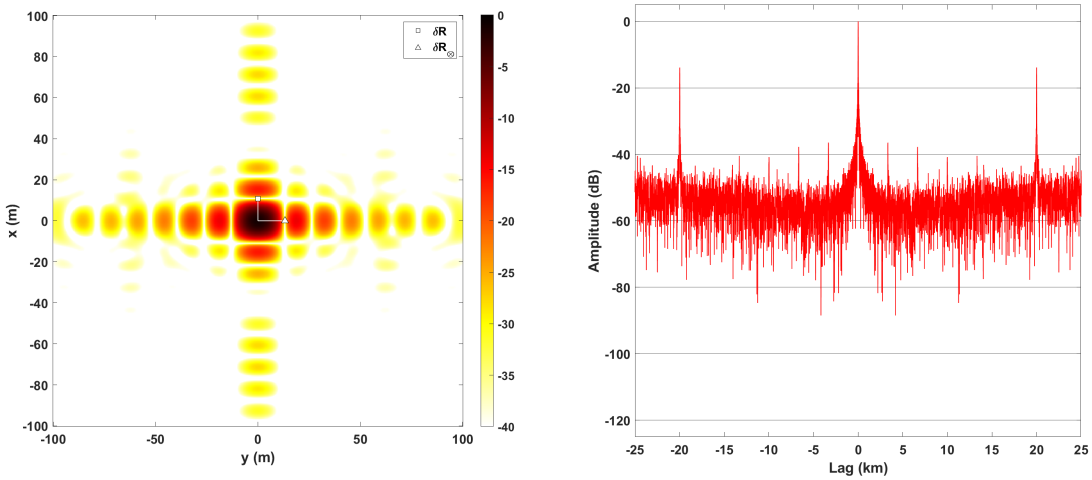

(a) PSF

(b) Magnified Range Profile

Figure 34: Resulting PSF and single range profile realization utilizing bandwidth-varying, frame-length pulses.

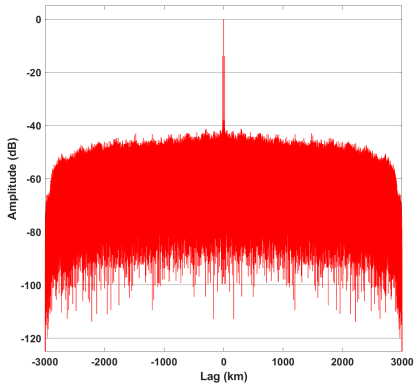

(a) Best Case, PSLR = -6.70 dB

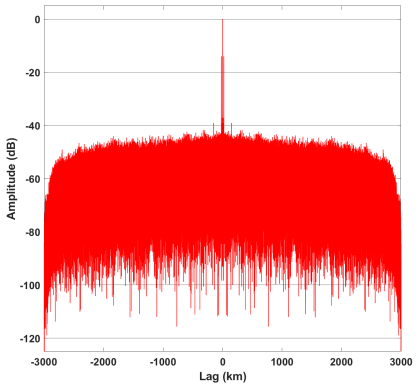

(b) Best Case, ISLR = 9.21 dB

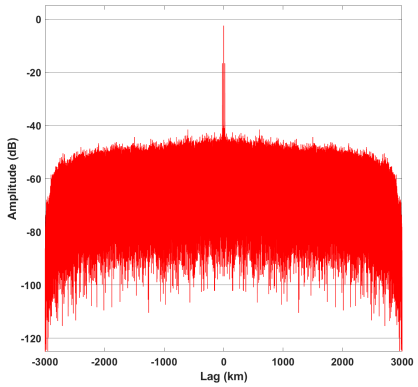

(c) Median Case, PSLR = -6.66 dB

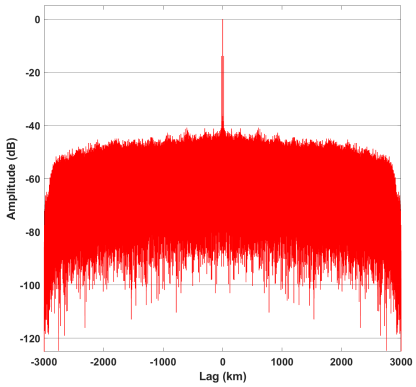

(d) Median Case, ISLR = 9.28 dB

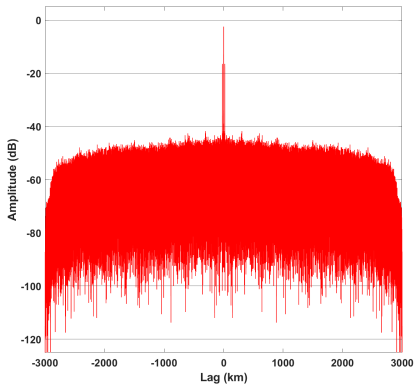

(e) Worst Case, PSLR = -6.60 dB

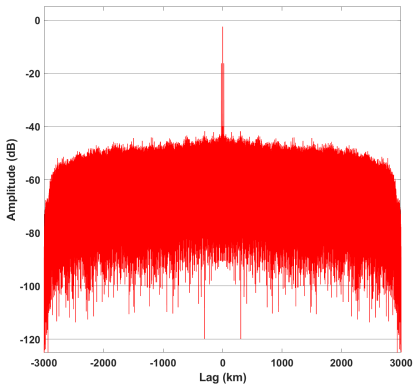

(f) Worst Case, ISLR = 9.96 dB

Figure 35: Range profiles for given cases of PSLR and ISLR utilizing variable bandwidth, frame-length pulses over the aperture.

4.2.2.2 Subframe

In this section, each pulse consists of one LTE subframe, see Figures 12b and 13b, which is 1 ms in length. New PDSCH data is generated, bandwidth selected, and the subframe index iterated for each subsequent pulse. The frame index is likewise iterated when necessary to maintain proper framework progression of the waveform across the aperture. At minimum, any given pulse contains cell-specific reference signal (CSRS), physical control format indicator channel (PCFICH), physical downlink control channel (PDCCH), physical hybrid ARQ indicator CH (PHICH), and PDSCH information at varying bandwidths. As the subframe index is iterated, some pulses will contain all cell and user data channels. Referencing Figure 36a, the PSF yields δR of 10.8 meters and $\delta R_{\otimes}$ of 12.8 meters. The best-case PSLR and ISLR resulting from Figure 37 are -6.74 dB and 13.60 dB, respectively.

PSF incurs a loss of 1.86 dB in relation to corresponding fixed-data results and maintains a response shape consistent with that using bandwidth-varying, frame-length pulses. The lower bandwidth pulses in the aperture contribute to range spreading, worsening δR and introducing range ambiguities along the cross-range extent. Considering Figure 36b, which depicts a range-magnified view of Figure 37e, intra-symbol sidelobes are evident at 3.3 km and 13.2 km. This particular range profile occurs on pulse 66 of 101, which corresponds to frame 6, subframe 5. Considering Figure 11, the subframe that generates this range profile does not contain any user data. Much like was discussed in Section 3.5.2.2, the low-response segments of Figures 37e and 37f are a result of empty symbols in subframe 5. While $\delta R_{\otimes}$ appears to improve over expectations, the inconsistent sidelobes resulting from and sparse-signal pulses and changing frequency support causes cross-range smearing and move the first cross-range minimum toward scene center. As more pulses are included in the aperture extent, $\delta R_{\otimes}$ degrades to expected bounds.

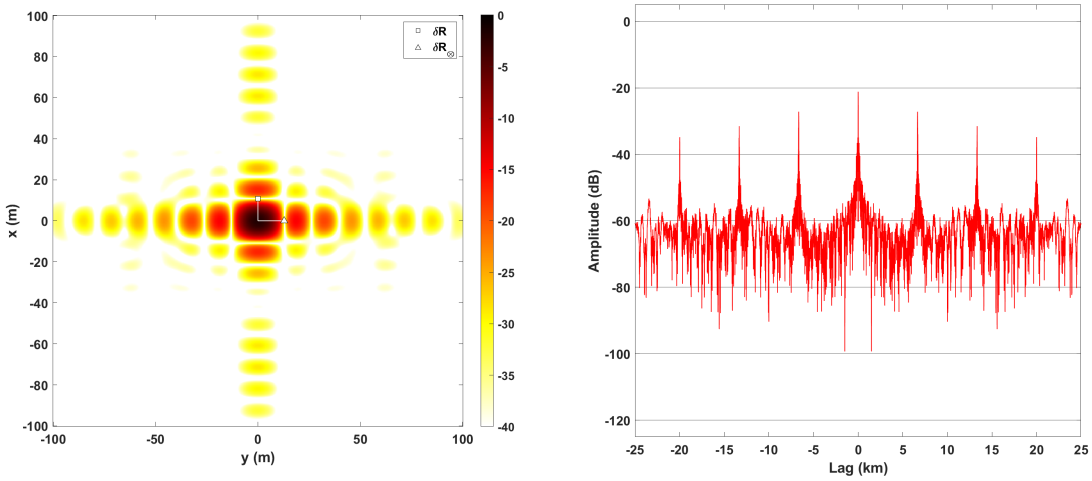

(a) PSF

(b) Magnified Range Profile

Figure 36: Resulting PSF and single range profile realization utilizing bandwidth-varying, subframe-length pulses.

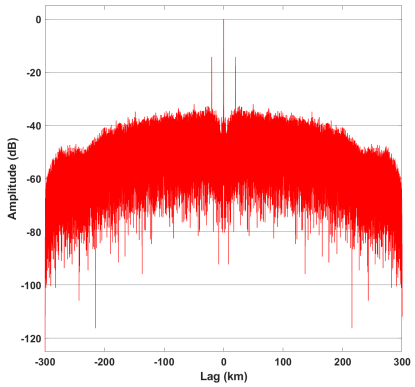

(a) Best Case, PSLR = -6.74 dB

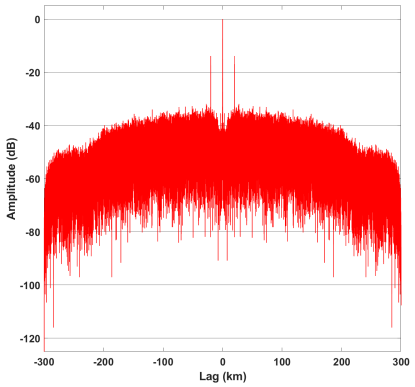

(b) Best Case, ISLR = 13.60 dB

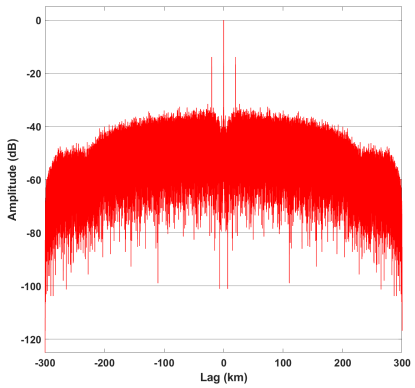

(c) Median Case, PSLR = -6.62 dB

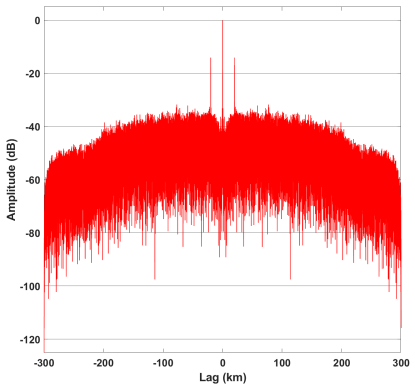

(d) Median Case, ISLR = 13.76 dB

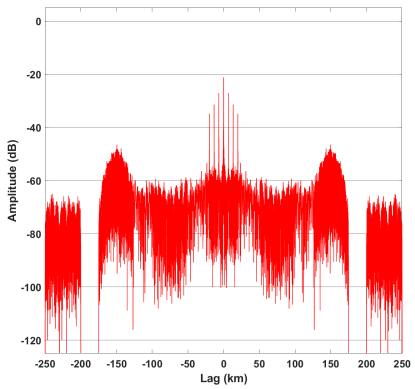

(e) Worst Case, PSLR = -2.93 dB

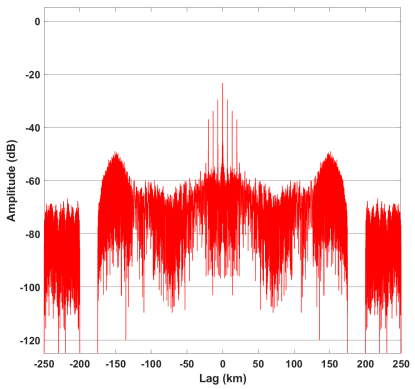

(f) Worst Case, ISLR = 25.11 dB

Figure 37: Range profiles for given cases of PSLR and ISLR utilizing variable bandwidth, subframe-length pulses over the aperture.

4.2.2.3 Slot

In this section, each pulse consists of one LTE slot, see Figures 12c and 13c, which is 0.5 ms in length. New PDSCH data is generated, bandwidth selected, and the slot index iterated for each subsequent pulse. The frame and subframe indices are likewise iterated when necessary to maintain proper framework progression of the waveform across the aperture. At minimum, any give pulse contains CSRS information. As the slot index is iterated, pulses will contain several combinations of cell and/or user data channels at varying bandwidths. Referencing Figure 38a, the PSF yields δR of 10.8 meters and $\delta R_{\otimes}$ of 12.8 meters. The best-case PSLR and ISLR resulting from Figure 39 are -6.90 dB and 13.89 dB, respectively.

A loss of 4.20 dB is observed in the PSF when normalized against the PSF generated in Section 3.3.2.3. Figure 38 displays cross-range ambiguities in addition to the range spreading and sidelobe effects identified up to this point. The inclusion of sparse-signal pulses in the aperture effectively decrease the aperture's pulse density and result in cross-range spreading and non-uniform sidelobes. While $\delta R_{\otimes}$ appears to improve over expectations, the inconsistent sidelobes move the first cross-range minimum toward scene center. As more pulses are included in the aperture extent, $\delta R_{\otimes}$ degrades to the expected bounds. As seen in Section 3.5.2.3, progression through the LTE framework creates considerable low points in the range profile response when the pulse is sourced from slot 1, subframe 5. These effects are displayed in Figure 39e.

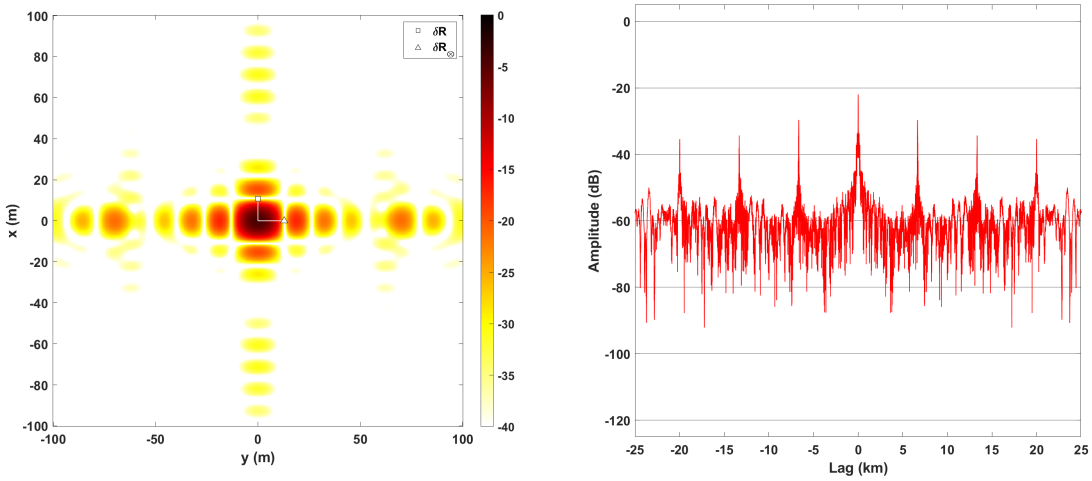

(a) PSF

(b) Magnified Range Profile

Figure 38: Resulting PSF and single range profile realization utilizing bandwidth-varying, slot-length pulses.

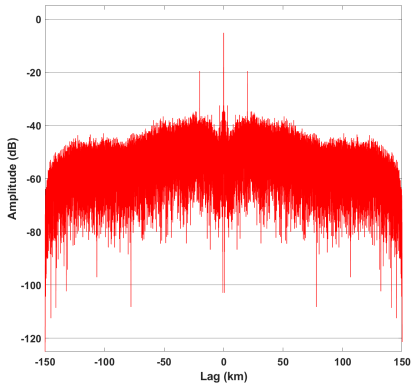

(a) Best Case, PSLR = -6.90 dB

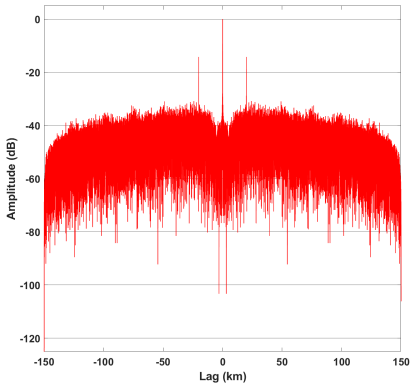

(b) Best Case, ISLR = 13.89 dB

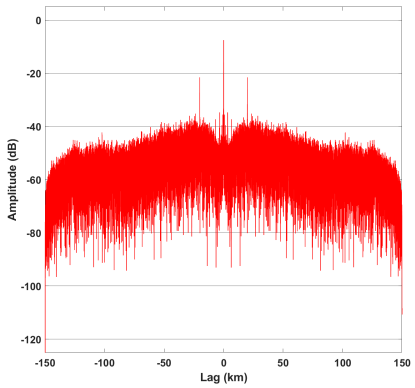

(c) Median Case, PSLR = -6.62 dB

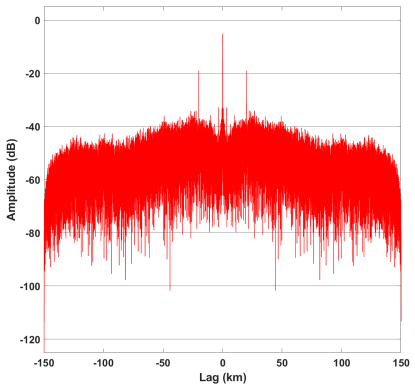

(d) Median Case, ISLR = 16.31 dB

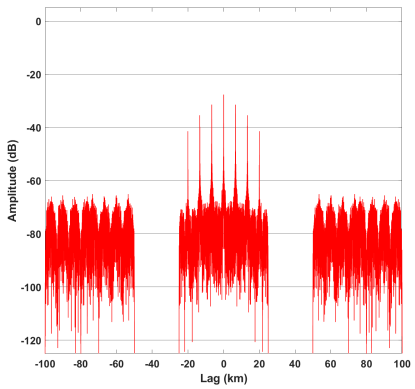

(e) Worst Case, PSLR = -1.94 dB

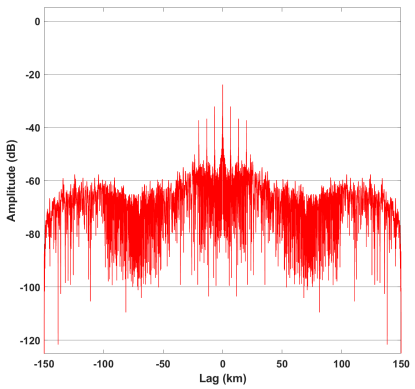

(f) Worst Case, ISLR = 25.78 dB

Figure 39: Range profiles for given cases of PSLR and ISLR utilizing variable bandwidth, slot-length pulses over the aperture.

4.2.2.4 Symbol

In this section, each pulse consists of one orthogonal frequency-division multiplexing (OFDM) symbol, see Figures 12d and 13d, which is 83.3 μs in length. Note that the symbol includes a CP. New PDSCH data is generated, bandwidth selected, and the symbol index iterated for each subsequent pulse. Frame, subframe, and slot indices are likewise iterated when necessary to maintain proper framework progression of the waveform across the aperture. At minimum, it is possible that a pulse will contain no signal whatsoever. This possibility only occurs at specific symbols within subframe 5 of each new frame. Otherwise, pulses may contain information from no less than one cell or user data channel. Referencing Figure 40, the PSF yields δR of 10.8 meters and $\delta R_{\otimes}$ of 12.4 meters. The best-case PSLR and ISLR resulting from Figure 41 are -6.96 dB and 15.28 dB, respectively.

Bandwidth variation results in a PSF loss of 4.6 dB. Range profiles are markedly similar to previous iterations of symbol-length pulses. Due to some symbols being devoid of any signal, the worst-case metrics are derived from zero-response range profiles. A combination of range spreading and cross-range smearing are visible in Figure 40. Notable cross-range effects are observed in the PSF resulting from the aperture pulse density, much like when using slot-length pulses. While $\delta R_{\otimes}$ appears to improve over expectations, the inconsistent sidelobes resulting from empty and sparse-signal pulses causes cross-range smearing and move the first cross-range minimum toward scene center. As more pulses are included in the aperture extent, $\delta R_{\otimes}$ degrades to expected bounds.

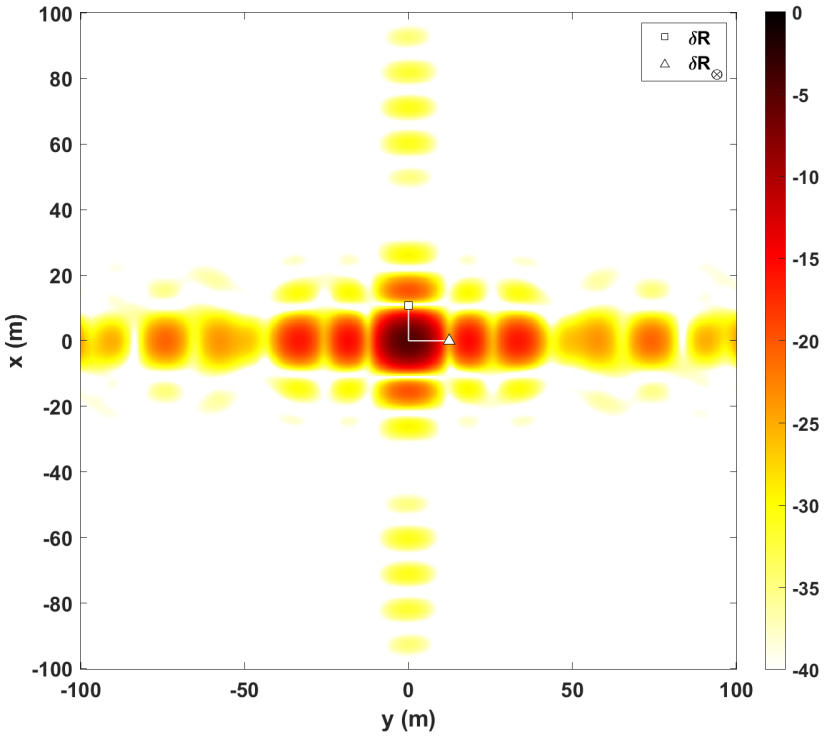

Figure 40: Resulting PSF utilizing bandwidth-varying, slot-length pulses.

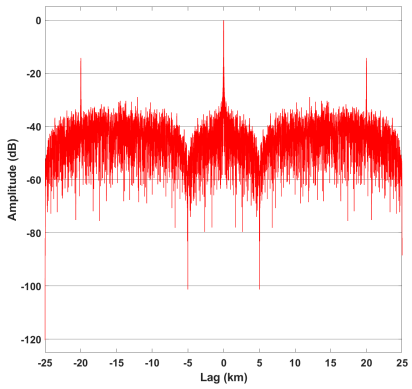

(a) Best Case, PSLR = -6.96 dB

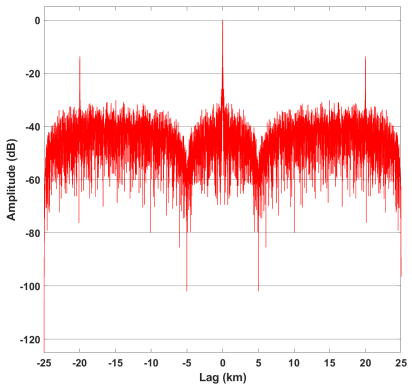

(b) Best Case, ISLR = 15.28 dB

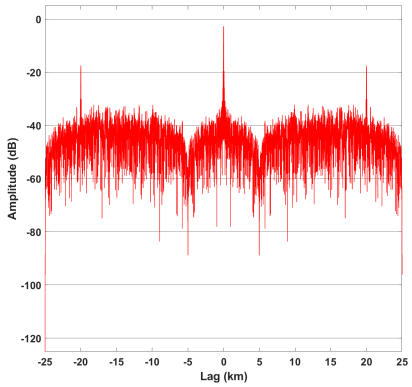

(c) Median Case, PSLR = -6.49 dB

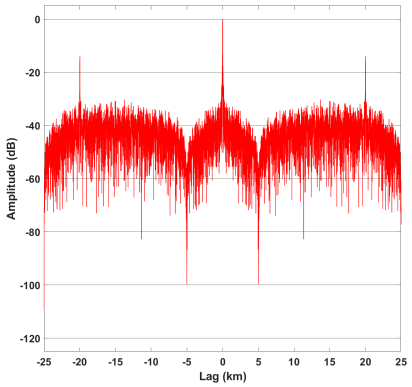

(d) Median Case, ISLR = 16.17 dB

Figure 41: Range profiles for given cases of PSLR and ISLR utilizing variable bandwidth, symbol-length pulses over the aperture.

4.3 Modulation Effects

User data modulation scheme for LTE networks is dependent mostly upon signal strength of the transmitted data at the receiver. This being the case, it is important to determine ramifications of pulse to pulse PDSCH modulation scheme fluctuations on image domain results.

4.3.1 Methodology and Assumptions

Up to this point, PDSCH has utilized QPSK modulation exclusively. In this section the modulation scheme varies uniformly randomly pulse to pulse between QPSK, 16-quadrature amplitude modulation (16QAM), and 64-quadrature amplitude modulation (64QAM). Each modulation scheme offers a unique number of complex values to which data may be assigned. With higher-rate modulation schemes, the increase in available complex values serves to better emulate entirely unique, random waveforms. Similar to dynamic changes in bandwidth, the modulation type for user data is not likely to change more frequently than frame-to-frame. This research explores impacts of a more agile approach to data modulation at each of the four LTE structure levels. Given modulation effect results from [2], it is expected that pulses utilizing higher-rate modulation schemes should provide improved image metrics over lower-rate schemes. Settings for eNB bandwidth, CPlength, and CFI are constant and designated to be 20 MHz, extended, and three control symbols, respectively. Given fixed aperture parameters and using possible effective simulation bandwidth of 18 MHz centered at 750 MHz, Equations (8) and (9) are utilized to determine an expected δR of 9.6 meters and $\delta R_{\otimes}$ between 13.1 and 13.4 meters for all pulse-lengths.

4.3.2 Results

4.3.2.1 Frame

In this section, each pulse consists of one LTE frame, see Figures 12a and 13a, which is 10 ms in length. Because the pulse is a full LTE frame, all cell and user data channels, see Section 2.4.3, are contained in every pulse. New PDSCH data is generated, modulation scheme selected, and the frame index iterated for each subsequent pulse. Referencing Figure 42a, the PSF yields δR of 9.6 meters and $\delta R_{\otimes}$ of 13.2 meters. The PSLR and ISLR resulting from Figure 43 are -6.73 dB and 9.23 dB, respectively.

The PSF is practically identical to those observed in Chapter III with a loss of 0.01 dB normalized to the corresponding fixed-data configuration. Range profiles, as seen in Figure 42b, replicate intra-symbol sidelobes noticed in less-variable waveforms. The continued reproduction of these particular sidelobes only strengthens support that they are influenced by the contents of PCFICH, PDCCH, PHICH, and CSRS, whether alone or in combination.

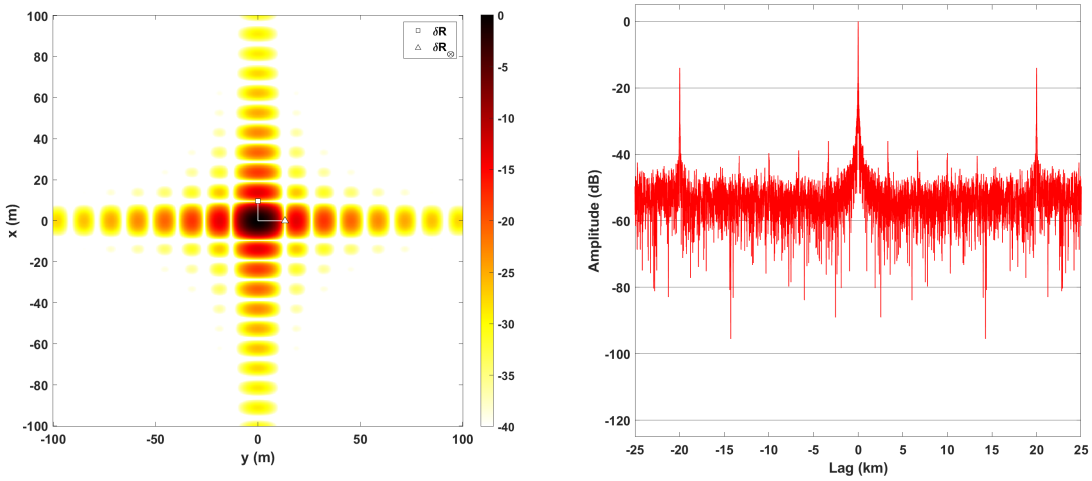

(a) PSF

(b) Magnified Range Profile

Figure 42: Resulting PSF and single range profile realization utilizing PDSCH modulation-varying, frame-length pulses.

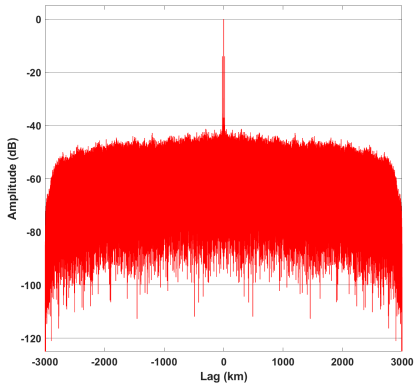

(a) Best Case, PSLR = -6.73 dB

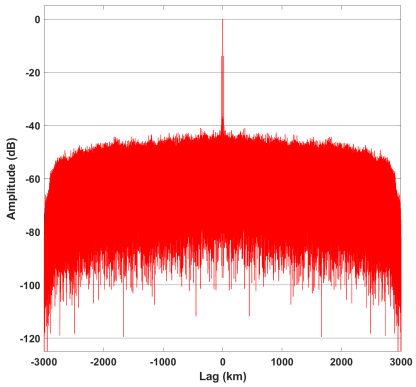

(b) Best Case, ISLR = 9.23 dB

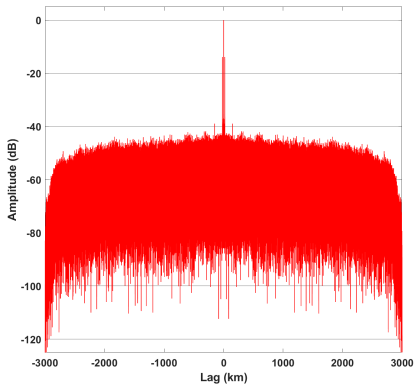

(c) Median Case, PSLR = -6.67 dB

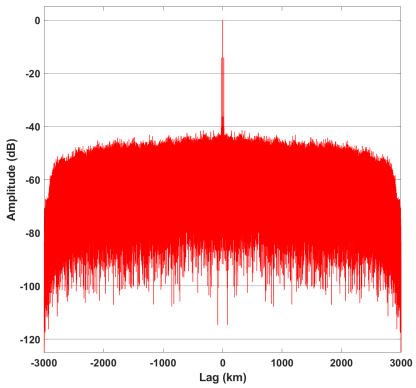

(d) Median Case, ISLR = 9.26 dB

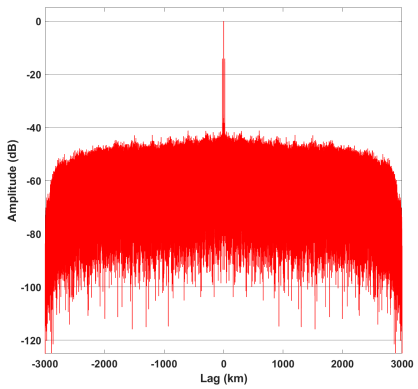

(e) Worst Case, PSLR = -6.61 dB

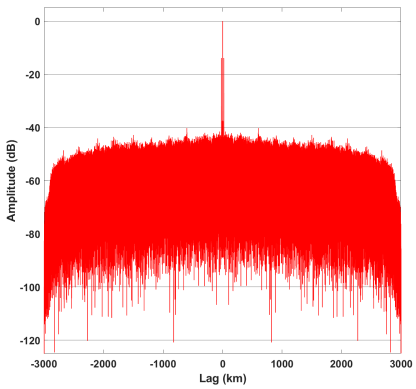

(f) Worst Case, ISLR = 9.32 dB

Figure 43: Range profiles for given cases of PSLR and ISLR utilizing variable modulation, frame-length pulses over the aperture.

4.3.2.2 Subframe

In this section, each pulse consists of one LTE subframe, see Figures 12b and 13b, which is 1 ms in length. New PDSCH data is generated, modulation scheme selected, and the subframe index iterated for each subsequent pulse. The frame index is likewise iterated when necessary to maintain proper framework progression of the waveform across the aperture. At minimum, any given pulse contains CSRS, PCFICH, PDCCH, PHICH, and PDSCH information. As the subframe index is iterated, some pulses will contain all cell and user data channels. Referencing Figure 44a, the PSF yields δR of 9.6 meters and $\delta R_{\otimes}$ of 13.2 meters. The best-case PSLR and ISLR resulting from Figure 45 are -6.81 dB and 13.62 dB, respectively.

PSF incurs a loss of 0.86 dB in relation to corresponding fixed-data results and maintains a response pattern consistent with Chapter III results. δR reverts to a level comparable to expectation due to lack of bandwidth effects and $\delta R_{\otimes}$ continues to be consistent. Much like other subframe-length pulse variations, some range profiles, as seen in Figure 44, contain intra-symbol sidelobes occurring about every 3 km outward from scene center. Sections of extremely low response, shown in Figures 45e and 45f, continue to appear as a result of pulses sourced from subframe 5 containing empty symbols.

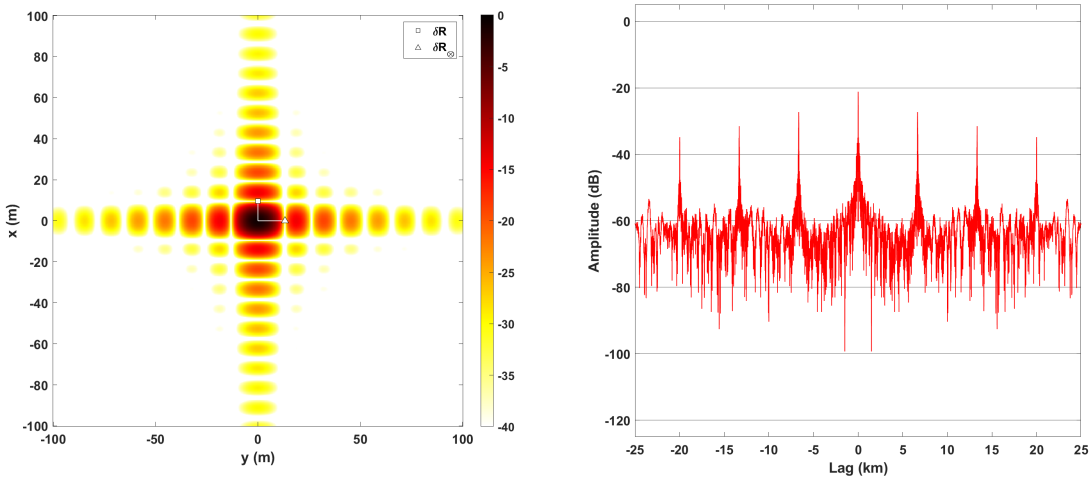

(a) PSF

(b) Magnified Range Profile

Figure 44: Resulting PSF and single range profile realization utilizing PDSCH modulation-varying, subframe-length pulses.

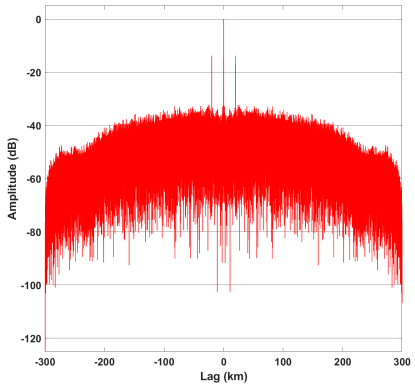

(a) Best Case, PSLR = -6.81 dB

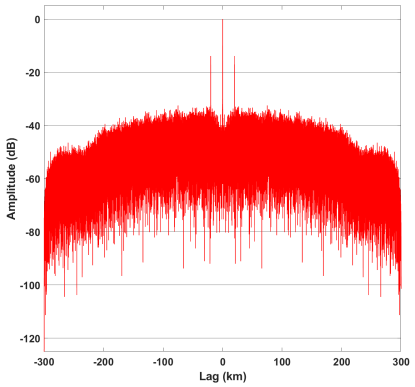

(b) Best Case, ISLR = 13.62 dB

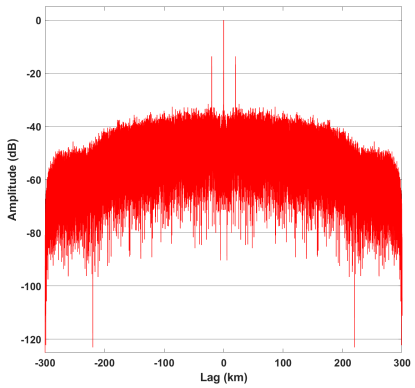

(c) Median Case, PSLR = -6.62 dB

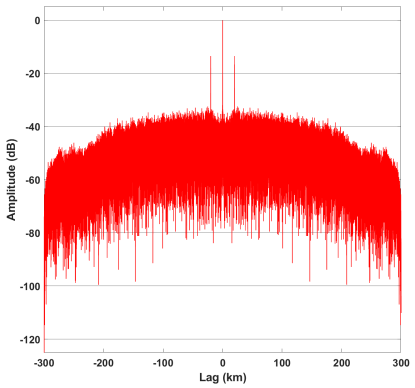

(d) Median Case, ISLR = 13.75 dB

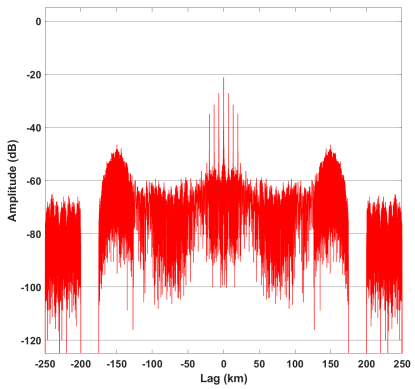

(e) Worst Case, PSLR = -2.93 dB

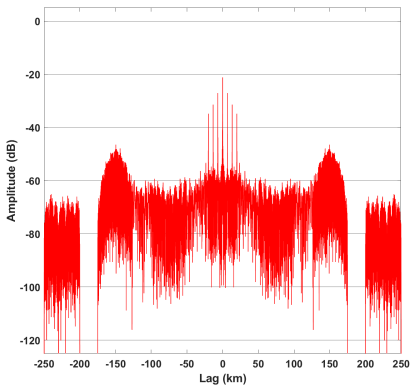

(f) Worst Case, ISLR = 24.44 dB

Figure 45: Range profiles for given cases of PSLR and ISLR utilizing variable modulation, subframe-length pulses over the aperture.

4.3.2.3 Slot

In this section, each pulse consists of one LTE slot, see Figures 12c and 13c, which is 0.5 ms in length. New PDSCH data is generated, modulation scheme selected, and the slot index iterated for each subsequent pulse. The frame and subframe indices are likewise iterated when necessary to maintain proper framework progression of the waveform across the aperture. At minimum, any give pulse contains CSRS information. As the slot index is iterated, pulses will contain several combinations of cell and/or user data channels at varying bandwidths. Referencing Figure 46a, the PSF yields δR of 9.6 meters and $\delta R_{\otimes}$ of 13.2 meters. The best-case PSLR and ISLR resulting from Figure 47 are -6.90 dB and 13.91 dB, respectively.

A loss of 3.09 dB is observed in the PSF when normalized against the PSF generated in Section 3.3.2.3. Cross-range ambiguities noted in Section 3.5 are evident here as well. As the pulses progress through the framework, some contain limited signal resulting in low-energy range profiles and impacting the aperture pulse density. Increasing the number of pulses in the aperture lessens the impact of sparse-signal pulses, thereby diminishing cross-range effects observed here. The range profile shown in Figure 46b is, much like some pulses in Section 3.5.2.3, the result of a pulse generated using slot 1, subframe 5. This further supports evidence that the intra-symbol sidelobes are a direct impact of the CSRS. The lack of response displayed in Figure 47e is an impact of empty symbols contained in the pulse sourced from slot 1, subframe 5.

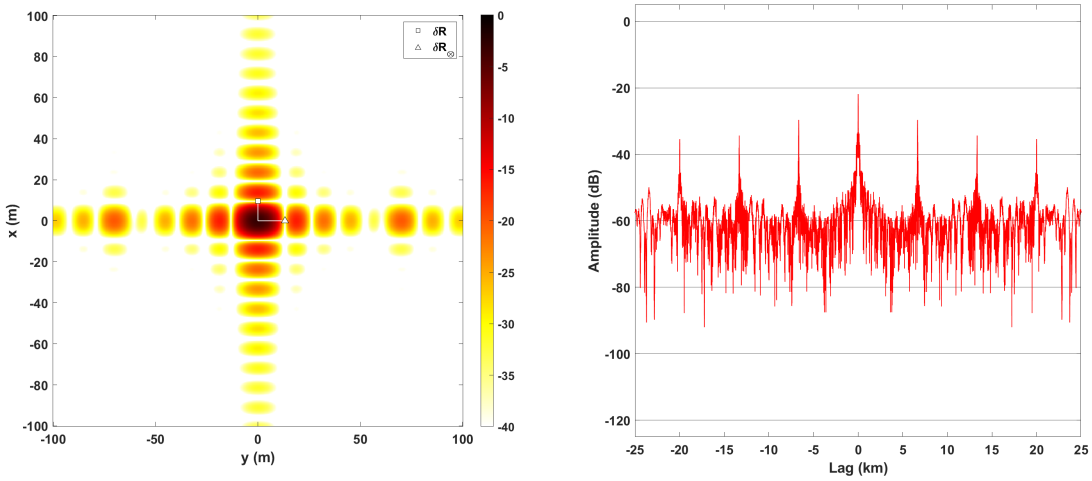

(a) PSF

(b) Magnified Range Profile

Figure 46: Resulting PSF and single range profile realization utilizing PDSCH modulation-varying, slot-length pulses.

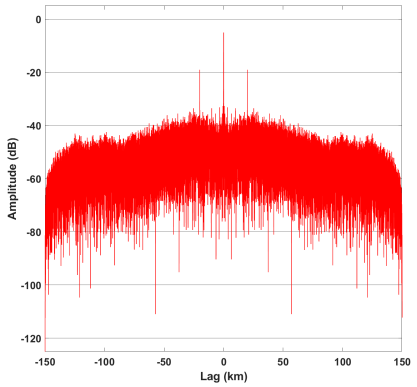

(a) Best Case, PSLR = -6.90 dB

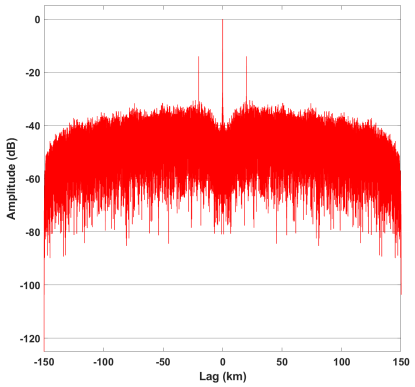

(b) Best Case, ISLR = 13.91 dB

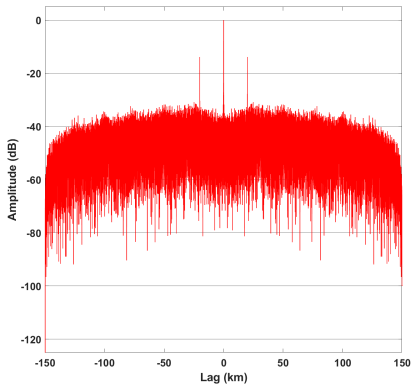

(c) Median Case, PSLR = -6.65 dB

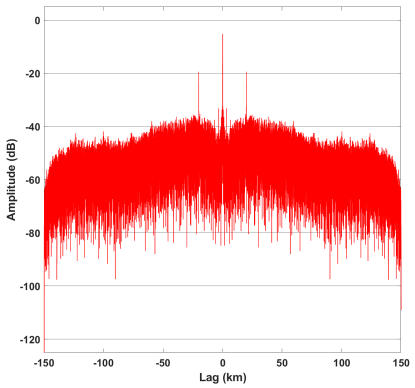

(d) Median Case, ISLR = 16.33 dB

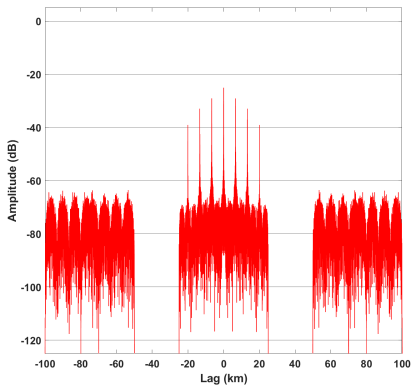

(e) Worst Case, PSLR = -1.96 dB

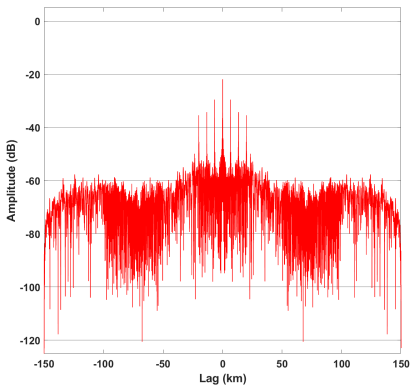

(f) Worst Case, ISLR = 25.53 dB

Figure 47: Range profiles for given cases of PSLR and ISLR utilizing variable modulation, slot-length pulses over the aperture.

4.3.2.4 Symbol

In this section, each pulse consists of one OFDM symbol, see Figures 12d and 13d, which is 83.3 μs in length. Note that the symbol includes a CP. New PDSCH data is generated, modulation scheme selected, and the symbol index iterated for each subsequent pulse. Frame, subframe, and slot indices are likewise iterated when necessary to maintain proper framework progression of the waveform across the aperture. At minimum, it is possible that a pulse will contain no signal whatsoever. This possibility only occurs at specific symbols within subframe 5 of each new frame. Otherwise, pulses may contain information from no less than one cell or user data channel. Referencing Figure 48, the PSF yields δR of 9.6 meters and $\delta R_{\otimes}$ of 12.4 meters. The best-case PSLR and ISLR resulting from Figure 49 are -6.97 dB and 15.12 dB, respectively.

PDSCH modulation variation results in a PSF loss of 3.44 dB. Range profiles are markedly similar to previous iterations of symbol-length pulses. Due to some symbols being devoid of any signal, the worst-case metrics are derived from zero-response range profiles. Cross-range aliasing is visible in Figure 48. Notable cross-range effects are observed in the PSF resulting from the aperture pulse density, much like when using slot-length pulses. While $\delta R_{\otimes}$ appears to improve over expectations, the inconsistent sidelobes resulting from empty and sparse-signal pulses causes cross-range smearing and move the first cross-range minimum toward scene center. As more pulses are included in the aperture extent, $\delta R_{\otimes}$ degrades to expected bounds.

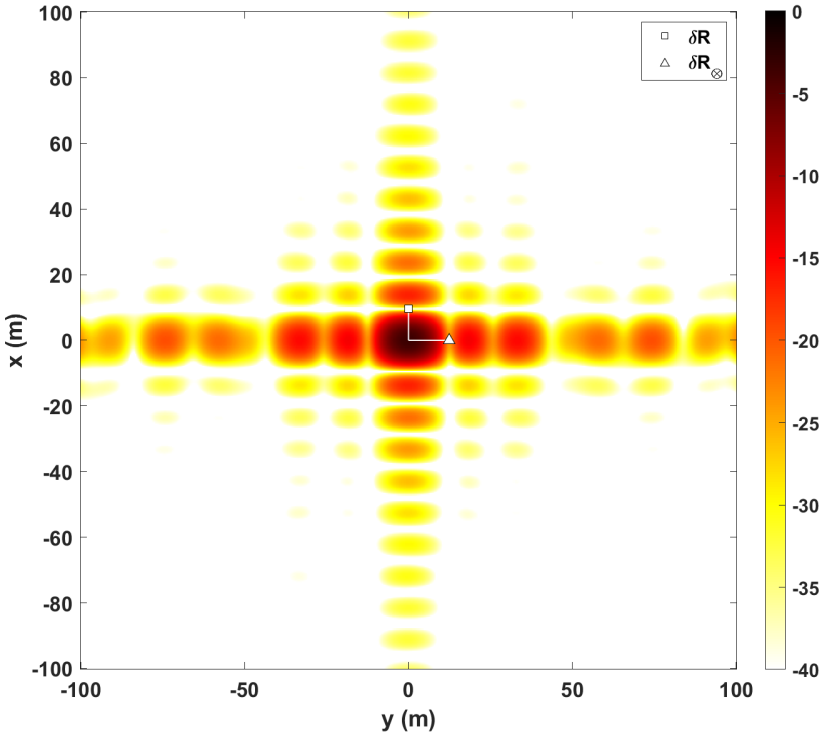

Figure 48: Resulting PSF due to varying data modulation on a symbol-by-symbol basis.

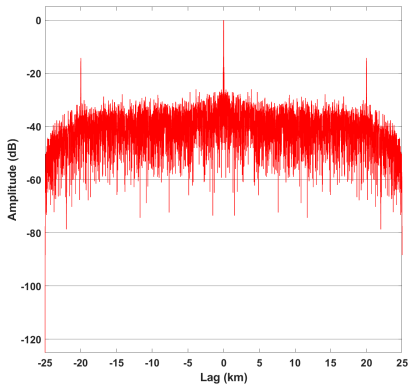

(a) Best Case, PSLR = -6.97 dB

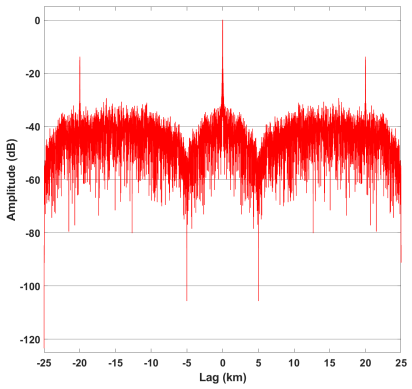

(b) Best Case, ISLR = 15.12 dB

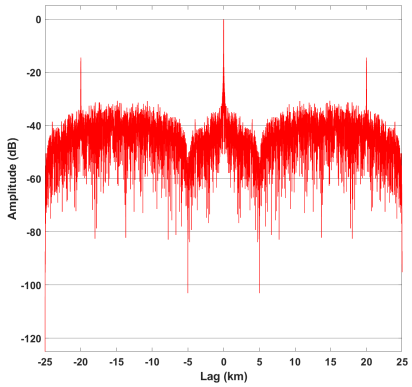

(c) Median Case, PSLR = -6.49 dB

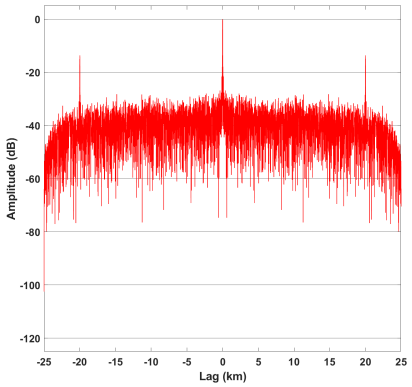

(d) Median Case, ISLR = 17.00 dB

Figure 49: Range profiles for given cases of PSLR and ISLR utilizing variable modulation, symbol-length pulses over the aperture.

4.4 Control Channel Effects

Control channel data is located in up to the first three symbols of each subframe. A reduction in number of control channels opens resources to more user data allocation. The number of control channels is set by the CFI which has the bit patterns shown in Table 2. The CFI setting is primarily dependent upon signal bandwidth.

4.4.1 Methodology and Assumptions

The number of control channels present in a given pulse is regulated by the CFI. For eNB bandwidth of 20 MHz, QPSK modulated PDSCH, and extended CP length, the CFI is uniformly randomly selected to be one, two, or three. Given fixed aperture parameters and using possible effective simulation bandwidth of 18 MHz centered at 750 MHz, Equations (8) and (9) are utilized to determine an expected δR of 9.6 meters and $\delta R_{\otimes}$ between 13.1 and 13.4 meters for all pulse-lengths.

4.4.2 Results

4.4.2.1 Frame

In this section, each pulse consists of one LTE frame, see Figures 12a and 13a, which is 10 ms in length. Because the pulse is a full LTE frame, all cell and user data channels, see Section 2.4.3, are contained in every pulse. New PDSCH data is generated, CFI selected, and the frame index iterated for each subsequent pulse. Referencing Figure 50a, the PSF yields δR of 9.6 meters and $\delta R_{\otimes}$ of 13.2 meters. The PSLR and ISLR resulting from Figure 35 are -6.72 dB and 8.40 dB, respectively.

Surprisingly, the PSF receives a gain of 0.81 dB over its fixed-data counterpart from Section 3.3.2.1. This gain is the result of more PDSCH data being represented in pulses where the number of control channels is less than three. Because the control channel symbols do not always contain signal across the entire spectrum of the

framework, introducing user data increases the energy in the overall signal. The PSF maintains a response pattern consistent with Chapter III results. Resulting δR and $\delta R_{\otimes}$ match expectations. Similarly to other frame-length pulse variations, some range profiles, as seen in Figure 50, contain intra-symbol sidelobes occurring about every 3 km outward from scene center.

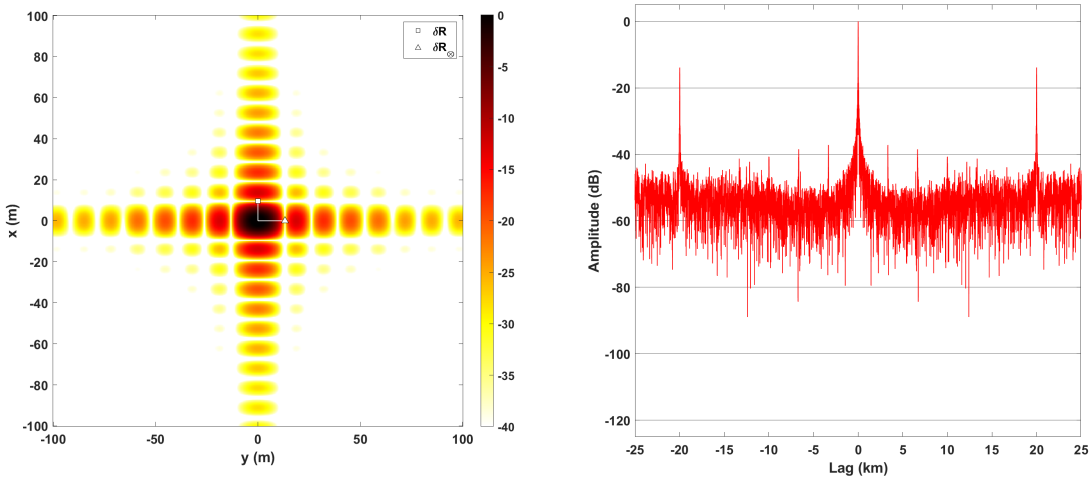

(a) PSF

(b) Magnified Range Profile

Figure 50: Resulting PSF and single range profile realization utilizing CFI-varying, frame-length pulses.

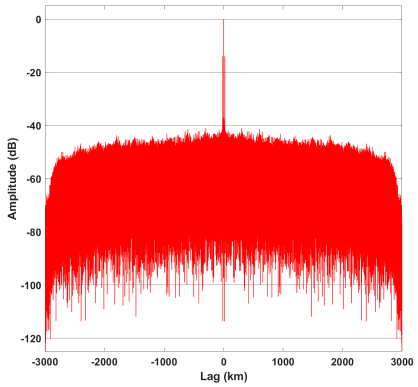

(a) Best Case, PSLR = -6.72 dB

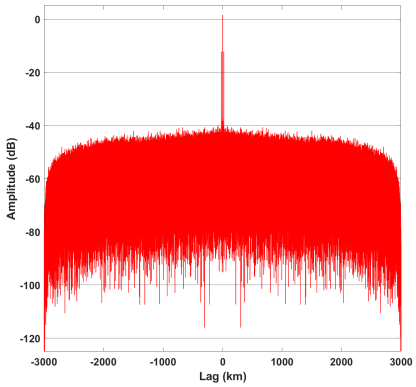

(b) Best Case, ISLR = 8.4 dB

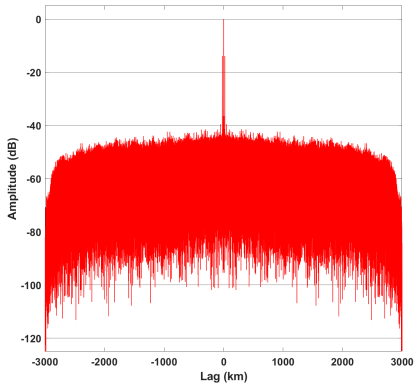

(c) Median Case, PSLR = -6.67 dB

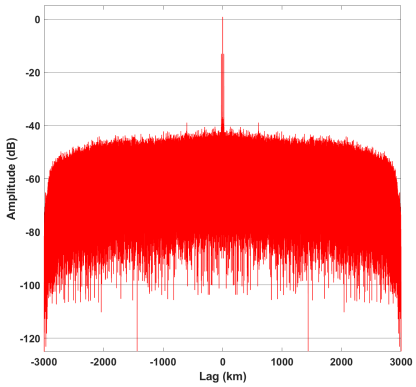

(d) Median Case, ISLR = 8.83 dB

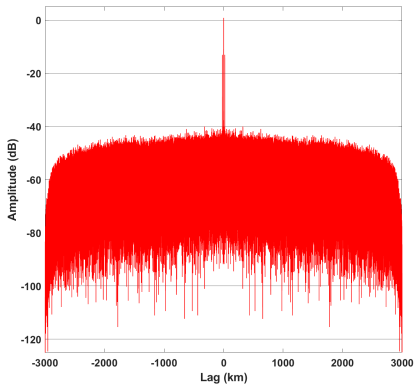

(e) Worst Case, PSLR = -6.63 dB

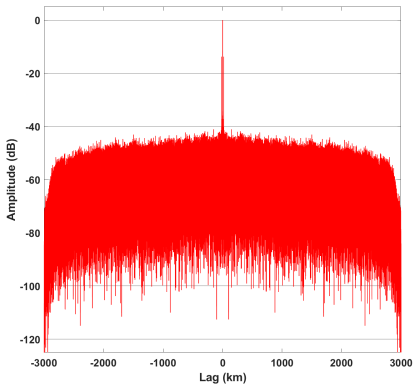

(f) Worst Case, ISLR = 9.29 dB

Figure 51: Range profiles for given cases of PSLR and ISLR utilizing variable control channel, frame-length pulses over the aperture.

4.4.2.2 Subframe

In this section, each pulse consists of one LTE subframe, see Figures 12b and 13b, which is 1 ms in length. New PDSCH data is generated, CFI selected, and the subframe index iterated for each subsequent pulse. The frame index is likewise iterated when necessary to maintain proper framework progression of the waveform across the aperture. At minimum, any given pulse contains CSRS, PCFICH, PDCCH, PHICH, and PDSCH information. As the subframe index is iterated, some pulses will contain all cell and user data channels. Referencing Figure 52a, the PSF yields δR of 9.6 meters and $\delta R_{\otimes}$ of 13.2 meters. The best-case PSLR and ISLR resulting from Figure 53 are -6.76 dB and 8.40 dB, respectively.

PSF incurs a loss of 0.06 dB in relation to corresponding fixed-data results and maintains a response pattern consistent with Chapter III results. Much like other subframe-length pulse variations, some range profiles, as seen in Figure 44, contain intra-symbol sidelobes occurring about every 3.3 km. Low-response regions shown in Figures 53e and 53f are a consequence of pulses generated using subframe 5 and the matching of empty symbols.

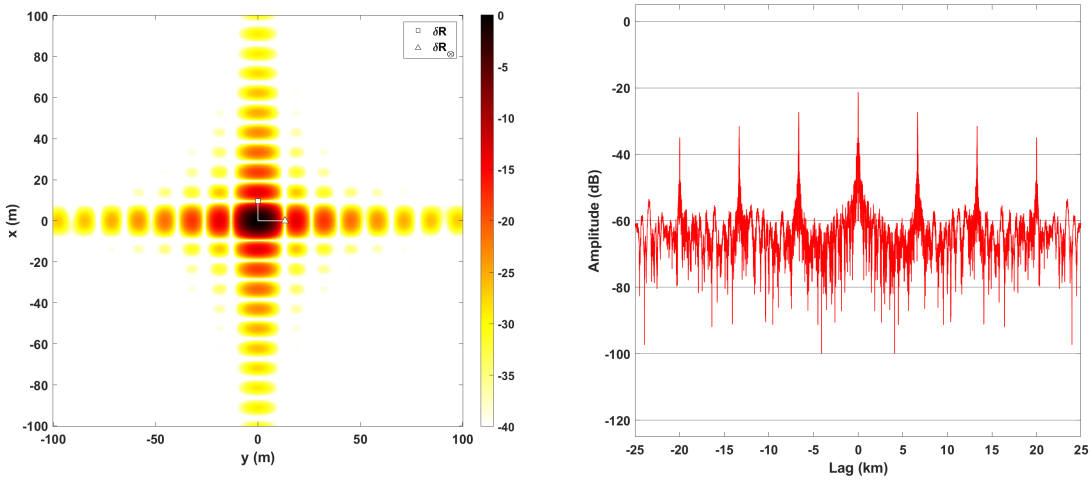

(a) PSF

(b) Magnified Range Profile

Figure 52: Resulting PSF and single range profile realization utilizing CFI-varying, subframe-length pulses.

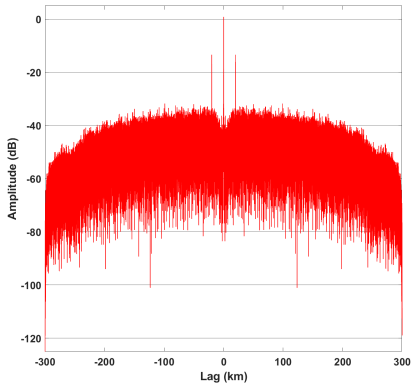

(a) Best Case, PSLR = -6.76 dB

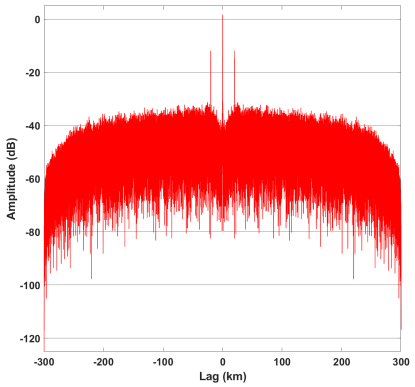

(b) Best Case, ISLR = 8.40 dB

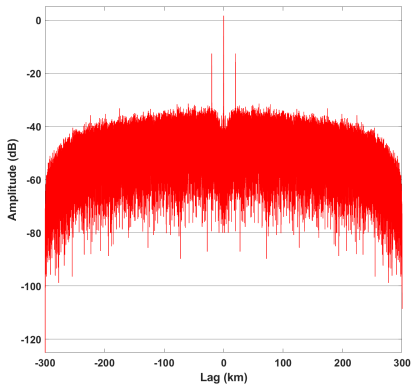

(c) Median Case, PSLR = -6.67 dB

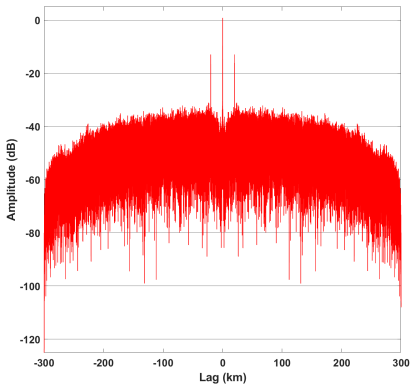

(d) Median Case, ISLR = 8.83 dB

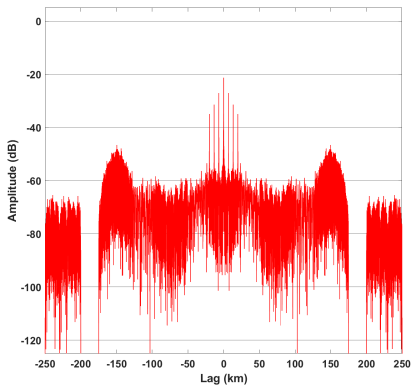

(e) Worst Case, PSLR = -2.90 dB

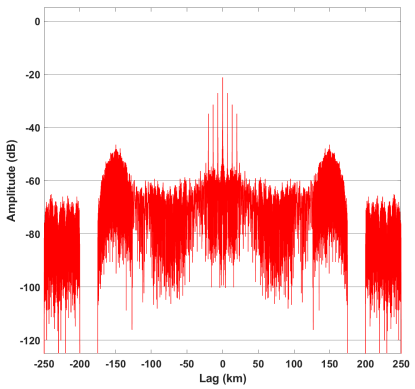

(f) Worst Case, ISLR = 24.44 dB

Figure 53: Range profiles for given cases of PSLR and ISLR utilizing variable control channel, subframe-length pulses over the aperture.

4.4.2.3 Slot

In this section, each pulse consists of one LTE slot, see Figures 12c and 13c, which is 0.5 ms in length. New PDSCH data is generated, CFI selected, and the slot index iterated for each subsequent pulse. The frame and subframe indices are likewise iterated when necessary to maintain proper framework progression of the waveform across the aperture. At minimum, any give pulse contains CSRS information. As the slot index is iterated, pulses will contain several combinations of cell and/or user data channels at varying bandwidths. Referencing Figure 54a, the PSF yields δR of 9.6 meters and $\delta R_{\otimes}$ of 12.8 meters. The best-case PSLR and ISLR resulting from Figure 55 are -6.78 dB and 13.82 dB, respectively.

A loss of 2.14 dB is observed in the PSF when normalized against the PSF generated in Section 3.3.2.3. Cross-range ambiguities noted in Section 3.5 are evident here as well. As the pulses progress through the framework, some contain limited signal resulting in low-energy range profiles and impacting the aperture pulse density. While $\delta R_{\otimes}$ appears to improve over expectations, the inconsistent sidelobes resulting from empty and sparse-signal pulses causes cross-range smearing and move the first cross-range minimum toward scene center. As more pulses are included in the aperture extent, $\delta R_{\otimes}$ degrades to expected bounds. The range profile shown in Figure 54b is, much like some pulses in Section 3.5.2.3, the result of a pulse generated using slot 1, subframe 5. This further supports evidence that the intra-symbol sidelobes are a direct impact of the CSRS. Near-null response observed in Figure 55e is a consequence of progression through the LTE framework and pulses generated from sections of framework that contain empty symbols.

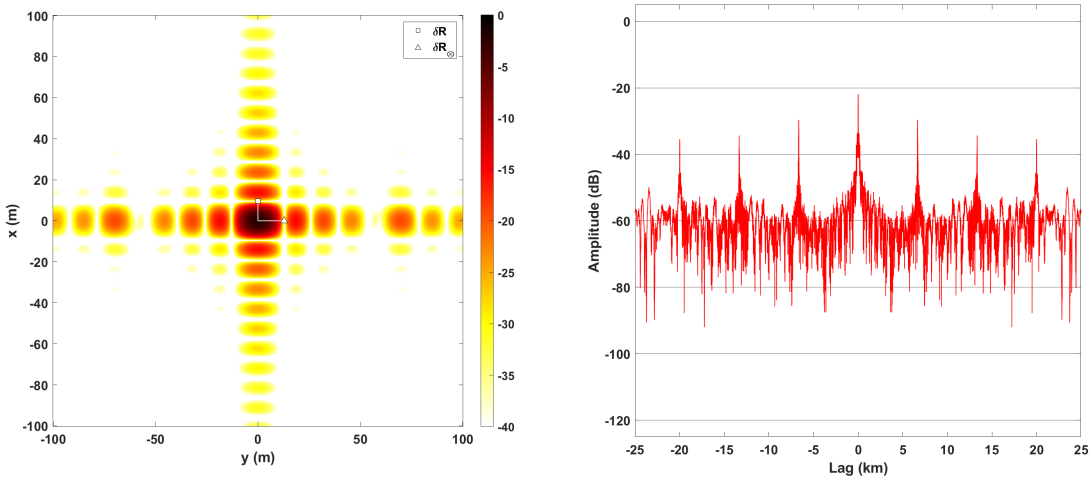

(a) PSF

(b) Magnified Range Profile

Figure 54: Resulting PSF and single range profile realization utilizing CFI-varying, slot-length pulses.

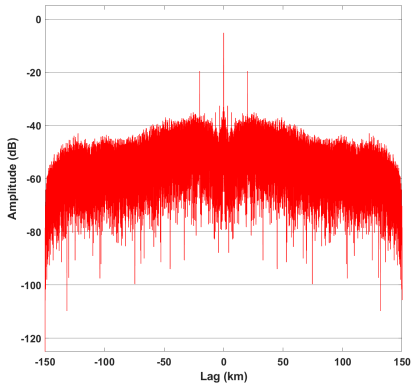

(a) Best Case, PSLR = -6.78 dB

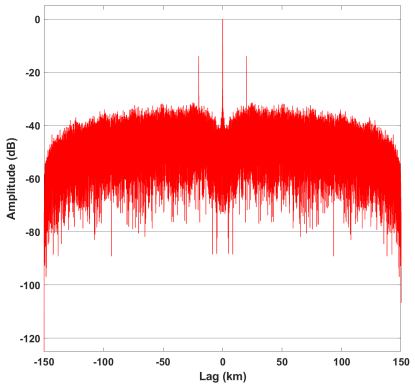

(b) Best Case, ISLR = 13.82 dB

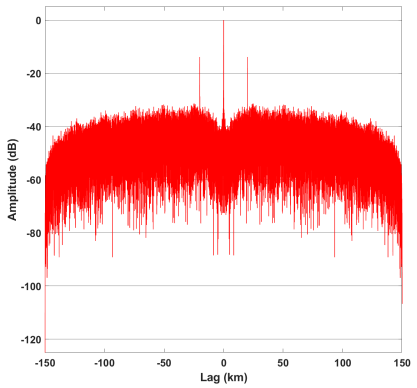

(c) Median Case, PSLR = -6.63 dB

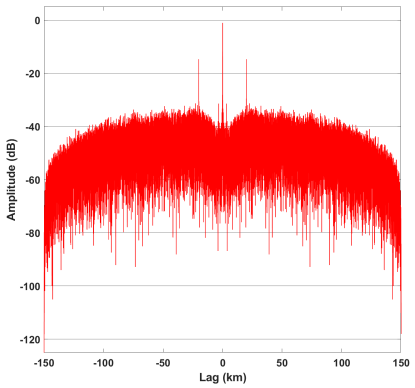

(d) Median Case, ISLR = 14.44 dB

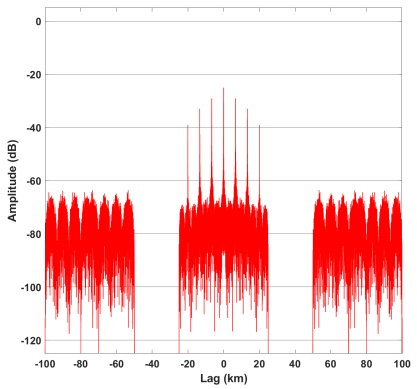

(e) Worst Case, PSLR = -1.96 dB

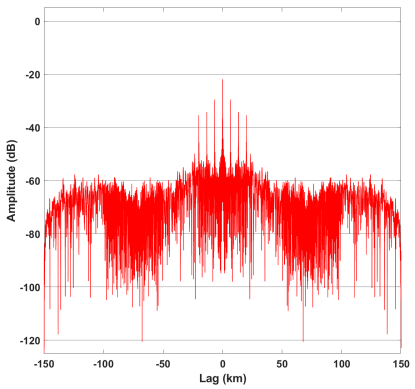

(f) Worst Case, ISLR = 25.53 dB

Figure 55: Range profiles for given cases of PSLR and ISLR utilizing variable control channel, slot-length pulses over the aperture.

4.4.2.4 Symbol

In this section, each pulse consists of one OFDM symbol, see Figures 12d and 13d, which is 83.3 μs in length. Note that the symbol includes a CP. New PDSCH data is generated, CFI selected, and the symbol index iterated for each subsequent pulse. Frame, subframe, and slot indices are likewise iterated when necessary to maintain proper framework progression of the waveform across the aperture. At minimum, it is possible that a pulse will contain no signal whatsoever. This possibility only occurs at specific symbols within subframe 5 of each new frame. Otherwise, pulses may contain information from no less than one cell or user data channel. Referencing Figure 56, the PSF yields δR of 9.6 meters and $\delta R_{\otimes}$ of 12.4 meters. The best-case PSLR and ISLR resulting from Figure 57 are -6.84 dB and 15.20 dB, respectively.

CFI variation results in a PSF loss of 3.44 dB. Range profiles are markedly similar to previous iterations of symbol-length pulses. Due to some symbols being devoid of any signal, the worst-case metrics are derived from zero-response range profiles. Cross-range aliasing is visible in Figure 56. Notable cross-range effects are observed in the PSF resulting from the aperture pulse density, much like when using slot-length pulses. While $\delta R_{\otimes}$ appears to improve over expectations, the inconsistent sidelobes resulting from empty and sparse-signal pulses causes cross-range smearing and move the first cross-range minimum toward scene center. As more pulses are included in the aperture extent, $\delta R_{\otimes}$ degrades to expected bounds.

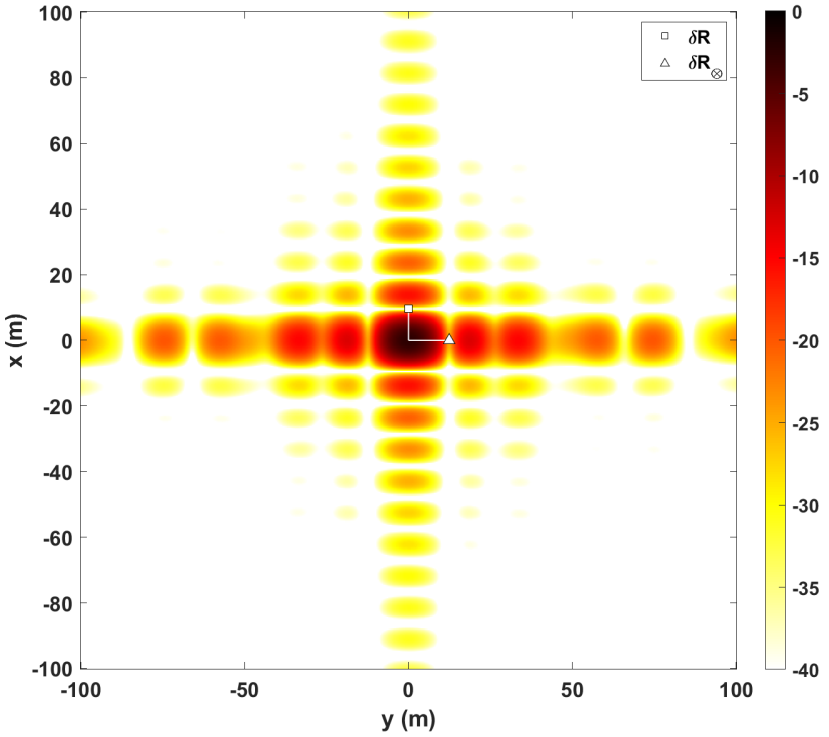

Figure 56: Resulting PSF due to varying number of control symbols on a symbol-by-symbol basis.

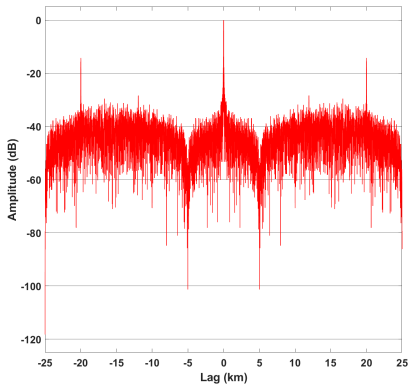

(a) Best Case, PSLR = -6.84 dB

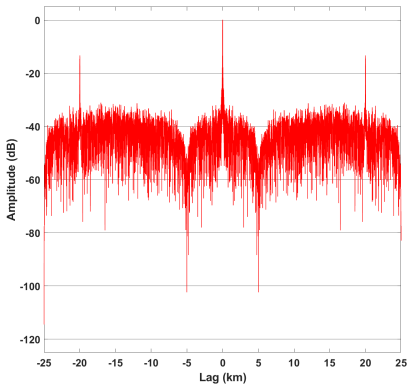

(b) Best Case, ISLR = 15.20 dB

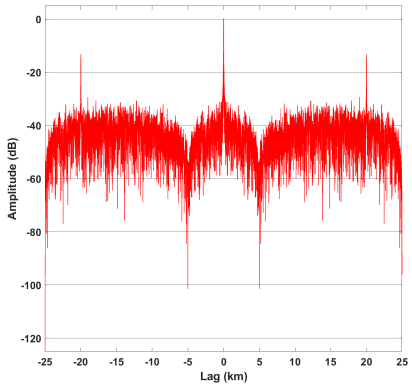

(c) Median Case, PSLR = -6.50 dB

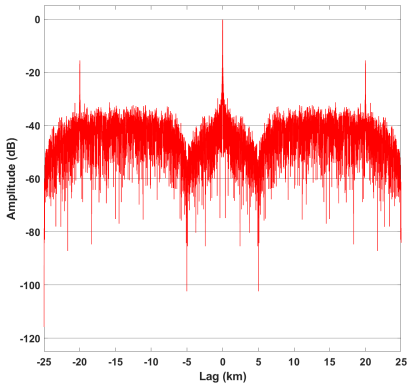

(d) Median Case, ISLR = 15.49 dB

Figure 57: Range profiles for given cases of PSLR and ISLR utilizing variable control channel, symbol-length pulses over the aperture.

4.5 Cyclic Prefix Effects

The CP for an LTE waveform varies dependent primarily on multipath impacts in the transmission environment. A normal CP length is preferred for active networks due to its greater data throughput. However, an extended CP waveform is simpler to process and handle being that all OFDM symbols are uniform in duration.

4.5.1 Methodology and Assumptions

The CP length is uniformly randomly varied between normal and extended with eNB bandwidth of 20 MHz, QPSK modulated PDSCH, and CFI of one. Because a normal CP length creates non-uniformly sized OFDM symbols, variation of the CP is not considered symbol-to-symbol. Attempting to fluctuate CP length symbol to symbol would require either truncation or extrapolation of the current symbol in order to maintain the timing of the LTE framework. Beyond the processing challenges of CP variation for symbol-length pulses, the introduction of such diversity is unlikely in a communications-focused waveform. Given fixed aperture parameters and using possible effective simulation bandwidth of 18 MHz centered at 750 MHz, Equations (8) and (9) are utilized to determine an expected δR of 9.6 meters and $\delta R_{\otimes}$ between 13.1 and 13.4 meters for all pulse-lengths.

4.5.2 Results

4.5.2.1 Frame

In this section, each pulse consists of one LTE frame, see Figures 12a and 13a, which is 10 ms in length. Because the pulse is a full LTE frame, all cell and user data channels, see Section 2.4.3, are contained in every pulse. New PDSCH data is generated, CP length selected, and the frame index iterated for each subsequent pulse. Referencing Figure 58a, the PSF yields δR of 9.6 meters and $\delta R_{\otimes}$ of 13.2 meters. The

PSLR and ISLR resulting from Figure 59 are -6.70 dB and 8.91 dB, respectively.

Like in the case of frame-length pulses with variations in PDSCH modulation, when CP length is set to be normal, more PDSCH data is contained in the pulse. The increase of user data in some pulses throughout the aperture facilitates a PSF gain of 0.15 dB. The PSF maintains a response pattern consistent with Chapter III results. Resulting δR and $\delta R_{\otimes}$ match expected values. Similarly to other frame-length pulse variations, some range profiles, as seen in Figure 58, contain intra-symbol sidelobes occurring at about 3 km intervals.

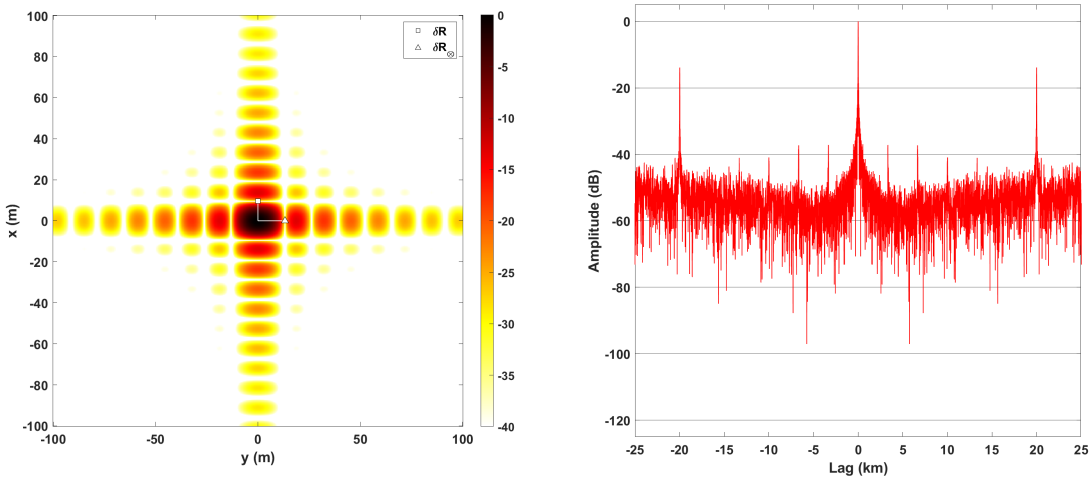

(a) PSF

(b) Magnified Range Profile

Figure 58: Resulting PSF and single range profile realization utilizing CP-varying, frame-length pulses.

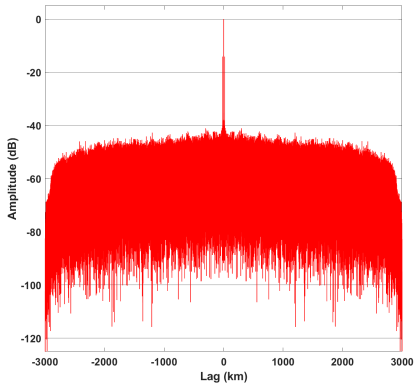

(a) Best Case, PSLR = -6.70 dB

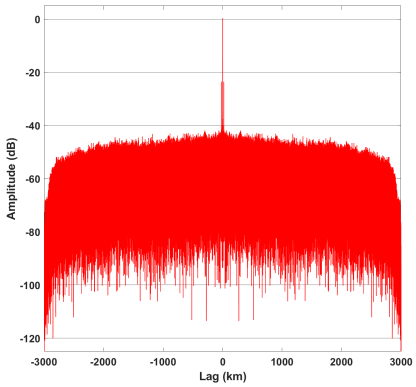

(b) Best Case, ISLR = 8.91 dB

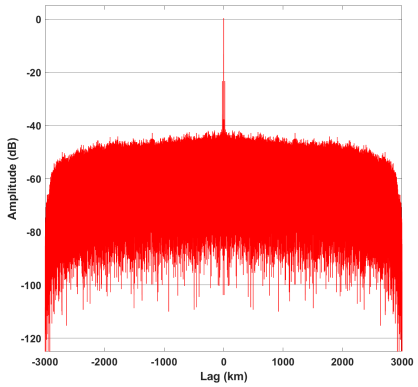

(c) Median Case, PSLR = -6.67 dB

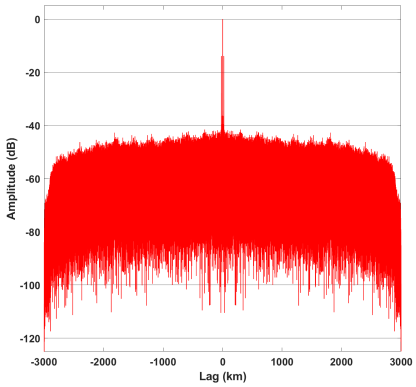

(d) Median Case, ISLR = 9.24 dB

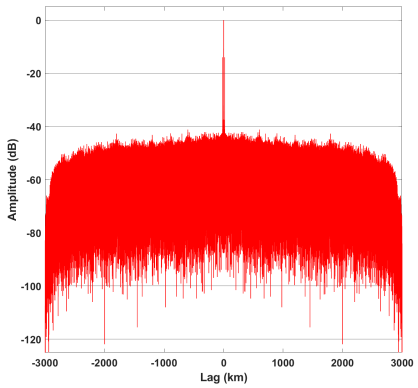

(e) Worst Case, PSLR = -6.63 dB

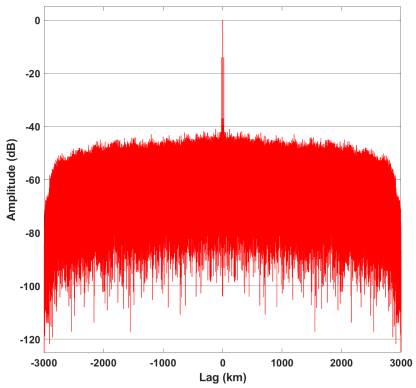

(f) Worst Case, ISLR = 9.29 dB

Figure 59: Range profiles for given cases of PSLR and ISLR utilizing variable cyclic prefix, frame-length pulses over the aperture.

4.5.2.2 Subframe

In this section, each pulse consists of one LTE subframe, see Figures 12b and 13b, which is 1 ms in length. New PDSCH data is generated, CP length selected, and the subframe index iterated for each subsequent pulse. The frame index is likewise iterated when necessary to maintain proper framework progression of the waveform across the aperture. At minimum, any given pulse contains CSRS, PCFICH, PDCCH, PHICH, and PDSCH information. As the subframe index is iterated, some pulses will contain all cell and user data channels. Referencing Figure 60a, the PSF yields δR of 9.6 meters and $\delta R_{\otimes}$ of 13.2 meters. The best-case PSLR and ISLR resulting from Figure 61 are -6.78 dB and 13.33 dB, respectively.

PSF incurs a loss of 0.72 dB in relation to corresponding fixed-data results and maintains a response pattern consistent with those observed in Chapter III. Much like other subframe-length pulse variations, some range profiles, as seen in Figure 44, contain intra-symbol sidelobes occurring about every 3.3 km. As part of progression through the LTE framework at the subframe level, Figures 61e and 61f depict examples of range profiles generated through use of pulses sourced from subframe 5 which contains empty symbols.

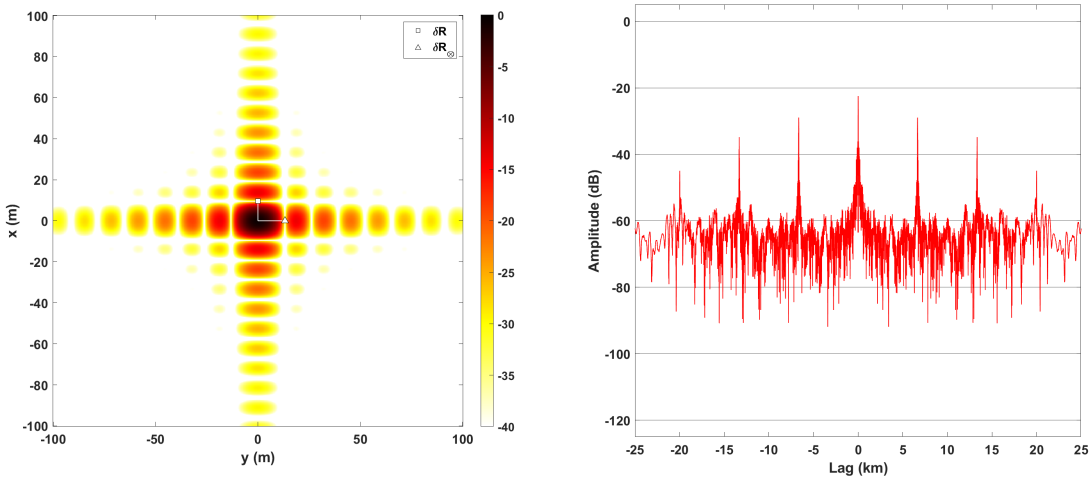

(a) PSF

(b) Magnified Range Profile

Figure 60: Resulting PSF and single range profile realization utilizing CP-varying, subframe-length pulses.

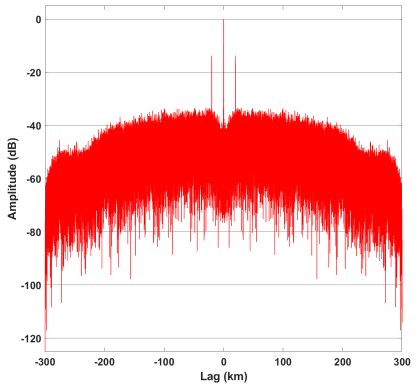

(a) Best Case, PSLR = -6.78 dB

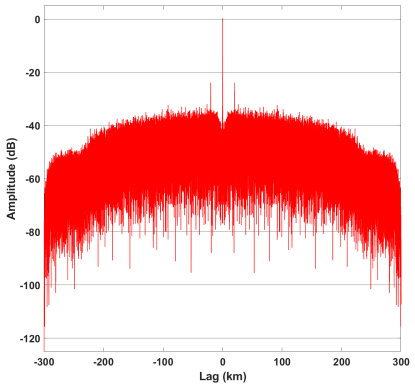

(b) Best Case, ISLR = 13.33 dB

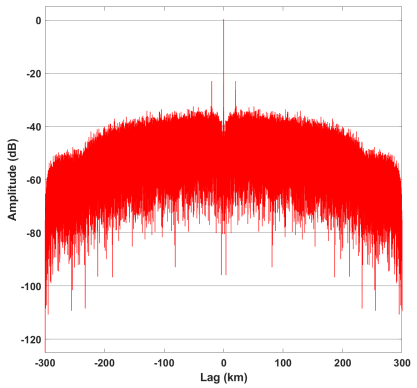

(c) Median Case, PSLR = -6.64 dB

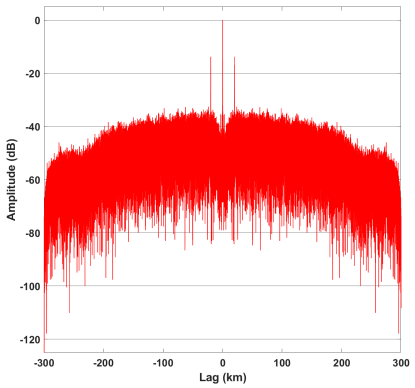

(d) Median Case, ISLR = 13.66 dB

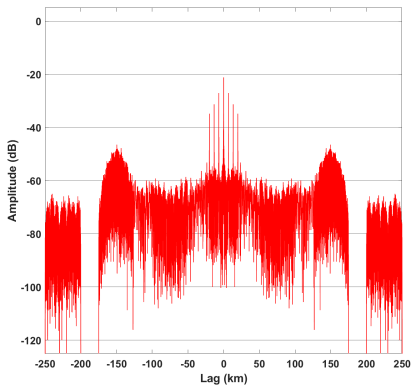

(e) Worst Case, PSLR = -2.93 dB

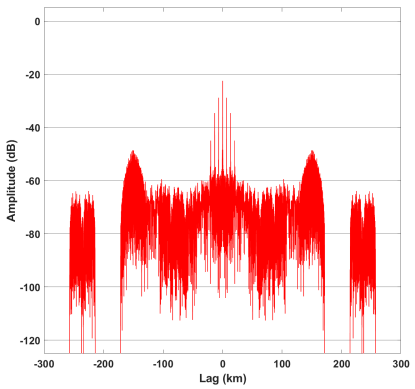

(f) Worst Case, ISLR = 24.79 dB

Figure 61: Range profiles for given cases of PSLR and ISLR utilizing variable cyclic prefix, subframe-length pulses over the aperture.

4.5.2.3 Slot

In this section, each pulse consists of one LTE slot, see Figures 12c and 13c, which is 0.5 ms in length. New PDSCH data is generated, CP length selected, and the slot index iterated for each subsequent pulse. The frame and subframe indices are likewise iterated when necessary to maintain proper framework progression of the waveform across the aperture. At minimum, any give pulse contains CSRS information. As the slot index is iterated, pulses will contain several combinations of cell and/or user data channels at varying bandwidths. Referencing Figure 54a, the PSF yields δR of 9.6 meters and $\delta R_{\otimes}$ of 13.2 meters. The best-case PSLR and ISLR resulting from Figure 55 are -6.82 dB and 13.81 dB, respectively.

A loss of 2.98 dB is observed in the PSF when normalized against the PSF generated in Section 3.3.2.3. Cross-range ambiguities noted in Section 3.5 are evident here as well. As the pulses progress through the framework, some contain limited signal resulting in low-energy range profiles and impacting the aperture pulse density. Increasing the number of pulses in the aperture lessens the impact of sparse-signal pulses, thereby diminishing cross-range effects observed here. The lack of response displayed in sections of Figure 63e is an impact of empty symbols contained in the pulse sourced from slot 1, subframe 5.

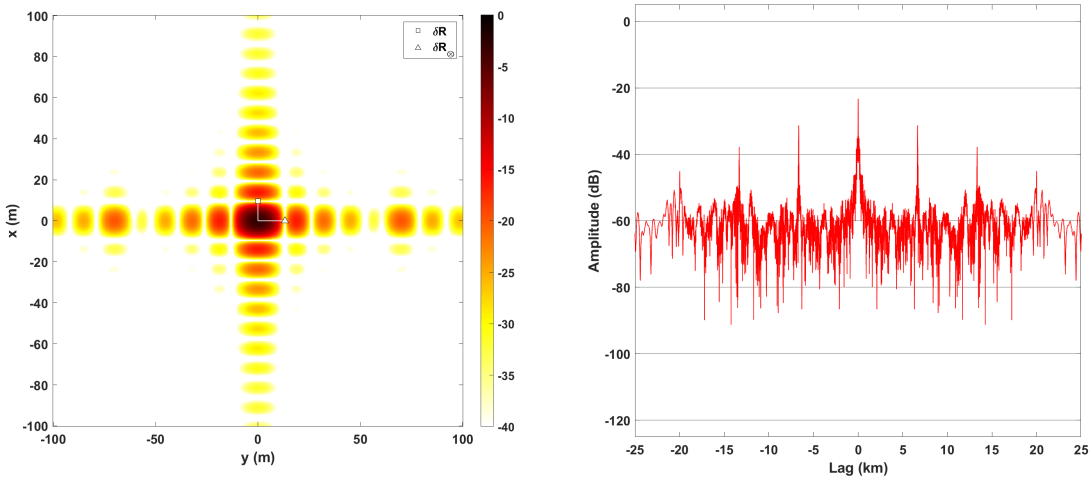

(a) PSF

(b) Magnified Range Profile

Figure 62: Resulting PSF and single range profile realization utilizing CP-length varying, slot-length pulses.

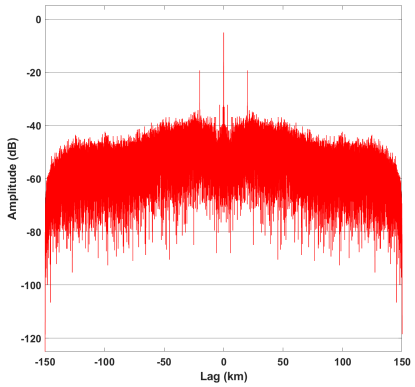

(a) Best Case, PSLR = -6.82 dB

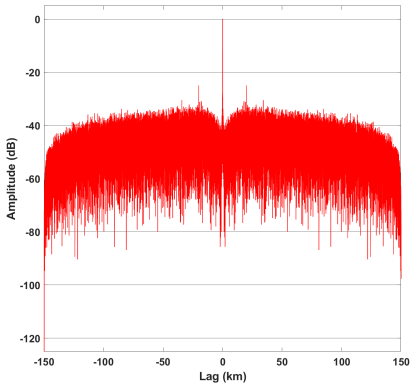

(b) Best Case, ISLR = 13.81 dB

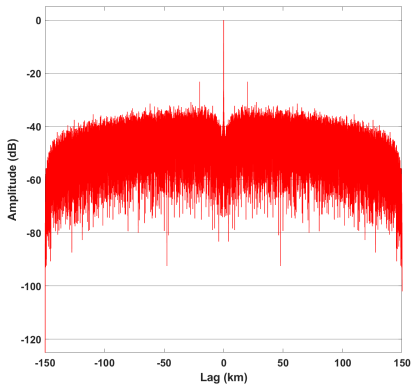

(c) Median Case, PSLR = -6.63 dB

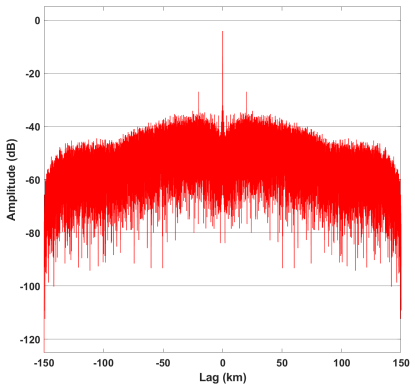

(d) Median Case, ISLR = 15.87 dB

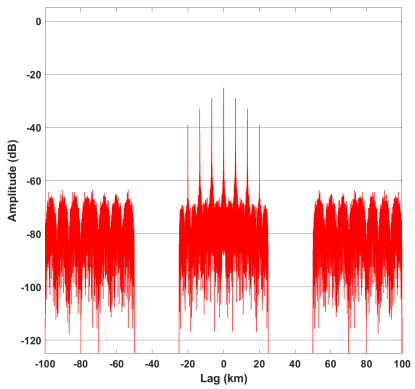

(e) Worst Case, PSLR = -1.96 dB

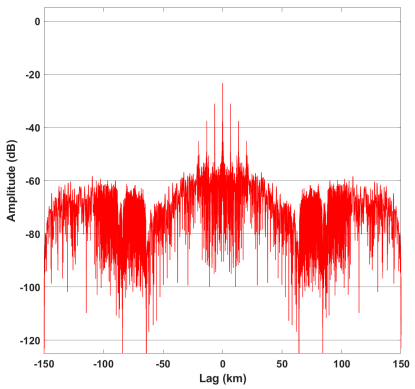

(f) Worst Case, ISLR = 25.93 dB

Figure 63: Range profiles for given cases of PSLR and ISLR utilizing variable cyclic prefix, slot-length pulses over the aperture.

4.6 Chapter Review

This chapter discussed advanced variations of the LTE waveform and demonstrated image domain and range profile effects of those variations. While bandwidth variations pulse to pulse produced significant range spreading at all pulse-lengths, other advanced variations produced little fluctuation in PSF when compared to basic variations in Chapter III. Use of variable CFI or CP length enable relatively small gains over their fixed-data counterparts at the frame-length level. At the slot and symbol level for each advanced variation, cross-range sidelobes occur as a result of aliasing introduced by significant pulse-diversity.

As waveform bandwidth and aperture extent dominate δR and $\delta R_{\otimes}$, these metrics are within expected bounds across most variations and pulse-lengths. Exceptions to this observation occur most notably at shorter pulse-lengths. Variation in bandwidth exacerbates the cross-range effects up to the subframe level while the apparent improvement to $\delta R_{\otimes}$ occurs at the slot and symbol level for CFI variation and only at the symbol level for modulation variations. The apparent improvement to $\delta R_{\otimes}$ in these cases is not an actual improvement, but an effect of non-uniform pulse repetition frequency and changing frequency support across pulses in the aperture. Given a great enough pulse density in the aperture, the apparent improvement to $\delta R_{\otimes}$ degrades to expected bounds for all cases. The waveform bandwidth and aperture pulse density dominate these metrics. Range profiles across the board do not contain significant sidelobes within 3 km, lending support to the potential effectiveness of LTE as a useful waveform for considerably-sized synthetic aperture radar (SAR) scenes. Range effects, across pulse-widths, within the 20 km range of the CP sidelobe are due in large part to PCFICH, PHICH, and CSRS information contained in the first symbol of each subframe. It is, however, difficult to discern which of these channels contributes most significantly to intra-symbol sidelobes in the range profiles.

Overall, PSLR improves with shorter pulse-lengths while ISLR is effected in the opposite manner, degrading with shorter pulse-lengths. Further, in the best-cases for each pulse length, both PSLR and ISLR improve marginally as more variation is introduced to the waveform. The primary trade off of additional variation is lower peak PSF, due mostly to lack of signal in all or sections of pulses. All PSLR and ISLR measures presented in the figures throughout this section are located in Table 7 for easy referencing.

Table 7: PSLR and ISLR results from all cases of advanced variations in decibels.

	Bandwidth		Modulation		CFI		CP Length		
	PSLR	ISLR	PSLR	ISLR	PSLR	ISLR	PSLR	ISLR	
Frame	-6.7	9.21	-6.73	9.23	-6.72	8.4	-6.7	8.91	Best
	-6.66	9.28	-6.67	9.26	-6.67	8.83	-6.67	9.24	Median
	-6.6	9.96	-6.61	9.32	-6.63	9.29	-6.63	9.29	Worst
Subframe	-6.74	13.6	-6.81	13.62	-6.76	12.81	-6.78	13.33	Best
	-6.62	13.76	-6.62	13.75	-6.63	13.31	-6.64	13.66	Median
	-2.93	25.11	-2.93	24.44	-2.9	24.44	-2.93	24.79	Worst
Slot	-6.9	13.89	-6.9	13.91	-6.78	13.82	-6.82	13.81	Best
	-6.62	16.31	-6.65	16.33	-6.62	14.44	-6.63	15.87	Median
	-1.94	25.78	-1.96	25.53	-1.96	25.53	-1.96	25.93	Worst
Symbol	-6.96	15.28	-6.97	15.12	-6.84	15.2	—	—	Best
	-6.49	16.17	-6.49	17	-6.5	15.49	—	—	Median
	NaN	NaN	NaN	NaN	NaN	NaN	—	—	Worst

V. Conclusions

5.1 Overview

This chapter revisits the overarching goal of this work, recaps experimental results, discusses contributions to the outlying synthetic aperture radar (SAR) community, and provides suggestions for future research topics.

5.2 Research Goal

The intent of this effort centers on broadening the knowledge base regarding the impacts of Long-Term Evolution (LTE) waveform variations on SAR image products. This topic area is still fairly new to Air Force Institute of Technology (AFIT), with previous efforts focusing on the established structures within LTE waveforms [1, 2]. This work sought to explore the effects of pulse-lengths corresponding to the four major structure levels of LTE on image domain metrics. This concept was built upon by including variation of bandwidth, physical downlink shared channel (PDSCH) modulation, control format indicator (CFI), or cyclic prefix (CP) pulse to pulse to determine what change might be affected by fluctuations in signal structure.

5.3 Results and Contributions

The work completed for this research builds upon a growing interest in the application of widely available communications waveforms to passive radar and provides an important step forward in that pursuit. Section 2.4 provides significant background on LTE structure and content. This information is expounded upon in Chapter III by stepping through the structural levels of the waveform and changes that take place at those structure levels. The information presented provides a springboard for newcomers to passive SAR interested in LTE.

The results observed throughout Chapter III establish a footing in fundamental LTE effects on the SAR image domain. The analysis of point-spread function (PSF) and range profiles affirm the dominating effects of signal bandwidth and collection aperture on primary image metrics. The use of several pulse-lengths enabled findings of peak sidelobe ratio (PSLR) improvement and integrated sidelobe ratio (ISLR) deterioration using shorter pulses. Results also show that pulse-diversity has the opportunity to improve both PSLR and ISLR when pulses are selected with an emphasis on maximizing PDSCH content. The observed outcomes may be leveraged towards waveform selection and prioritization as the SAR community continues to vet the radar applications of communications waveforms.

Waveform parameters in real LTE networks are very likely to be dynamic over time. Chapter IV breaks down four of these parameters — bandwidth, PDSCH modulation, CFI, and CP length — and quantifies the consequences of their fluctuation. Of the parameters considered, variations in bandwidth are the most influential in that a decrease in bandwidth may significantly worsen resolution and introduce range and cross-range smearing. While changes to waveform parameters are most likely to occur no more frequently than frame to frame, this work attempts to look ahead and establish background for the future as consumer pressure for ever faster networks lead to the emergence of more dynamic waveforms [12].

5.4 Future Work

This research provides a foundation for further exploration of LTE effects in SAR systems. The following are areas open to future endeavors.

- Bistatic modeling: Process waveform in bistatic environment
- Aliasing mitigation: Characterize consequences of including empty symbols in pulses and relate to cross-range aliasing metrics.

- Error introduction: Noise or flight-path error may be introduced to processing chain to establish statistical characteristics of PSF.
- Cell synchronization: Consideration of system synchronization with cell and associated impacts on image formation.
- Multipath effects: The influence of signal variation due to LTE multipath mitigation be explored to broaden the knowledge base.
- Multi-provider waveform: The use of multiple providers' signals from the same cell has the potential improve effective bandwidth.
- Pulse spacing: Use of uniform but non-adjacent LTE structure to prioritize desirable waveform attributes may improve image metrics.

Bibliography

1. Aaron Evers and Julie A. Jackson. Cross-ambiguity characterization of communication waveform features for passive radar. *IEEE Transactions on Aerospace and Electronic Systems*, 51(4):3440–3455, Oct 2015.

2. Forrest D Taylor. Orthogonal frequency division multiplexed waveform effects on passive bistatic radar. MS Thesis, Air Force Institute of Technology, March 2019.

3. Charles V. Jakowatz, Daniel E. Wahl, Paul H. Eichel, Dennis C Chiglia, and Paul A. Thompson. *Spotlight-mode synthetic aperture radar: a signal processing approach*. Springer Science Business Media, New York, 1996.

4. Scott L. Miller and Donald G. Childers. *Probability and random processes with applications to signal processing and communications*. Elsevier/Academic Press, Waltham, 2012.

5. Samuel D. Stearns and Don R. Hush. *Digital signal processing with examples in MATLAB*. CRC Press, Boca Raton, 2011.

6. Anil K. Jain. *Fundamental of digital images processing*. Prentice Hall, Upper Saddle River, 1989.

7. William L. Melvin and Jim Scheer, editors. *Principles of Modern Radar, Volume 2 - Advanced Techniques*. Institution of Engineering and Technology, Edison, 2013.

8. Hugh D. Griffiths and Nicholas J. Willis, editors. *Advances in Bistatic Radar*. SciTech Publishing, Inc., Raleigh, 2007.

9. Mark A. Richards, James A. Scheer, and William A. Holm, editors. *Principles of modern radar*. SciTech Publishing, Raleigh, 2015.

10. LTE; Evolved Universal Terrestrial Radio Access (E-UTRA); Physical channels and modulation. https://portal.3gpp.org/desktopmodules/Specifications/SpecificationDetails.aspx?specificationId=2425, January 2019. Accessed August 2019.

11. Jaeku Ryu. Sharetechnote. http://sharetechnote.com/, 2011. Accessed August 2019.

12. Bob O'Donnell. 5g latency improvements are still lagging. https://www.forbes.com/sites/bobodonnell/2020/02/18/5g-latency-improvements-are-still-lagging/#3b946d9b48f1, Feb 2020. Accessed 18 February 2020.

Acronyms

16QAM 16-quadrature amplitude modulation. 18, 19, 78

64QAM 64-quadrature amplitude modulation. 18, 19, 78

AFIT Air Force Institute of Technology. 114

BPA back-projection algorithm. 9, 10

CFI control format indicator. 19, 20, 65, 66, 78, 91, 94, 97, 100, 103, 112, 114, 115

CP cyclic prefix. 3, 14, 15, 16, 19, 20, 22, 25, 26, 27, 29, 32, 34, 36, 38, 39, 40, 46, 49, 60, 63, 65, 66, 75, 78, 88, 91, 100, 103, 104, 106, 109, 112, 114, 115

CSRS cell-specific reference signal. 16, 17, 21, 25, 34, 36, 43, 46, 51, 54, 57, 63, 69, 72, 79, 82, 85, 94, 97, 106, 109, 112

DL downlink. 14, 16, 17, 18, 23

eNB Evolved Node B. 23, 24, 25, 66, 78, 91, 103

FDD frequency-division duplexing. 14

GMTI ground moving target indication. 21

ISI inter-symbol interference. 19

ISLR integrated sidelobe ratio. iv, 2, 13, 32, 33, 34, 35, 36, 37, 38, 39, 40, 42, 43, 45, 46, 48, 49, 50, 51, 53, 54, 56, 57, 59, 60, 62, 63, 64, 66, 68, 69, 71, 72, 74, 75, 77, 79, 81, 82, 84, 85, 87, 88, 90, 91, 93, 94, 96, 97, 99, 100, 102, 104, 105, 106, 108, 109, 111, 113, 115, 1

LFM linear-frequency modulation. 5, 7, 11

LTE Long-Term Evolution. iv, 1, 2, 3, 4, 11, 14, 15, 16, 17, 18, 19, 20, 21, 22, 23, 24, 26, 27, 28, 32, 34, 36, 39, 40, 43, 46, 51, 53, 54, 56, 57, 59, 62, 63, 64, 65, 66, 69, 72, 78, 79, 82, 85, 91, 94, 97, 103, 106, 109, 112, 114, 115, 116, 1

MF matched filter. 5, 7, 8, 13

OFDM orthogonal frequency-division multiplexing. 14, 15, 16, 17, 18, 19, 20, 32, 34, 38, 43, 49, 60, 75, 88, 100, 103

PBCH physical broadcasting channel. 18, 34, 43

PCFICH physical control format indicator channel. 18, 34, 36, 43, 46, 54, 63, 69, 79, 82, 94, 106, 112

PDCCH physical downlink control channel. 18, 20, 34, 36, 43, 46, 51, 54, 69, 79, 82, 94, 106

PDSCH physical downlink shared channel. 18, 28, 34, 36, 38, 39, 40, 43, 46, 51, 54, 57, 60, 65, 66, 69, 72, 75, 78, 79, 80, 82, 83, 85, 86, 88, 91, 94, 97, 100, 103, 104, 106, 109, 114, 115

PHICH physical hybrid ARQ indicator CH. 18, 34, 36, 43, 46, 51, 54, 63, 69, 79, 82, 94, 106, 112

PSF point-spread function. iv, 2, 3, 10, 11, 12, 22, 23, 28, 32, 33, 34, 35, 36, 37, 38, 39, 40, 41, 43, 44, 46, 47, 49, 51, 52, 54, 55, 57, 58, 60, 61, 63, 65, 66, 67, 69, 70, 72, 73, 75, 76, 79, 80, 82, 83, 85, 86, 88, 89, 91, 92, 94, 95, 97, 98, 100, 101, 103, 104, 106, 107, 109, 110, 112, 113, 115, 116, 1

PSLR peak sidelobe ratio. iv, 2, 13, 32, 33, 34, 35, 36, 37, 38, 39, 40, 42, 43, 45, 46, 48, 49, 50, 51, 53, 54, 56, 57, 59, 60, 62, 63, 64, 66, 68, 69, 71, 72, 74, 75, 77, 79, 81, 82, 84, 85, 87, 88, 90, 91, 93, 94, 96, 97, 99, 100, 102, 104, 105, 106, 108, 109, 111, 113, 115, 1

PSS primary synchronization signal. 16, 17, 25, 34, 43

QPSK quadrature phase-shift keying. 18, 19, 66, 78, 91, 103

RB resource block. 15, 16, 17, 18, 25

SAR synthetic aperture radar. iv, 1, 2, 3, 4, 5, 6, 7, 8, 17, 18, 21, 23, 63, 112, 114, 115, 1

SNR signal-to-noise ratio. 5, 19

SSS secondary synchronization signal. 16, 17, 25, 34, 43

TDD time-division duplexing. 14

UE user equipment. 19

UL uplink. 14

REPORT DOCUMENTATION PAGE

Form Approved
OMB No. 0704–0188

1. REPORT DATE *(DD–MM–YYYY)*	2. REPORT TYPE	3. DATES COVERED *(From — To)*
19–03–2020	Master's Thesis	Sept 2018 — Mar 2020

4. TITLE AND SUBTITLE

Effects of Long-Term Evolution Waveform on Synthetic Aperture Radar Image Quality Metrics

5a. CONTRACT NUMBER

5b. GRANT NUMBER

5c. PROGRAM ELEMENT NUMBER

6. AUTHOR(S)

Colson, Blake M., Captain, USAF

5d. PROJECT NUMBER

5e. TASK NUMBER

5f. WORK UNIT NUMBER

7. PERFORMING ORGANIZATION NAME(S) AND ADDRESS(ES)

Air Force Institute of Technology
Graduate School of Engineering and Management (AFIT/EN)
2950 Hobson Way
WPAFB OH 45433-7765

8. PERFORMING ORGANIZATION REPORT NUMBER

AFIT-ENG-MS-20-M-011

9. SPONSORING / MONITORING AGENCY NAME(S) AND ADDRESS(ES)

Air Force Research Laboratory - Sensors Directorate
Dr. Braham Himed, AFRL/RYMD Division Research Fellow
2241 Avionic Circle, Bldg. 620, WPAFB, OH 45433
(937) 713-8124
brahan.himed@us.af.mil

10. SPONSOR/MONITOR'S ACRONYM(S)

AFRL/RYMD

11. SPONSOR/MONITOR'S REPORT NUMBER(S)

12. DISTRIBUTION / AVAILABILITY STATEMENT

DISTRIBUTION STATEMENT A:
APPROVED FOR PUBLIC RELEASE; DISTRIBUTION UNLIMITED.

13. SUPPLEMENTARY NOTES

14. ABSTRACT

Passive radar allows for data collection by referencing signals already established in the environment. LTE is a prolific waveform that could be leveraged for discrete collection of image intelligence. Seeking to build a base of knowledge, simulations of SAR systems are carried out using the LTE framework. Variations in waveform content, structure, and signal components are established and used to generate PSF responses characterizing the image domain impacts of given fluctuations. Overall, PSF responses for most variations are highly similar, incurring slight losses as pulses become more diverse and slight gains when maximizing the amount of user data contained in pulses. Notable sidelobes in range profiles occur at predictable intervals and may be easily managed for adequately-sized scenes. PSLR and ISLR results show marginal improvement when pulses are diverse. Range and cross-range resolution, while remaining mostly unchanged throughout variations, are observed to be worse in simulation than is expected.

15. SUBJECT TERMS

Synthetic Aperture Radar, Long-Term Evolution, Passive Radar, Image Metrics

16. SECURITY CLASSIFICATION OF:			17. LIMITATION OF ABSTRACT	18. NUMBER OF PAGES	19a. NAME OF RESPONSIBLE PERSON
a. REPORT	b. ABSTRACT	c. THIS PAGE			Dr. J. A. Jackson, AFIT/ENG
U	U	U	UU	133	19b. TELEPHONE NUMBER *(include area code)* (937) 255-3636, ext 4678; julie.jackson@afit.edu